

THE UNIVERSITY OF CHICAGO

LIFE HISTORY EVOLUTION IN CYCLICAL ENVIRONMENTS

A DISSERTATION SUBMITTED TO
THE FACULTY OF THE DIVISION OF THE BIOLOGICAL SCIENCES
AND THE PRITZKER SCHOOL OF MEDICINE
IN CANDIDACY FOR THE DEGREE OF
DOCTOR OF PHILOSOPHY

COMMITTEE ON EVOLUTIONARY BIOLOGY

BY

JOHN SOOKWON PARK

CHICAGO, ILLINOIS

AUGUST 2021

Contents

LIST OF FIGURES	V
LIST OF TABLES	X
ACKNOWLEDGMENTS	XI
INTRODUCTION	1
1 PHENOLOGICAL PATTERNS AND THEIR EVOLUTION ON A CYCLICAL EARTH	5
1.1 ABSTRACT	5
1.2 INTRODUCTION	6
1.3 GLOSSARY OF ESSENTIAL TERMS	10
1.4 PHENOLOGY: DELINEATING THE DIMENSION OF TIME TO STANDARDIZE CYCLICAL PATTERNS	11
1.4.1 <i>Temporal contingency</i>	14
1.4.2 <i>Scale relativity</i>	15
1.5 EVOLUTION OF PHENOLOGIES	16
1.6 HOW DOES LIFE HISTORY EVOLUTION PRODUCE CYCLICALLY REPEATING PHENOLOGICAL PATTERNS?	20
1.7 HOW DO SPECIES INTERACTIONS PRODUCE AND MAINTAIN DIVERSE PHENOLOGIES IN THE SAME SPACE?	23
1.8 IMPORTANT UNRESOLVED QUESTIONS	26
1.9 SUMMARY AND OUTLOOK	28
1.10 ACKNOWLEDGEMENTS	30
2 CYCLICAL ENVIRONMENTS DRIVE VARIATION IN LIFE HISTORY STRATEGIES: A GENERAL THEORY OF CYCLICAL PHENOLOGY	31
2.1 ABSTRACT	31
2.2 INTRODUCTION	32
2.3 METHODS	35
2.3.1 <i>Model construction</i>	35
2.3.2 <i>Fitness</i>	37
2.3.3 <i>Life history trade-offs</i>	38
2.3.4 <i>Fitness landscapes and optimal life history strategies</i>	39
2.3.5 <i>Empirical investigation in <i>Tigriopus californicus</i></i>	39
2.3.6 <i>Likelihood and model fitting</i>	40
2.4 RESULTS	41
2.4.1 <i>Cycle periodicity alters optimal life history predictions</i>	41
2.4.2 <i>Periodicity and trade-offs interact to produce diverse life histories</i>	43
2.4.3 <i><i>Tigriopus</i> trade-offs predict life history variation across a periodicity gradient</i>	44
2.5 DISCUSSION	46
2.5.1 <i>Stochasticity, ESS models, and gene flow</i>	48
2.5.2 <i>Trade-off functions</i>	50
2.5.3 <i>Links to evolution of seasonal phenologies</i>	50
2.6 ACKNOWLEDGEMENTS	53

3 SLOWER ENVIRONMENTAL CYCLES INCREASE LIFE HISTORY VARIATION WITHIN POPULATIONS	54
3.1 ABSTRACT	54
3.2 INTRODUCTION	55
3.3 METHODS.....	59
3.3.1 <i>Demography and life history of Tigriopus californicus</i>	59
3.3.2 <i>Agent-based model (ABM) of life-history evolution in fluctuating environments</i>	60
Birth, growth & death of individuals	60
Environmental fluctuation regimes	62
Phenotypic variance	62
3.3.3 <i>Multi-generational life history selection experiment</i>	63
Fecundity (f) measurements	64
Maturation rate (μ) measurements	65
3.3.4 <i>Statistical analyses</i>	65
3.4 RESULTS	66
3.4.1 <i>Shifting distributions in simulated populations during transience</i>	66
3.4.2 <i>Higher variance in Slow simulated environments</i>	68
3.4.3 <i>Experimental corroboration of higher variance in Slow environments</i>	70
3.4.4 <i>Speed of purifying selection and sustained variance in simulations</i>	71
3.5 DISCUSSION	72
3.6 ACKNOWLEDGEMENTS	76
4 SYNTHESIS AND EPILOGUE	77
APPENDIX I: SUPPORTING INFORMATION FOR CHAPTER 2 (CYCLICAL ENVIRONMENTS DRIVE VARIATION IN LIFE HISTORY STRATEGIES: A GENERAL THEORY OF CYCLICAL PHENOLOGY)	87
SI-1.1 MODEL DESCRIPTION	87
SI-1.1.1 <i>Continuous stage-structured population dynamics</i>	87
SI-1.1.2 <i>Incorporating periodic disturbance</i>	89
SI-1.1.3 <i>Fitness of a periodically disturbed population</i>	91
SI-1.2 DATA COLLECTION & ANALYSIS	91
SI-1.2.1 <i>Tigriopus californicus</i>	91
SI-1.2.2 <i>Local disturbance periods</i>	93
SI-1.2.3 <i>Disturbed demographic dynamics</i>	93
SI-1.2.4 <i>Life history measurements</i>	94
SI-1.2.5 <i>Parameterization for model analysis</i>	95
SI-1.3 SUPPLEMENTARY FIGURES	96
SI-1.4 SUPPLEMENTARY TABLES	101
APPENDIX II: SUPPORTING INFORMATION FOR CHAPTER 3 (SLOWER ENVIRONMENTAL CYCLES INCREASE LIFE-HISTORY VARIATION WITHIN POPULATIONS)	103
SI-2.1 SIMULATION SCHEMATIC	103
<i>Demographic dynamics</i>	103
<i>Periodic disturbance-induced death</i>	104
SI-2.2 EXPERIMENTAL SCHEMATIC	105
SI-2.3 PERMUTATION DISTRIBUTIONS OF EXPERIMENTAL POPULATION VARIANCES	106

SI-2.4 PHENOTYPIC MEANS IN EXPERIMENTAL POPULATIONS	108
SI-2.5 DETERMINISTIC <i>VS.</i> STOCHASTIC VARIANCE TRAJECTORIES AND ENDPOINTS	110
SI-2.6 POPULATION STRUCTURE AND SIZE DYNAMICS IN SIMULATIONS	112
REFERENCES	113

List of Figures

Figure 1.1 Distribution patterns in finite units of space or time. (A) Repeated patterns in space are often innately obvious to human observers, such as zonation of rocky shore intertidal communities, even if space in nature is realistically messy and unbounded. (B) Repeated patterns in time, such as seasonal phenology, can be seen over longer observations. (C) Patterns can only be defined and quantitatively measured given finite boundaries. In space, standardized delineations such as transects and grids are commonplace. (D) Just as in space, one must delineate unbounded time into relevant units such as years or climatic growing seasons to quantify time points occupied by phenological expression. (E) Only within standardized arenas of measurement are comparative studies possible and can eco-evolutionary theories of how patterns form and change be developed and tested. (F) Similarly, an explicit view of timing patterns within standardized time windows sets the basis for systematic hypotheses of how phenology is shaped by ecological and evolutionary forces..... 7

Figure 1.2 Phenology is a study of repeated patterns of events in the dimension of time. Delimiting the continuous arrow of time into natural units such as years or climatic growing seasons allows observers to compare patterns between cycle periods and quantify change such as phenological shifts. Shapes of seasonal patterns (colored curves), peak dates (location of stars), or number of peaks (e.g. species 1 has two peaks in Window 3) can be taken as measures of change. Systematic quantification and comparisons then provide the necessary groundwork for studying ecological and evolutionary causality. 14

Figure 1.3 Disaster. High-tide wave disturbance brings unwelcome inconvenience to tidepool *Tigriopus californicus* populations, the focal field system that will be introduced in the subsequent chapters. Imaged here is a perspectives study I conducted on Tatoosh Island, WA to gain more insight into how I myself might arrange my life history in such a setting. A major logical flaw was later identified that precluded any fair comparison between *Tigriopus* life history scheduling and mine, namely access to the NOAA tide table. 18

Figure 1.4 The manner in which phenology evolves at the single-species level requires consideration of trade-offs and temporal contingencies both within an individual's life time and across generations. Phenology treated as a correlative response to meteorological forcing per year overlooks how evolution is shaped by trait covariance and demographic lag effects. Here we illustrate four examples of connections in phenological cycles across two adjacent years or generations. Curve shows fluctuations in abundance or event timing (peaks) which are typical representations of phenology. Green circles paired with pictorial representations of flower development denote points in the life-cycle, and arrows indicate correlative links between two points. A) Biological functions early in life such as development and growth can be negatively correlated with those later in life such as reproduction. B) Conversely, reproductive investment in one generation can influence the next generation's offspring performance. Success of the previous generation can also shape the standing genetic variation available for selection in the next generation. C) In some species, a proportion of offspring or seeds of a population will proceed to development while others enter diapause. These unrealized offspring carry over to subsequent years and influence population dynamics and selection landscapes in the future. D) If the timing of a phenological trait such as flowering is related to fitness in the context of the environment, selection can shape the frequency distribution of its mean in the population,

balanced out by potentially antagonistic forces such as those connections represented by A, B, and C. 19

Figure 1.5 Community interactions promote phenological variation within bounded windows of time. In addition to external seasonal cues and internal mechanisms of optimization at the single-species level, ecological interactions can influence the phenologies of coexisting species in a community. Colored curves show hypothetical phenological curves of species, measured as change in abundance reflecting seasonal emergence or number of individuals expressing a trait such as flowering. Stars show peak phenology. Dashed curves show phenologies prior to shifts, and arrows show direction of shifts. Certain interactions may favor (A) co-occurrence between species, such as plant-pollinator interactions and other mutualistic relationships, and others (B) avoidance, such as competition for a time-related resource. 25

Figure 2.1 Three hypothetical cost functions between μ —rate at which juveniles mature into reproducing adults—and f —adult fecundity—are analyzed while setting linear trade-offs between μ and f , and between those two traits and their respective stage-specific background survival rates (d and γ). Stage-specific survival terms associated with cyclical disturbance are set at $S_A = 0.9$ & $S_J = 0.6$. Colors of cost functions in A correspond to colors of fitness profiles of μ in B and C. Dashed lines in B and C show peaks of fitness profiles which correspond to optimal values of μ . Periodicity of cyclical perturbation to population structure is set to be much greater than generation time in B ($T=365$), and at a relevant time scale ($<$ generation time) in C ($T=1$). Under short periods (C), all cost functions produce higher optimal μ values, wider fitness profiles, and an exactly reversed relationship between cost and optimality compared to long periods (B). 42

Figure 2.2 Example fitness landscapes of two focal life history traits, μ (rate of maturity) and f (reproductive rate) which assumes lower juvenile survival with each disturbance event ($S_A = 0.9$, $S_J = 0.6$), and trade-offs between μ and f , between μ and d , and between f and γ . Heat shows normalized fitness of a life history strategy compared to all other strategies in a disturbance regime (T). Curves track the optimal (maximum fitness) life history trait across T 44

Figure 2.3 Mean (\pm se) values of the two focal life history traits μ and f across 19 *T. californicus* populations, against mean (\pm se) disturbance period determined by timeseries analysis of wave disturbance signals in each pool. Curves are optimal life history functions across periodicity (T) fit simultaneously to μ and f 46

Figure 3.1 Optimality model of life histories in cyclical environments, and hypotheses for variance. (A) The deterministic theoretical model (Park 2019) takes the life-history strategy of a genotype—which consists of life-history traits and trade-offs among them—and calculates the asymptotic growth rate (dominant eigenvalue λ of the matrix model) as a continuous function of traits and environmental periodicity. (B) The resulting landscape gives optimal life histories (peaks on trait axis) across the axis of environmental cycle periodicity. Note that asymptotic growth on the z-axis is scaled by the matrix projection intervals which vary along the cycle periodicity axis. Here we take two near-extreme cases of periodicity, namely “Fast” (low period) and “Slow” (high period),

and investigate trait distribution hypotheses. (C) Relative (to the optimal trait in each regime) vs. absolute asymptotic growth rate profiles across the trait axis give contrasting hypotheses for whether higher variance should be expected in Fast or Slow environments. 58

Figure 3.2 Means of life-history traits evolving in simulated populations. (A) and (B) show evolving mean of μ (maturation rate) in deterministic and stochastic regimes, respectively; (C) and (D) show evolving mean of f (fecundity) in deterministic and stochastic regimes, respectively. Each scenario is repeated for 100 realizations. 67

Figure 3.3 Purifying selection in action. Morphing distribution of μ (maturation rate) in one example realization of a population under Fast environmental fluctuation shows early selection towards lower μ ; this reflects short-term benefit for fast reproducers (high f) that are simply adding more offspring that resemble them quickly. Thereafter, costs associated with high reproduction allow alternate phenotypes to resurge in frequency ($\sim t=75$), which momentarily raises population mean as well as variance. Soon, the distribution narrows towards an optimum and variance declines (yellow peak at $t=150$). 68

Figure 3.4 Higher phenotypic variance in Slow environments in simulation and in experiment. (A-B) Simulated trajectories of intrapopulation variance over 150 time-steps (5~6 generations) exhibit common qualitative patterns of 1) dropping early on because fast reproducers proliferate quickly (by definition) and distributions become concentrated at high f and low μ values; 2) briefly spiking as alternate phenotypes rise in frequency due to life-history costs associated with high f and low μ ; and 3) beginning to gradually decline. (C-D) Intrapopulation variances at simulation endpoints are higher in Slow environments than Fast for both traits. Diamond points show means of variances in realizations (i.e. means of intrapopulation variance), and error bars the standard deviation among the realization variances. (E-F) Measurements of intrapopulation phenotypic variances after the 150-day experiment (5~6 generations) also showed higher variance in Slow treatments for both traits. Square points show means of intrapopulation variances among replicate populations, and error bars the standard error of the variance measurements. 69

Figure 3.5 Sustained high variance in Slow environments. A longer simulation ($t=300$; 10~12 generations) of realizations for each regime, shows that phenotypic variances of populations in Slow environments steadily decrease as well, but much more gradually than those in Fast environments. Temporary spikes of variance in the Fast regime realizations are explained by compensatory resurgence of fast growers (high μ) after short-term dominance of fast reproducers. By $\sim t=150$, most simulated populations in the Fast regime have markedly low variance as a result of emergent purifying selection. 71

Figure 4.1 Nonlinear functional response of a life history trait (juvenile survival) as a function of time since last disturbance event..... 79

Figure 4.2 Timeseries of disturbance event intervals in the four environmental fluctuation scenarios considered. 81

Figure 4.3 Frequency distributions of disturbance event intervals in the four environmental fluctuations scenarios considered. 82

Figure 4.4 Response in fitness predictions as standard deviation (σ) of event intervals—i.e. amount of noise—increases, across the four environmental fluctuation scenarios considered.... 83

Figure 4.5 Frequency distributions of consecutive events with negative deviations from the mean interval, across the four environmental fluctuation scenarios considered. 84

Figure SI-1.1 Optimality curves of all model variants which include varying life history trade-off assumptions. Each model’s trade-off inclusion is denoted above the pair of plots by the double-sided arrow between traits. In each pair of plots the left panel is the curve representing optimal μ (fitness maximizing) across cycle period T , and right is optimal f across T . First column of paired plots contains models with single trade-offs, second column models with secondary trade-offs (but only ones that include μ or f out of all possible combinations among the four traits) and the last column the one model with tertiary trade-offs in which μ and f trade off with each other and with their respective stage mortalities d and γ . All realizations in this figure were run with $S_A > S_J$ (0.9, 0.6), which represent stage-specific (Adults vs. Juveniles) mortalities associated with cyclical disturbance. Magnitude of $S_A > S_J$ does not qualitatively change shapes of optimality curves. 96

Figure SI-1.2 Landscapes of log-transformed absolute fitness (eigenvalue of P) as opposed to relative fitness (normalized per T , as in Figure 2 in main text). Areas of $\log(\lambda) < 0$ would represent negative long-term population growth, therefore potential troughs in evolutionary trajectories. These areas are shown in gray, appearing in the bottom-left corner of the μ landscape and top-left corner of the f landscape. Curves of optimal life history across T are identical to those in relative fitness landscapes, and do not cross areas of $\log(\lambda) < 0$. The general incline in $\log(\lambda)$ as T increases is a result of higher long-term population growth due to less frequent disturbances. 97

Figure SI-1.3 High tide periodicity regimes in Neah Bay (A) and Friday Harbor (B) in northern Washington, which are near the mouth of and further inside the Strait of Juan de Fuca respectively. Data are hourly tide heights from NOAA’s National Data Buoy Center (Stations # 9449880 and # 9443090 respectively). Red lines that bound red shaded areas show typical range of heights where *T. californicus* populations are found on rocky shores. Yellow triangles show hypothetical disturbance events when high tide reaches height of a *T. californicus* pool, to illustrate that pools in Neah Bay are generally subject to longer periods and a wider spectrum of periods, and pools in Friday Harbor are generally subject to shorter periods. Disturbance events generally induce higher mortality in juveniles than adults (C), incurring not only population decline but also structural perturbation. 98

Figure SI-1.4 Temperature regimes of sample populations plotted against pools’ tidal disturbance periods (data in Table S1), between June – September 2017. Point is mean daily mean temperature, and line spans mean daily minimum and mean daily maximum temperature per

pool. Blue curve is second order polynomial fit on mean daily means. Generalized linear model (Mean daily mean \sim Period) showed non-significant difference across pools ($p = 0.28$). 99

Figure SI-1.5 Observed trade-offs between μ and f per mother in each population. Each point is a pair of a mother (used for f measurement) and her clutch (used for μ measurement), and 19 independent populations are represented by different colors. Dashed black line is the regression of μ against f across all populations. 100

Figure SI-2.1 Permutation distribution used to calculate the p-value of the disparity between intrapopulation maturation rate variances of deterministic Fast and Slow treatment populations. 106

Figure SI-2.2 Permutation distribution used to calculate the p-value of the disparity between intrapopulation fecundity variances of deterministic Fast and Slow treatment populations. 106

Figure SI-2.3 Permutation distribution used to calculate the p-value of the disparity between intrapopulation maturation rate variances of deterministic and stochastic Slow treatment populations. 107

Figure SI-2.4 Permutation distribution used to calculate the p-value of the disparity between intrapopulation fecundity variances of deterministic and stochastic Slow treatment populations. 107

Figure SI-2.5 Phenotypic measurements from selection experiment. Colored scatter points show individual measurements, and black dots with bars show mean \pm sd of each replicate population. Panels show replicate populations of each treatment. 108

Figure SI-2.6 Intrapopulation variance trajectories of fecundity (f) and maturation rate (μ) in deterministic and stochastic simulation iterations. The deterministic panels (first and third rows; panels A, E & I, and C, G & K) are identical to Fig. 4 of main text. The second and fourth rows (panels B, F & J, and D, H & L) are the stochastic analogs. Note that in panels J and L, there is only one treatment, Stochastic Slow. 110

Figure SI-2.7 Simulation endpoint variances (identical data as second column of Fig. SI-2.6, presented for easier visual comparisons across treatments). 111

Figure SI-2.8 Stage-structure dynamics in deterministically and stochastically slow and fast regimes in one representative realization of the simulation. 112

Figure SI-2.9 Population size dynamics in deterministically and stochastically slow and fast regimes in one representative realization of the simulation. 112

List of Tables

Table 1.1 Cyclical phenological patterns exist on various organizational scales of natural systems, within bounded spans of time such as a year or climatic growing seasons.	13
Table 3.1 Comparing intrapopulation phenotypic variances among experimental populations. Hypothesis testing with Monte Carlo permutation showed that intrapopulation variances of both traits were significantly different between Fast and Slow treatments across replicate populations (p -values under significance level $\alpha = 0.05$ in bold). However, variances under Slow and Stochastic Slow treatments were not significantly different.	70
Table SI-1.1 Temperature regimes of all 19 sample pools decomposed into mean daily min, mean daily mean, and mean daily max (plotted in Fig. S1). Population # is arbitrary codes of HOBO temperature loggers that were used to obscure association of each pool with its region or disturbance regime while conducting analyses. “FH” is Friday Harbor and “NB” is Neah Bay. Period is result of time series analysis for each pool’s 5-minute interval temperature data over the summer of 2017 that detected signals of wave disturbance and their intervals.	101
Table SI-1.2 Log-likelihoods of all models, obtained by maximum likelihood search through the space of $S_A \geq S_J$ (stage-specific mortalities associated with cyclical disturbance), while simultaneously fitting μ and f . Arrows denote trade-offs between life history traits. Model variants have different trade-off inclusions, but have the same number of estimated parameters because linear trade-offs were included computationally by setting parameter ranges of those traits in opposing (increasing vs. decreasing) order. Therefore model comparison criteria that penalize number of parameters were not needed. Highlighted (last model) is the best (likelihood-maximizing) model, which is reproduced as Figure 2 in the main text.	102
Table SI-2.1 Tests of differences in phenotypic means at the replicate population level. P-values are from two-tailed nonparametric Mann-Whitney tests using population means (black dots in Fig. SI-2.5).	109
Table SI-2.2 Comparisons of intrapopulation phenotypic variances between simulation realizations. Welch’s two-sample t-tests with log-transformed measures of variance showed strong differences between Fast and Slow regimes for both traits, both in statistical significance and magnitude. Deterministic and stochastic analogs produced smaller, and less significant differences in intrapopulation variance overall (though more significant for μ than f).	111

Acknowledgments

I would like to thank my PhD committee for challenging, encouraging, and supporting me. First, I thank my adviser Tim Wootton for always keeping an open door, both literally and figuratively. Feeling genuinely comfortable walking into that corner of the 4th floor of the Zoology building to chat about any question I was thinking through was a great joy. His broad knowledge was inspiring and helpful, both in the field and in the lab. Our three-hour lunch chats and weekly milkshake sessions will be missed. I thank Greg Dwyer for teaching me how to model, and providing some important lifelines early on in my PhD. His mathematical intuition and clear style of communicating quantitative concepts was refreshing and at times critically helpful, both intellectually and emotionally. I am grateful to Mercedes Pascual for being a perpetual fountain of good ideas, and often staying behind longer after committee meetings to dig deeper into ideas. She was a master at connecting the dots, which was invaluable when things felt particularly hazy in my mind. Cathy Pfister's positive and passionate spirit gave me a real sense in the beginning that I could do good research; this is critical for graduate students and does not go unnoticed. I am very grateful for her continued dedication to me and other students. I thank Trevor Price for relentlessly pushing me to be a more precise thinker. He was simultaneously sharply critical and immensely encouraging, which helped me to mature as a scientist and enjoy my time in graduate school. I will miss sharing pitchers with Trevor at Jimmy's, while debating about the definition of phenology.

Many colleagues and collaborators outside of the University of Chicago helped broaden my horizon. I would like to thank Dave Iles, who has been a great intellectual and personal friend since my undergraduate arctic fieldwork days. Eric Post at UC Davis has become an important mentor and collaborator during my PhD years. Our many philosophical discussions about the dimension of time and how organisms use it have energized me over and over again. I would like

to thank Roberto Salguero-Gómez, who will be my postdoc supervisor at Oxford, for being a great colleague and mentor. He has graciously welcomed me into the lab virtually, which was an immense source of joy and hope during the year we spent in quarantine during the COVID-19 pandemic of 2020-2021.

I am deeply grateful to Stephen Stearns, my mentor from my undergraduate days at Yale. I owe him much for introducing me to the wonderful world of life history theory, and planting in me a burning passion for chasing after ever bigger questions. He profoundly shaped the way I am as a scientist. I thank him for graciously continuing to critique many papers and applications through graduate school, and being an endless source of personal and intellectual inspiration.

My time in Chicago was joyous primarily because of the irreplaceable friends I made there. Among many, I especially thank Charles Washington III, Allison Haungs, Joe Marcus, Manny Rocha, Gabriel Vargas, Connie de la Fuente, Katherine Silliman, Joel Mercado-Díaz, Mark Bitter, Cassie Halls, Arjun Biddanda, Haley Jones, and Wynn Sullivan for the sweet memories. I was also incredibly lucky to have the support of friends from Toronto and college who were far away during graduate school but continued to be crucial fixtures in my life: Andrew Marburg, Will Kronick, Evan Frondorf, Henry Davidge, Greg Santoro, Thomas Rokholt, Ira Slomski-Pritz, Dan Hughes, Graham Clark, Lesley Tulipano, and Ishaan Kumar. I thank them for visiting me during grad school, listening to me ramble on about nature, and the deep friendships that don't seem to fade.

I thank Katherine Lawrence for being an endlessly loving support figure. I am inspired everyday by her kindness, intellect, and generosity. I thank my family for providing me with all the foundations for an enjoyable life. I am lucky to benefit from their sacrifices and unconditional support; I am forever grateful.

Introduction

Seasons are central to life on Earth. Indeed, the fixed 365.25-day harmonic oscillation of the physical environment preceded the origin of life itself, and has shaped its evolution globally ever since. However, zooming in and out in scale, we find that annual seasons are but one example of a more fundamental theme that temporally structures nature: that all environments fluctuate cyclically on scales such as daily, tidal, seasonal, and even decadal.

Organisms tend to schedule their life cycles—or 'life-histories'—to fit with the cycles of the physical environments in which they reside. At the seasonal timescale, this familiar timing of biological activity is called phenology. Shifts in phenology are now deemed the most conspicuous, most rapid, and most widely documented consequence of global climate change. From the ever-growing body of observational studies of phenological change emerges one clear message: effect sizes and even direction of phenological change are extremely incongruent between populations and species. For instance, two closely-related flowering plant species residing in the same habitat, undergoing the same seasonal change, often show divergent evolutionary responses where one flowers earlier in the season, and the other later. We understand little about life-cycle adaptations to environmental cycles. As seasons are arguably the best studied scale of environmental cycles, we understand even less about the other scales that surround us everywhere such as daily, tidal, and decadal.

Correlative and observational studies, while important for the specific system under investigation, offer limited insight into the deep forces of causality such as the influence of environmental cycles on life cycles. Incongruent phenological shifts offer a good example. Observational studies of phenological shifts typically associate local environmental change to

change in phenological traits, necessarily making each explanation proximate and unfocused on the forces shared by all systems that produced the wonderful explosion of life-history, behavioral, plastic, social, and genetic mechanisms organisms have employed, through the history of life, to survive in a cyclical world. At the outset of my doctoral research I asked the question: “what is the fundamental evolutionary force driving the need for such diverse innovations across the tree of life?”

A push towards a more ultimate causality perspective, which is necessarily simple but flexible, is a way to break out of the box of system-specific inquiry to tackle such a ubiquitous, fundamental, and urgent topic more directly. The goal of developing simple theory is not to explain every system. Rather, simple theory of a more ultimate causality is an exercise in formulating a null model, which is conspicuously absent in the discipline of phenology, and evolution in cyclical environments more broadly. Without a null model, we currently cannot argue precisely why certain observed changes like phenological shifts should be interpreted as surprising. I believed that it was worth spending my entire doctoral research, and perhaps my whole career, trying to understand how environmental cycles at multiple scales have shaped the temporal patterns of life since life began.

My doctoral work consists of a three-pronged approach of theory, fieldwork, and experiment. Striving to formulate a simple but flexible theory, I constructed a species-agnostic and scalable framework of life-history evolution in cyclical environments. Field and experimental work was based on the species-agnostic model, but tailored for the specific system of marine intertidal copepod *Tigriopus Californicus*. The goals of the field and experimental work were always to test the basic assumptions and dynamics of the theory, with an eye towards general applicability.

Before delving into the above three elements, Chapter 1 is a synthesis of theoretical concepts surrounding evolutionary phenological change in nature. We present a framework that ties together disparate cases of shifts and generates testable questions about selective forces, beyond reviewing ecological evidence of phenology. We build three sequential arguments: 1) Currently, phenology lacks a standard definition amenable for evolutionary theory. We offer one grounded in the idea that recurrent windows of time in natural systems such as seasons constitute a fitness-related dimension, and that phenological evolution is the process of optimizing the use of that dimension. We draw analogies from the more familiar examination of the spatial dimension in ecology and evolution, and review recent studies from which this perspective emerges. 2) We outline eco-evolutionary forces that shape the scheduling of life cycle events at the single-species level. We describe how quantitative tools from the disciplines of evolutionary demography and life-history theory can help study the evolution of holistic life-cycle schedules, moving beyond idiosyncratic examination of phenological traits. 3) We discuss how interspecific interactions shape the divergent evolution of species' phenologies in ecological communities: interactions such as mutualisms promote co-occurrence in time, and competition for temporal resources promotes asynchrony between coexisting species. We offer a future outlook on drivers and consequences of phenological evolution in multispecies communities under novel climatic conditions.

Chapter 2 consists of two parts. First, I formulate a mathematical model to explore how ecological processes (population dynamics and changes in the underlying environmental cycle) influence the evolution of life history strategies. Notably, this approach is scale-free in that it can be applied to daily, tidal, seasonal, multiannual cycles, or any period length in between, and is easily adjustable for any species of interest given simple parameterization. I discuss the conceptual implications of the theory as it connects to the literatures of life-history evolution and population

ecology. Then, I demonstrate the model framework's power by parameterizing it for the marine intertidal copepod *Tigriopus californicus*, for which I determined data can be accrued at amounts and speeds that are unusually high for life-history studies of wild populations. I show that the theoretical framework had surprisingly strong predictive power in explaining patterns of life-history variation in wild populations.

Chapter 3 also consists of two integrative approaches. First, to more rigorously test how cyclical perturbations shape moments of the distribution of life history traits in populations, I conducted a long-term selection experiment with *T. californicus* populations in the laboratory. I show that cycle periodicity is a strong driver of intrapopulation trait variance—even more so than random noise in the environment—which adds a novel contribution to the popular topic of how phenotypic variation is maintained in nature, as well as a possible first theoretical explanation of why so much phenological divergence is observed today under climate change. To strengthen the link between theory and experiment, I conduct an agent-based simulation study that corroborates the finding that slower environmental cycles increase life history variation in populations.

Finally, in a fourth and concluding chapter I synthesize what I have learned about life history evolution in cyclical environments, and reemphasize the broad relevance of this pursuit across systems and temporal scales. I illustrate a final simple model to demonstrate why cyclical fluctuations of the environment is different from other fluctuation modes for evolutionary considerations, and how these considerations might be useful for gaining a deeper understanding of a fundamental theme in nature.

1 Phenological patterns and their evolution on a cyclical Earth

1.1 ABSTRACT

Phenology—the seasonal timing of biological events—is a common feature of life across ecosystems, and its shifts are the most widely documented consequence of climate change around the planet. Yet, we still lack a general understanding of the selection pressures that drive evolutionary change in the phenology of individuals, populations, or species. Most studies have associated proximate environmental variables with phenological responses in ways that are case-specific, making it difficult to contextualize observed changes against an evolutionary predictive framework. At the very least, we need null theories of phenological evolution that will help organize the overwhelming literature of phenological change in a systematic manner and distinguish when cases are surprising, and why. To do so, it is important to first explicitly recognize that time is a fitness-related dimension, and that phenology can be defined as recurrent patterns contained within time windows set by fundamental oscillations in the environment (e.g. seasons), regardless of scale or system. Within this framework, we identify clear opportunities for developing and testing theories of phenological selection pressures—borrowing tools from demography, life-history evolution, and community ecology—to synthesize a first-principles understanding of this ubiquitous process across the planet.

1.2 INTRODUCTION

Phenology—the seasonal timing of biological events on scales ranging from individual life history dynamics to global cycles—is a universal feature across plants and animals, from ecosystems (e.g. insect emergence, flowering, migration) to human systems (e.g. agriculture) (Schwartz 2003; Cleland et al. 2007; Forrest and Miller-Rushing 2010). This is perhaps unsurprising considering that the revolution of the Earth around the Sun preceded the origin of life itself and has shaped its evolution ever since. Phenology is commonly investigated as a phenomenon that responds dynamically to climate change (Forrest and Miller-Rushing 2010; Visser et al. 2010). But explanations of phenological change are typically system-specific and centered around idiosyncratic cues and responses; this focus has not been matched by developments of a higher-order understanding of selective rules behind the near-global existence of phenology and its recent changes (Williams et al. 2017; Kharouba and Wolkovich 2020). A first-principles approach to phenology is urgently needed to synthesize and contextualize the large body of disparate reports of phenological divergence unfolding under climate change, and to produce a systematic suite of testable hypotheses for its eco-evolutionary drivers.

It is worth emphasizing that phenology—regardless of scale or system—is distinctly a description of repetitive patterns in the dimension of time (Fig. 1.1). Historically, spatial pattern-thinking has inspired many fundamental frameworks in ecology and evolution from island biogeography (MacArthur and Wilson 1967) to regional-local community hierarchies (Ricklefs 1987) to species ranges (Guisan and Zimmermann 2000), perhaps due to the immediate obviousness of spatial patterns. Decades of rigorous phenological observations show that there are repeatable and predictable biological patterns in the dimension of time. The Earth’s physical environment is structured by temporal cycles especially at the seasonal scale, even in

comparatively less seasonal environments such as the Tropics (van Schaik et al. 1993). Such physical cycles frame the windows for predictable repetitions of biological dynamics such as seasonal timing of an individual's life history event (e.g. emergence, flowering, migration), oscillations in the number of individuals in a population expressing such a trait, or in the number of species engaged in expressing such a trait.

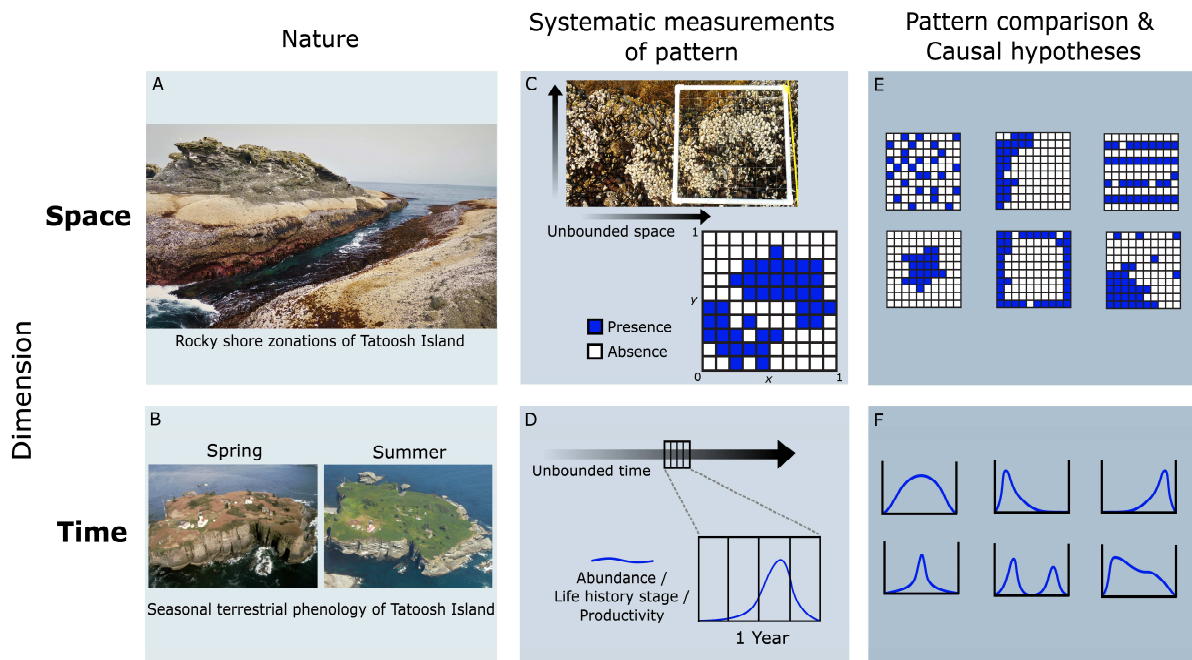


Figure 1.1 Distribution patterns in finite units of space or time. (A) Repeated patterns in space are often innately obvious to human observers, such as zonation of rocky shore intertidal communities, even if space in nature is realistically messy and unbounded. (B) Repeated patterns in time, such as seasonal phenology, can be seen over longer observations. (C) Patterns can only be defined and quantitatively measured given finite boundaries. In space, standardized delineations such as transects and grids are commonplace. (D) Just as in space, one must delineate unbounded time into relevant units such as years or climatic growing seasons to quantify time points occupied by phenological expression. (E) Only within standardized arenas of measurement are comparative studies possible and can eco-evolutionary theories of how patterns form and change be developed and tested. (F) Similarly, an explicit view of timing patterns within standardized time windows sets the basis for systematic hypotheses of how phenology is shaped by ecological and evolutionary forces.

Climate change alters phenologies through two modes of influence. The first is overall warming (Piao et al. 2019), *e.g.* increases in mean annual temperature, which influences rates of biological processes such as development. Consequences are well documented in plants on large scales such as the latitudinal gradient of phenological advancement rates across the Northern Hemisphere (Post et al. 2018). Research on phenological shifts has disproportionately focused on warming, at least in part due to the conventional practices of measuring annual averages of temperature data. The second takes a view that entire thermal or ‘climatic’ growing seasons (*e.g.* the continuous frost-free period of the year) are being extended as a consequence of warming, demonstrated by conspicuous trends such as earlier springs (Linderholm 2006; Kukul and Irmak 2018; Richardson et al. 2018; Piao et al. 2020). Importantly, the climatic growing season is a period when biological activity is favorable (Varpe 2017), especially for high latitude or altitude zones. Thus, extended climatic growing seasons represent a warp in the temporal template available for biological life cycles, local population dynamics, and larger scale ecosystem processes. There is mounting evidence that the warping of the seasonal time window induces evolution of individual phenological traits (Varpe 2017; Williams et al. 2017; Post 2019), and whole durations of phenophases (Ehrlén 2015).

What arises from operationalizing phenology as patterns within finite—and recurrent—windows of time, and overwhelming evidence that the warping of seasonal windows induces heritable change in the way organisms use time, is a view that time is a fitness-related dimension in its own right. This view provides the first important step towards conceptualizing general selective rules of phenology.

A complex puzzle that continues to draw researchers to phenology is that the same change in seasonal parameters, such as growing season length, often induces quite different phenological

shifts among organisms occupying the same habitat in both direction (when) and magnitude (by how much), causing what are known as phenological mismatches. These discrepancies are seen among individuals of the same species, which perturbs the standing variation of phenological traits (Miller-Rushing et al. 2010), among different traits in a single species, such as early-life traits shifting more than late-life traits (Post 2019), and among species in interactive communities (CaraDonna et al. 2014). Longer climatic growing seasons are not necessarily beneficial, nor do they have the same evolutionary consequence for different populations and species, due to complex physiological trade-offs within and between seasons, and nonlinear dynamics of populations over multiple generations and years. For instance, longer growing seasons have benefited some species [e.g. orchids in Norway (Sletvold and Ågren 2015) or yellow-bellied marmots in the US (Ozgul et al. 2010)], while spelled disaster for others [e.g. mustard white butterflies in the US (Kerr et al. 2020)]. It is currently difficult to generalize the long-term evolutionary consequences of seasonality change for phenological change. Fortunately, we are now in an age of immense phenological data from around the world that both urgently require causal synthesis, and make it possible.

We aim to articulate a timely framework to organize the higher-level causes of phenology and its changes. In our first section, we will expound on the conceptualization of time as a fitness-related dimension. Drawing analogies from spatially-oriented thinking, we highlight that treating the dimension of time in meaningfully bounded units, instead of as a boundless axis, enables synthesis and comparison of phenomena across systems. Then, we identify clear opportunities to study selection pressures driving phenological patterns, first at the scale of individuals and populations, and then at the scale of ecological communities in which interspecific interactions produce and maintain phenological diversity. Our overarching goal in this synthesis is to introduce

theorists to the interesting and unsolved questions about phenological selection pressures, and invite empiricists to test hypotheses of phenological causality to advance cross-system understanding.

1.3 GLOSSARY OF ESSENTIAL TERMS

- **Phenological shift:** change in the timing or phase duration of life cycle schedules within the context of geophysically fixed annual oscillations in the environment
- **Eco-evolutionary dynamics:** the concurrent and reciprocal dynamics of ecological and evolutionary processes where one shapes the context of the other, usually described as a feedback
- **Phenophase:** the duration of a categorically distinct phase of a life cycle, such as adolescence or reproductive period
- **Life-history evolution:** the evolution of the holistic suite of life cycle traits in the context of the ecology of populations as well as predictable fluctuations in the environment
- **Evolutionary demography:** selection dynamics that produce, as well as directly result from dynamics in the size and structure (proportions of stages, ages, sizes or sexes) of populations
- **Proximate phenological causality:** system-specific triggers that induce the expression of phenological traits
- **Ultimate phenological causality:** broad evolutionary forces that influence the seasonal timing of universal life-history traits such as birth, growth, reproduction, and death, considering that the timing of each trait contributes to fitness and all are constrained by trade-offs with one another (e.g. earlier birth may incur costs on growth)

1.4 PHENOLOGY: DELINEATING THE DIMENSION OF TIME TO STANDARDIZE CYCLICAL PATTERNS

First, it is crucial to explicitly recognize that annual ‘phenological cycles’ are different from emergent phenomenological cycles that arise from systems dynamics (e.g. predator-prey cycles) or Markovian transition processes (e.g. ecological succession). Instead, phenological patterns are adapted strategies repeatedly manifested within periods of geophysical environmental cycles. This is particularly clear in high latitude environments where winters largely induce biological dormancy and spring marks a new iteration of phenological sequences. Studying the selective causality of phenology first requires defining phenology as patterns repeated across subsequent finite windows of time (Fig. 1.1).

Patterns, in any dimension, can only be quantified and systematically compared when measured within the context of defined boundaries and scales. Drawing analogies from the more familiar spatial dimension helps crystallize this point (Fig. 1.1). Ecologists readily discretize infinite space into appropriately sized frames to set the stage for the question at hand even though the chosen delineation is often imperfect, and always arbitrary (Levin 1992). Consider a quadrat or transect: we impose a grid or line on nature at a manageable size, and use statistical tools to translate what we encounter on it to an idea of how entities are distributed in space. We can take this ruler anywhere in the world, follow the same sampling method, and thus systematically compare patterns between systems. Finite spatial delineations enable human observers to quantify, understand, and compare patterns, though a vector crossing the surface of a spherical planet is in reality infinite. Similarly, while time is in reality boundless, phenological adaptation can only be quantified when measured within bounds such as a calendar year.

In fact, a calendar year is a much more physically meaningful unit than a convenient

delineation of time. While correlated cycles such as temperature and precipitation in ecosystems are variable, a year is an example of a ‘phase-locked oscillation’ in the language of physics, whose cycle is externally fixed by the planetary rotation at least on scales relevant for evolution. Within each iteration of a calendar year, individual organisms follow sequences of life-cycle transitions, populations exhibit individual variations in these transition schedules, and communities display turnover in species composition (Table 1), all in a reasonably predictable manner. While each annual period is but one snapshot sample of a practically infinite unfolding event (e.g. population dynamics, community composition changes), it provides a standard ruler of the temporal dimension that allows iteration-to-iteration, as well as system-to-system comparisons (Fig. 1.2). What is relatively underdeveloped is a null model of how such iterative patterns should evolve. A null model provides the standard for knowing when a case is surprising and why; then, proving the null model wrong with data helps formulate better models. Much of today’s interpretation of phenological evolution happens independent of a structured theoretical framework (Kharouba and Wolkovich 2020).

Before moving forward to a discussion about phenological selection pressures, two caveats are crucial when one attempts to infer the evolutionary processes that produce patterns within bounded and repeating time windows: *temporal contingency* in biological and abiotic dynamics, and *scale relativity* between life-cycles and seasonal cycles.

Scale	Measured Patterns	Potential causal mechanisms
Individual organisms	<p>Life history schedule such as timing of birth, reproduction, and death</p> <p>Duration of phenophases</p>	<p>Physiological trade-offs between past, current, and future life-history traits</p> <p>Seasonal resource pulses and environmental oscillations</p> <p>Plastic responses to near-past environmental conditions</p>
Populations	<p>Peak timing of life history events</p> <p>Inter-individual variations in timing, manifested as oscillations in number of individuals expressing a life history trait</p>	<p>Evolved optimal timing governed by within- and across-generational trade-offs (e.g. parent-offspring conflict between reproduction and survival)</p> <p>Demographic stochasticity (variation in birth and death rates)</p> <p>Variation in resource acquisition rate and allocation decisions among individuals, including bet-hedging strategies</p> <p>Standing variation shaped by selection</p>
Communities	<p>Turnover of observed species through time</p> <p>No-analog communities observed at different points through the course of a year</p>	<p>Predator-prey tracking of periodic activity</p> <p>Symbiotic synchrony of periodic activity</p> <p>Competitive avoidance of periodic activity</p>

Table 1.1 Cyclical phenological patterns exist on various organizational scales of natural systems, within bounded spans of time such as a year or climatic growing seasons.

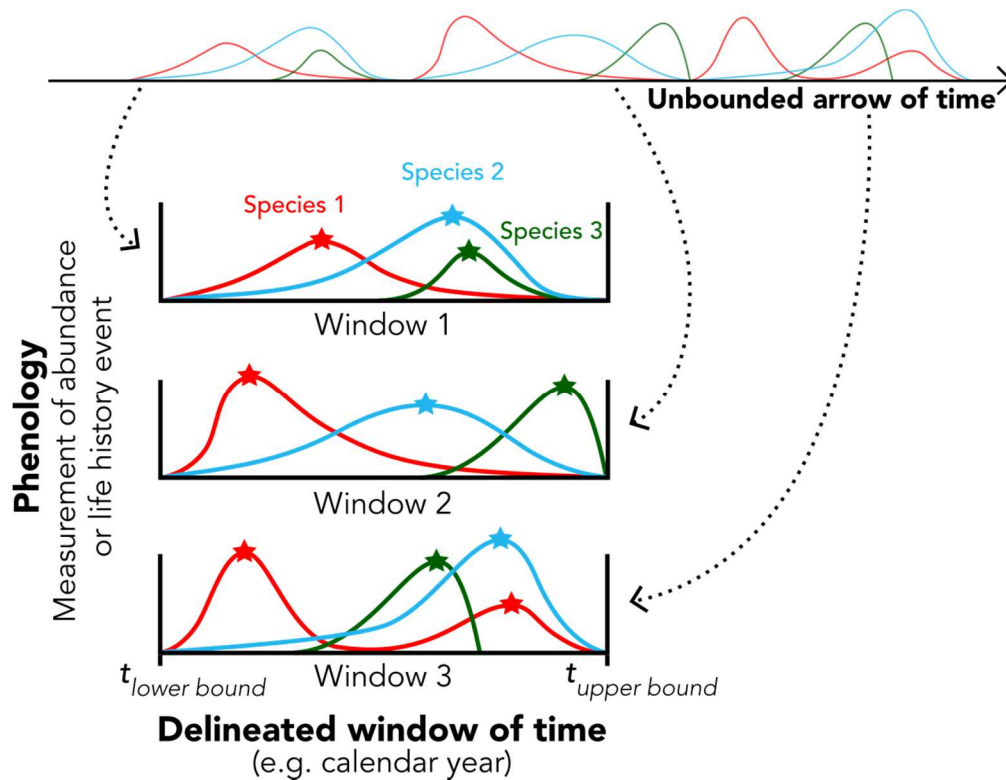


Figure 1.2 Phenology is a study of repeated patterns of events in the dimension of time. Delimiting the continuous arrow of time into natural units such as years or climatic growing seasons allows observers to compare patterns between cycle periods and quantify change such as phenological shifts. Shapes of seasonal patterns (colored curves), peak dates (location of stars), or number of peaks (e.g. species 1 has two peaks in Window 3) can be taken as measures of change. Systematic quantification and comparisons then provide the necessary groundwork for studying ecological and evolutionary causality.

1.4.1 Temporal contingency

Phenological patterns in future seasonal time windows are dependent on patterns in past windows, importantly with respect to both the physical environmental fluctuations and the biological dynamics simultaneously. The identification and consequences of anisotropic (unidirectional) temporal dependencies within a system, i.e. autocorrelation, have been extensively studied in the contexts of population ecology and dynamical systems (Sugihara and May 1990; Vasseur and Yodzis 2004), and life-history evolution (Metcalf and Koons 2007; Paniw et al. 2018). However, the effect of such temporal autocorrelation in the physical environment on the evolution of iterative

phenological timing from year to year is much less well understood. In evolutionarily explicit models of phenology, both the temporal contingency of current biological functions on past events (e.g. energy expenditure in early life negatively impacting future investments into growth, survival, or reproduction; Fig. 1.2), and of the current abiotic environment on past environments (e.g. climate change causing overall upward trends in temperature, producing a positive autocorrelation) must be simultaneously considered. One clear starting point is to adopt modeling methods developed in evolutionary demography and life history theory which set up the environmental regime and biological dynamics separately, as we will outline in the following section.

1.4.2 Scale relativity

A collection of species that exhibits a repeatable sequence of phenological or compositional turnover year to year in the same space may consist of strikingly different generation times or activity schedules; hence, sympatric species' population dynamics actually operate on very different scales of time [e.g. community of phytoplankton and zooplankton in Lake Washington, USA shows predictably synchronized seasonal temporal patterns but the two trophic levels are characterized by very different generation times (Winder and Schindler 2004)]. Annual organisms fit one generation within one period of an annual cycle, whereas perennial organisms experience multiple periods per generation, and shorter-lived organisms fit multiple generations within an annual cycle (Stearns 1976). Temporal scale discrepancies among species' population dynamics may be one source of the persistent tendency to study each species' seasonal phenology independently without a standardized evolutionary framework (Jenouvrier and Visser 2011; Reed et al. 2015). However, it helps to remember that such scale incongruencies among species are almost always present in studies of spatial patterns. For instance, a collection of species found

within a delineated space represents an eclectic mix of species-specific spatial range sizes. Local patterns are influenced by processes larger than the scope of study, which are invisible to the local observer. Analogously, longer processes are invisible to the ‘brief’ observer of natural systems. The key point is that delineation of a dimension into bounded units facilitates conceptual organization and construction of a standardized framework. The goal is to develop principled theories that can explain why predictable cyclical patterns are so common within and across natural systems despite the wide discrepancies in species’ temporal scales of life histories and population dynamics.

Towards that goal, we ask a general guiding question: how do organisms that live in periodically changing environments and ecological systems evolve to occupy non-random portions of each period? We discuss two broadly applicable hierarchies: single species phenological evolution, and community interactions that influence multiple coexisting phenologies.

1.5 EVOLUTION OF PHENOLOGIES

Analyzing phenological traits independently oversimplifies the manner in which life-cycles are structured by trade-offs and contingencies between life history traits (Inouye 2008; Post et al. 2008) (Fig. 1.3). The expression of a trait is dependent on those that occurred earlier in the season as well as in previous seasons. Selection on traits therefore depends intimately on the covariance structures of holistic life-history strategies (Sheriff et al. 2011; Burghardt et al. 2015; Park 2019). Models that account for such covariance structures are typically exercises in optimization. They ask how the potential fitness benefits of a particular phenological timing such as flowering relative to the environmental cycle is balanced out by costs on fitness through trade-offs (Roff et al. 2006). Costs are incurred on an individual at the current moment in the form of decreased survival, or through any lag effects on the same individual via future survival or on its progeny in subsequent

generations. Life-history theory asks which of all possible combinations of interlinked traits would confer the highest fitness in the long run and eventually invade the population.

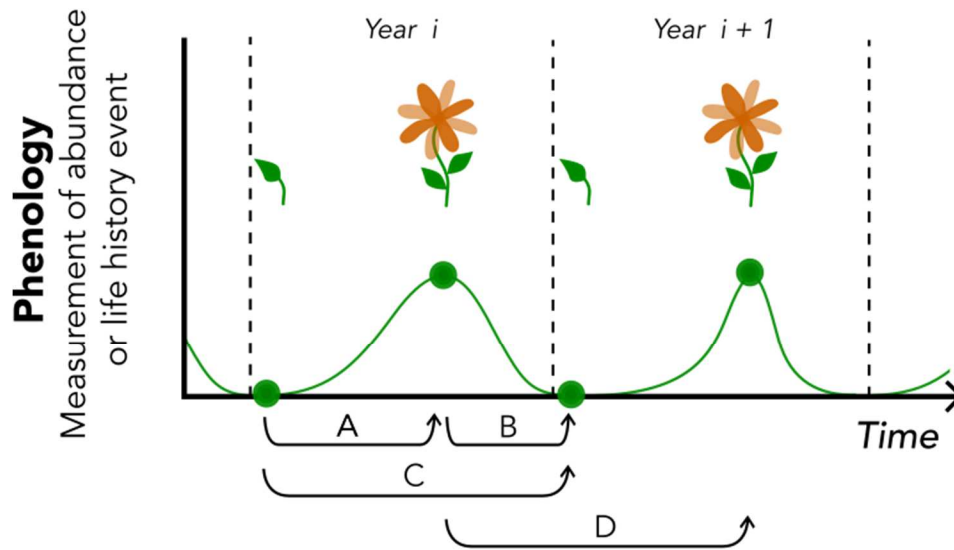
Although optimization approaches built upon assumptions of constant environments are powerful and widely used, theorists recognize that stochasticity in the environment can produce very different outcomes with respect to population dynamics and evolution (Koons et al. 2008, 2009; Tuljapurkar et al. 2009; Tuljapurkar 2013; Hastings et al. 2018). Stochastic demography has been applied to many interesting life-history and phenology questions (Caswell 2001). For example, decreased predictability of the environment may induce the evolution of bet-hedging strategies wherein risks of potentially ‘incorrect’ life-history timing are spread among individuals, maintaining multimodal or broad distributions of life-history strategies in the population (Metcalf and Koons 2007; Simons and Johnston 2006; Childs et al. 2010; Gremer and Venable 2014). Further refining our understanding of variability of the environment, recent work has investigated how the strength of temporal autocorrelation in stochastic environments influences life-history evolution (Metcalf and Koons 2007; Paniw et al. 2018).

However, the manner in which life-history timings are shaped by non-random cyclical temporal structures in the environment—such as those governed by Earth’s rotation around the sun which is geophysically locked—remains much less well understood theoretically (Lande et al. 2017). Specifically, we have limited knowledge of how structural parameters like amplitude or period of abiotic variables, beyond just how strongly those variables are autocorrelated through time, influence life-history evolution. Climate change is perturbing parameters of seasonal cycles



Figure 1.3 Disaster. High-tide wave disturbance brings unwelcome inconvenience to tidepool *Tigriopus californicus* populations, the field system that will be introduced in the subsequent chapters. Imaged here is a perspective study I conducted on Tatoosh Island, WA to gain more insight into how I myself might arrange my life history in such a setting. A major inconsistency was later identified that precluded any fair comparison between *Tigriopus* life history scheduling and mine, namely access to the tide table.

[e.g. longer growing seasons (Walther et al. 2002; Schwartz et al. 2006) and greater amplitudes of annual CO₂ cycle (Keeling et al. 1996)] and phenological timing around the planet. Understanding how parameters of cycles shape life-history evolution will help to explain and predict continued phenological shifts under future change (Park 2019).



Causal connections between time points in phenological cycles due to life history trade-offs and demographic contingencies within and across generations

Figure 1.4 The manner in which phenology evolves at the single-species level requires consideration of trade-offs and temporal contingencies both within an individual's life time and across generations. Phenology treated as a correlative response to meteorological forcing per year overlooks how evolution is shaped by trait covariance and demographic lag effects. Here we illustrate four examples of connections in phenological cycles across two adjacent years or generations. Curve shows fluctuations in abundance or event timing (peaks) which are typical representations of phenology. Green circles paired with pictorial representations of flower development denote points in the life-cycle, and arrows indicate correlative links between two points. A) Biological functions early in life such as development and growth can be negatively correlated with those later in life such as reproduction. B) Conversely, reproductive investment in one generation can influence the next generation's offspring performance. Success of the previous generation can also shape the standing genetic variation available for selection in the next generation. C) In some species, a proportion of offspring or seeds of a population will proceed to development while others enter diapause. These unrealized offspring carry over to subsequent years and influence population dynamics and selection landscapes in the future. D) If the timing of a phenological trait such as flowering is related to fitness in the context of the environment, selection can shape the frequency distribution of its mean in the population, balanced out by potentially antagonistic forces such as those connections represented by A, B, and C.

1.6 HOW DOES LIFE HISTORY EVOLUTION PRODUCE CYCLICALLY REPEATING PHENOLOGICAL PATTERNS?

Phenological timing is typically studied as a response variable to abiotic cues that are associated with seasonal transitions in the abiotic environment (e.g. temperature, snow melt, photoperiod, precipitation frequency). Responses to seasonal environmental variables constitute proximate phenological causality. Environmental cues often have tractable effects on the expression of phenotypic traits, and will continue to be important targets of research as cue timings will likely continue to shift and become more unpredictable under climate change (Forrest and Miller-Rushing 2010; Schär et al. 2004; Katz and Brown 1992). However, proximate investigations have fallen short of explaining or predicting phenological shifts in many cases; species or even individuals in the same space experiencing the same change in seasonal cycles often exhibit varied phenological shift trends (Post et al. 2008; Both et al. 2009; Primack et al. 2009; Thackeray et al. 2010, 2016; CaraDonna et al. 2014). These formerly surprising discrepancies appear to be commonplace as evidence grows, and confirm three notions: 1) there is of course no single optimal phenological timing for all species, 2) there is also no single optimal way for phenology to change in response to environmental change, and 3) investigating the correlative trait responses to environmental variables is not sufficient for understanding the selective pressure acting on phenological change. Correlative approaches typically cannot integrate responses across the lifespan to reveal their impact on lifetime reproductive success and evolution over multiple generations, and thus offer explanations of ultimate causality or generalized tools for predictions of unmeasured future phenological shifts. Most importantly, an evolutionarily grounded framework can allow one to quantify how unexpected the observed discrepancies in phenological shifts really are against null expectations. For instance, (Park 2019) theoretically showed that with

small differences in life-history trade-offs, individuals or species can have vastly different shifts in phenologies even when given the same change in environmental seasonality.

Life-history theory and evolutionary demography have consistently provided biologists with remarkable causal explanation power delivered by simple, species-agnostic frameworks (Stearns 1992; Caswell 2001). These frameworks consider fundamental traits that are universal across living organisms such as birth, growth, reproduction, and death. The classic models are free from species-specific assumptions [e.g. (Cole 1954; Gadgil and Bossert 1970; Law 1979; Michod 1979)], and draw broad conclusions about the direction in which life-history evolution should proceed if, for example, certain age classes of a population experience selective mortality. They have motivated decades of life-history research across vastly different systems (Reznick 1982; Stearns 1992; Stearns et al. 2000). The philosophy of such models is not to precisely explain every system but to provide a framework that defines null expectations, and one that can be flexibly parameterized by practitioners to study their specific systems.

There is general consensus that integration of life history theory and evolutionary demography into phenological research is necessary and timely, but efforts are so far nascent and disconnected (Kharouba and Wolkovich 2020). To streamline the path forward, we argue that the key benefits for phenology that these disciplines offer are modelling tools to deal with temporal contingencies within and across seasonal time windows. Namely, life-history models specify temporal contingency in two main forms: 1) an individual organism's current investments into biological functions influence future investments, and 2) biological investments in one generation have rippling consequences for future generations (Stearns 1989, 1992). Thus, selection on phenological timing within one seasonal window depends on selection in past and future seasonal windows (Fig. 1.3). Demographic theory integrates temporal contingencies in the numerical

dynamics of stage-/age-/size-/sex- structures of populations into selection dynamics. For example, age- or stage-structures of populations, as opposed to simply population size, influence population growth trajectories, as well as optimal vital rates (Caswell 2001). Calculations of selection on life-histories when such real structural complications are considered can be very different from when they are not considered (Tuljapurkar et al. 2009; Lande et al. 2017). Another real complication of natural populations that demographic models help deal with is that individuals in populations exhibit variations in phenological schedules. For example, sexes of the same species often have different courses of seasonal developmental sequences and are affected differently by change in seasonality. Seasonal synchrony of sexes is important for mating or even predator swamping (Ims 1990). For Scottish red deer, climate change has induced unequal advancements of phenological traits between males and females, leading to a contraction of their seasonal breeding window (Moyes et al. 2011). Further, different life stages of a single species can be differentially shifted by climate change. For example, in yellow-bellied marmots, advancements in dates of emergence from hibernation and weaning, but not of the onset of hibernation, led to the lengthening of their growing season, and to increases in body mass, reproduction, and population size (Ozgul et al. 2010).

Above examples of studies that incorporated life-history interdependencies and demographic structure into phenological analysis demonstrate that phenology is a highly evolutionary process. For example: phenological selection shapes the individual variation of life cycle schedules within a seasonal window. The life cycle decisions made in that seasonal window have consequences on the survival and life cycles of genotypes that make it to future seasons due to intergenerational life-history trade-offs. These genotypes then shape the standing variation of traits and population structure that form the raw material available for selection in future windows,

completing the eco-evolutionary loop. Such a demographically explicit conceptualization of phenological evolution, we believe, is one of the most obvious targets of theoretical progress.

In integrating phenological data with evolutionary theory, a crucial conceptual gap that remains to be bridged is one between how ‘rate’ evolves and how ‘timing’ evolves. *Rates* are the parameters typically manipulated in demographic and life-history models. Conceptions of rate, such as growth, force the theorist to confront the fact that all phenology-related traits require time for processes such as metabolism and development. For example, when a flowering event is detected, it represents the culmination of a series of upstream biological steps leading up to that point; these can be aggregated to express a rate to reach that point. Therefore, one should consider the correlated and sometimes antagonistic selection pressures involved prior to the detectable timing of an event, and this is done well with theory. But the actual *timing* of an event is often what affects intra- and interspecies interactions such as mating or predator avoidance, therefore a measurable point event that affects survival, and thus is potentially most ‘visible’ to selection (Forrest and Miller-Rushing 2010). Events like flowering reflect actual categorical change with a binomial property where timing is a measurable point in time. Likely for these reasons, data on timing dominate phenological studies [e.g. (Menzel et al. 2006)]. For annual organisms that can be assumed to start their lives in the beginning of each year, conceiving phenological patterns as adaptive occupations of temporal niches within seasonal time windows equates rate and timing (i.e. *fast-growers* mature *earlier* in a season). Our understanding of phenological evolution will be significantly improved with a better mathematical marriage of life-history rates and phenological timing for organisms beyond annuals.

1.7 HOW DO SPECIES INTERACTIONS PRODUCE AND MAINTAIN DIVERSE PHENOLOGIES IN THE SAME SPACE?

Phenological evolution occurs in the context of ecological communities. The challenge is to understand how periodic interactions between coexisting species influence each species' adaptive occupation of different portions of seasonal windows. Empirical evidence shows that different types of ecological interactions such as competition, invasion, or consumer-resource dynamics can alter the occurrence or phenotypic expression timing of species in a community. Broadly, periodic interactions can favor overlap (Fig. 1.4A) or segregation (Fig. 1.4B) of phenologies between two species within seasonal time windows. Mechanisms depend on context and history. For example, experimental reduction of plant species diversity in a serpentine grassland community in California, USA advanced the phenology of remaining species, suggesting an infilling of newly available temporal niches (Wolf et al. 2017). This suggests that competition may limit co-occurrence. Analogously, exotic plant species may invade a new community by exploiting early-season phenological niches in which competition by co-occurrence with native species is lower (Waterton and Cleland 2016). A similar pattern can be achieved through a consumer-resource dynamic: introduction of large vertebrate herbivores may have selected for advanced flowering time in forage species in the US Southwest because earlier flowering reduces herbivory-induced loss of reproductive structures (Smith et al. 2015). Mismatches in phenological shifts across trophic levels can have adverse effects on reproduction, survival and fitness of coexisting species, and cause rapid increases in extinction probability of populations (Simmonds et al. 2020) or health of whole ecosystems (Williams et al. 2017); some trophic links such as plant-pollinator pairs appear capable of advancing constituent phenologies fairly synchronously (Bartomeus et al. 2011; Post and Avery 2019), possibly suggesting that at least in some cases the selective forces on phenology imposed by species interactions are dominant over those imposed by single-species life history optimization. One fruitful avenue of theoretical advancement will be

to incorporate the various modes of periodic phenological interaction into models of single-species phenological evolution. Interactions can be treated as dynamic time-dependent parameters that modify fitness landscapes of each involved species. Viewing phenological communities as dynamical systems in this way might help explain many of the differential cases of phenological shifts that appear unintuitive when studied out of the context of the community.

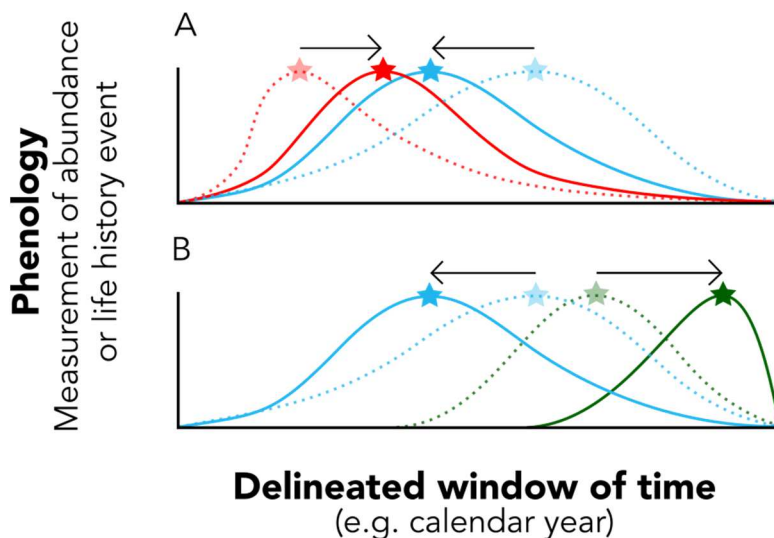


Figure 1.5 Community interactions promote phenological variation within bounded windows of time. In addition to external seasonal cues and internal mechanisms of optimization at the single-species level, ecological interactions can influence the phenologies of coexisting species in a community. Colored curves show hypothetical phenological curves of species, measured as change in abundance reflecting seasonal emergence or number of individuals expressing a trait such as flowering. Stars show peak phenology. Dashed curves show phenologies prior to shifts, and arrows show direction of shifts. Certain interactions may favor (A) co-occurrence between species, such as plant-pollinator interactions and other mutualistic relationships, and others (B) avoidance, such as competition for a time-related resource.

The key ecological consequence of the differential expansions, contractions, and shifts among species is that interaction potentials between the species change within seasonal time windows (Encinas-Viso et al. 2012; CaraDonna et al. 2014), and novel ‘*no-analog*’ communities (*sensu* (Williams and Jackson 2007)) form through the season. For example, a recent 12-year observational study of 14 co-existing vascular plant species at a low-Arctic study site in Greenland

revealed that differential advancement of spring emergence among the species (Post et al. 2016) increased temporal segregation of the early- and late-phenology species from other species (Post 2019). Among species of coexisting plants in a subalpine meadow in Colorado, USA, differential rates of advance of first, peak, and last flowering time have altered the phenological sequence and co-flowering patterns through the season (CaraDonna et al. 2014). Similar phenomena are now documented across a broad range of biological systems including butterflies (Gezon et al. 2018), anurans (Todd et al. 2010; Rudolf and McCrory 2018), vascular plants (CaraDonna et al. 2014; Hart and Salick 2018; Prevéy et al. 2019), and vertebrate herbivores (Post 2019). These cases of temporal shuffling of phenological communities highlight the issue that co-existence in the same space does not necessarily mean co-occurrence. Interaction potentials are as periodic as the occurrence of each species in seasonal systems, and are being perturbed under climate change. One important question that emerges—connected to the broader disciplines of species coexistence and biodiversity research—is how perturbations to multi-phenological systems influence interaction dynamics among species within seasonal time windows, and thus long-term ecological community stability and maintenance of phenological diversity.

1.8 IMPORTANT UNRESOLVED QUESTIONS

Within our framework of conceiving phenological phenomena as patterns of distribution in the dimension of time (Fig. 1), we propose a set of questions for theorists and empiricists moving forward:

- Are environmental cycles themselves agents of phenological selection? Does this perspective help explain phenological shifts in the context of global change, wherein parameters of environmental cycles are being altered?

- How do life cycle traits—which are intricately connected in time due to trait covariance and trade-offs—evolve upon a template of environmental cycles, which are themselves structured by temporal autocorrelation and lag effects? Recognizing connections among phenological traits, borrowing from life-history theory, will advance our understanding of phenological shifts beyond correlative approaches that focus on single traits. We have highlighted that marrying concepts of timing and rate in models will be important.
- Autocorrelation can occur at various temporal scales that may constructively or destructively interfere with seasonal cycles (e.g. monthly or multiannual cycles). How do multi-resonance autocorrelative regimes influence the evolution of seasonal phenology?
- Do phenologies of organisms with different numbers of generations per seasonal window evolve in fundamentally different ways, as the window expands, contracts, or becomes otherwise distorted (e.g. less predictable seasonal boundaries) by environmental change?
- How do different modes of adaptation (e.g. adaptive phenotypic plasticity; adaptive genetic change) influence the capacity for, speed of, and constraints on phenological change?
- How can we better integrate empirical approaches to enhance our general understanding of phenological evolution? As an example, can quantitative genetic / life history models that make probabilistic predictions about optimal phenology (e.g. reproductive timing) as a function of environmental cycle parameters (e.g. period of temperature fluctuations) be corroborated by genetic associations with associated traits in individuals in a population?
- How is the timing of a trait that is important from the perspective of the community (e.g. flowering) controlled simultaneously by life history optimization at the species level and periodic interactions with other species that favor co-occurrence or temporal segregation? Are

there general rules regarding if and when single-species evolution or multi-species interaction is a stronger driver of phenology in nature?

- How do changes in seasonal time windows alter interaction potentials in ecological communities, create novel no-analog communities in different portions of the season, and affect phenological diversity?

1.9 SUMMARY AND OUTLOOK

On a revolving planet where life has evolved in inherently oscillatory environments everywhere, phenology appears to be ubiquitous. Here we have argued for the need to investigate the deep selective pressures of phenology to help scaffold the overwhelming literature of disparate case studies. To do so, we make the case that general theory of the selective rules of phenology is lacking and is an important key for progress. The ubiquity of phenology simply warrants this investigation, but the speed, magnitude, and complexity with which phenology is shifting under climate change makes it urgent. Global change is associated with perturbations to the duration and predictability of biologically favorable seasonal windows. Perturbations to seasonal windows— analogous to spatial perturbation of habitats such as deforestation—are unravelling familiar phenological patterns contained within those windows (Fig. 1.1) such as species occurrence or activity times (CaraDonna et al. 2014; Post et al. 2016). Correlative approaches to explaining phenological changes across years using candidate meteorological variables yield limited lessons for a general understanding of such dynamic changes because even when the hunt for the best correlate is complete for a given system, the next system will require an independent list of assumptions and candidate drivers to test.

We have focused on phenotypic (life history) evolution to draw attention to general selection *pressures* acting on individuals, populations, and communities to enable cross-system understanding. Such pressures have led species to innovate a myriad of physiological, genetic, behavioral, plastic, and neuronal *mechanisms* to utilize the dimension of time to maximize evolutionary fitness; those rich literatures are discussed better elsewhere (Visser et al. 2010; Wilczek et al. 2010; Pau et al. 2011; Helm et al. 2013; Kaiser et al. 2016; Williams et al. 2017; Chmura et al. 2019). Our aim here is to ask why the seemingly universal need for such a diversity of innovations exists in the first place. We believe that streamlined progress can be made by explicitly recognizing that time is a fitness-related dimension, and that time can be delineated in bounded units that organize pattern in a systematic way such as years, or climatic growing seasons. We remind readers that convenient delineation of the spatial dimension is already foundational to ecology and evolution, and has produced much of the useful theories we use today. Building on our framework, the microevolutionary *process* of phenological evolution—for example how population genetic processes such as recombination and drift are constrained by the seasonally fluctuating rates of encounter among individuals, which limit periodic opportunities for mating and gene exchange—will be another obvious frontier of phenological understanding. Then, studying how all of those processes per species are simultaneously influenced by multiple interacting species in ecological communities is the next challenge. We have strived to distill key questions for future investigators, particularly those interested in developing general evolutionary theory. Simultaneously, empirical test of broad applicability of theory will be important going forward. Fortunately, global scale open-access phenological databases continue to grow rapidly, such as the USA National Phenology Network (www.usanpn.org) and the Pan-European

Phenology Database (www.pep725.eu), and will make such interdisciplinary and comparative investigations possible.

Finally, many general ideas about time windows we discussed reveal interesting theoretical questions fundamental to ecology and evolution of natural systems, beyond the temporal scale of seasons. While life history and phenological research have focused on the seasonal scale, cycles in the physical environment in fact exist on other temporal scales as well such as daily, tidal, and multiannual (e.g. El Niño-Southern Oscillation cycle), with ‘phenological’ scales to match [e.g. diel vertical migration of zooplankton (Lampert 1989)]. Geophysically-driven oscillations of the environment clearly constitute a pervasive theme of temporal structure and pattern in natural systems. Scalable theory of how organisms evolve to occupy meaningful windows of ecological time, as a function of the relative scales of such windows and generation time of species, would be a rich avenue of exploration beyond seasonal phenological understanding.

1.10 ACKNOWLEDGEMENTS

We thank CA Pfister, TD Price, SC Stearns, and JT Wootton for helpful discussions and improving earlier drafts. JSP was supported by NSF OCE 1851489, U.S. Department of Education GAANN Fellowship, and University of Chicago Donald Steiner Award; EP was supported by NSF OPP 1525636 and 1748052.

2 Cyclical environments drive variation in life history strategies: a general theory of cyclical phenology¹

2.1 ABSTRACT

Cycles, such as seasons or tides, characterize many systems in nature. Overwhelming evidence shows that climate change-driven alterations to environmental cycles—such as longer seasons—are associated with phenological shifts around the world, suggesting a deep link between environmental cycles and life cycles. However, general mechanisms of life history evolution in cyclical environments are still not well understood. Here I build a demographic framework and ask how life history strategies optimize fitness when the environment perturbs a structured population cyclically, and how strategies should change as cyclicity changes. I show that cycle periodicity alters optimality predictions of classic life history theory because repeated cycles have rippling selective consequences over time and generations. Notably, fitness landscapes that relate environmental cyclicity and life history optimality vary dramatically depending on which trade-offs govern a given species. The model tuned with known life history trade-offs in a marine intertidal copepod *T. californicus* successfully predicted the shape of life history variation across natural populations spanning a gradient of tidal periodicities. This framework shows how environmental cycles can drive life history variation—without complex assumptions of individual responses to cues such as temperature—thus expanding the range of life history diversity explained by theory and providing a basis for adaptive phenology.

¹ A version of this chapter has been published as: Park, J. S. 2019. Cyclical environments drive variation in life-history strategies: a general theory of cyclical phenology. *Proceedings of the Royal Society B: Biological Sciences* **286**:20190214.

2.2 INTRODUCTION

Natural populations in all systems must survive environmental fluctuations. Biologists have long known that a particularly common and powerful mode of fluctuations in nature is cyclical, such as seasons. Species around the planet exhibit predictable and sensitive life history transitions that are tightly associated with seasonal cycles, also referred to as phenology. Environmental cycles in fact occur beyond just the timescale of seasons, such as daily, tidal, lunar, flood, fire and decadal oscillations, and life histories of species are often associated with cycles at these timescales as well (Lampert 1989; Sponaugle and Cowen 1994; Post and Stenseth 1999; Keeley and Bond 1999; Schaubert et al. 2002; Lytle and Poff 2004). Despite the ubiquity of cycles in nature, and clear empirical evidence of the importance of cycles for life histories, we lack a general theory of how life history evolution is shaped by cycles.

Over the last few decades perturbations to environmental cycles due to climate change have driven dramatic life history changes such as phenological timing in many species (Post et al. 2001; Walther et al. 2002; Parmesan and Yohe 2003; Edwards and Richardson 2004; Parmesan 2006; Bradshaw and Holzapfel 2008; Cleland et al. 2007; Thackeray et al. 2010; Cohen et al. 2018). In fact, phenological shifts are widely regarded as the most conspicuous and rapid consequence of climate change across marine, freshwater, and terrestrial systems (Thackeray et al. 2010). Notably, different species' phenologies are shifting in different directions, creating phenological mismatches with profound consequences on ecosystem function and health (Post et al. 2001; Parmesan 2006; Post et al. 2008; Both et al. 2009; Chuine 2010; Richardson et al. 2010). Disparate case studies of shifts that typically invoke individual-level responses to environmental cues such as temperature may be limited in their potential to explain general evolutionary forces due to system-specific idiosyncrasies. On the trailing edge of rapidly accumulating empirical evidence of

shifts, questions regarding general mechanisms of life history evolution in cyclical environments have emerged to the forefront of theoretical population biology, biodiversity, and climate change science (Forrest and Miller-Rushing 2010; Visser et al. 2010; Lande et al. 2017).

A first step in understanding the mechanics of life history evolution in cyclical environments may be to conceptualize cycles as sequential arrivals of harsh conditions whose periodicity is not reciprocally affected by local ecological dynamics. An example is the arrival of winter in seasonal systems. A typical consequence of such cyclical events for a population is heightened mortality as well as some perturbation to population structure [e.g. seedling mortality in plants (Cook 1979)]. This consequence not only reduces population size at a given time, but also impacts the long-term trajectory and fitness of the population (Charlesworth 1994; Caswell 2001). It follows that, if periodic disturbance is an inherent feature of a habitat, fitness is determined by how well a resident population survives repeated demographic perturbations at regular intervals.

Population ecologists have long been interested in demographic dynamics in variable environments, including cyclically variable environments (Lande et al. 2017; Tuljapurkar 1985; Orzack 1993; Caswell and Trevisan 1994; Lytle 2001; Tuljapurkar et al. 2009; Koons et al. 2009). Life history theorists, on the other hand, have classically focused on how time-invariant (i.e. constant) perturbations on age-, size- or stage-classes of populations, mediated by trade-offs between biological processes, shape life history strategies broadly (Gadgil and Bossert 1970; Charnov and Schaffer 1973; Law 1979; Michod 1979; Stearns 1992). For example, theory predicts that heightened juvenile mortality should induce the evolution of reduced reproductive effort. Such predictions have been widely tested empirically, and effects are often strong, rapid, and heritable (Roff 1984; Hairston and Walton 1986; Reznick et al. 1996; Ernande et al. 2004; Olsen et al. 2004;

Walsh and Post 2011). So far, modern models of life history evolution that do incorporate time-variance in the environment have mainly focused on how optimality predictions are altered by stochasticity (i.e. randomly variable environments), which yield convenient analytical probabilistic conclusions (Lande et al. 2017; Koons et al. 2009; Orzack and Tuljapurkar 2001; Metcalf and Koons 2007; Childs et al. 2010). What is not well understood is how life histories are generally shaped by non-random cycles, despite biological attention to fundamentally cyclical environments such as seasonal systems (Lande et al. 2017), and the fact that parametric changes to cycles such as season length are repeatedly associated with life history changes across systems.

Here I explore the general relationship between periodicity of cycles and evolutionarily optimal life history strategy. Proximate triggers of phenological expression, such as plastic response to temperature cues, mechanistically vary widely across species and habitats (Forrest and Miller-Rushing 2010). By taking a demographic life history theory approach agnostic to system-specific plastic responses, I address the ultimate selective force behind phenological traits and their shifts, given that phenology is fundamentally a study of how life cycle transitions are fit to environmental cycles.

I hypothesize that rates of life cycle transitions relative to the periodicity with which environmental cycles incur predictable population perturbations influence fitness. I test this prediction by calculating which life history strategy in a population confers maximum fitness in a given periodic regime, and then studying how that optimal life history changes with changes in periodicity. Further, I hypothesize that fitness, and thus optimal life history strategies, will be influenced by trade-offs underlying these life cycle transitions. Thus I explore how various trade-offs impact the relationship between periodicity and optimality to understand how different species

in nature—whose life histories are in reality shaped by different sets of trade-offs—might be differentially affected by the same change in periodic regime.

Next I test my theoretical predictions in the copepod *Tigriopus californicus* (Copepoda: Harpacticoida), a crustacean found in rock pools in the supralittoral (upper tidal) zone along the North American Pacific coast. Populations are disturbed periodically by wave-wash at high tide, and experience population decline and heightened juvenile mortality periodically. Periodicity of disturbance varies among populations depending on regional tidal patterns and pool height on the shore. *T. californicus* provides an ideal system to study life history variation in cyclical systems across populations due to its short generation time and short disturbance cycles, the rare opportunity to sample from homogenized whole populations, and ease of quick sampling and trait measurements yielding large amounts of within- and across-population data. Across 19 natural populations of *T. californicus* in two regions of northern Washington I ask: do disturbance cycle periodicity and known trade-offs together predict life history variation across populations?

2.3 METHODS

2.3.1 Model construction

To uncover general predictions of evolutionarily optimal life history traits in cyclical environments, untied to species-specific idiosyncrasies such as plastic responses to meteorological cues, I describe a hypothetical population in two linked stages of broad applicability: juveniles and reproducing adults. I consider continuous-time demographic dynamics of the stage-structured population and impose stage-specific mortalities at given periodicities (full model description in Appendix I, SI-1.1).

First, I express constant-environment dynamics as a system of ordinary differential equations

$$\begin{aligned}\frac{dJ}{dt} &= -(\mu + d)J + fA \\ \frac{dA}{dt} &= \mu J - \gamma A\end{aligned}\tag{1}$$

which can be expressed as matrix \mathbf{M} :

$$\mathbf{M} = \begin{bmatrix} -(\mu + d) & f \\ \mu & -\gamma \end{bmatrix}\tag{2}$$

where J is juveniles, A is adults, μ is the rate at which juveniles mature into reproducing adults, d is background mortality of juveniles, f is the reproductive rate of adults, and γ is background mortality of adults. Then, via eigendecomposition of \mathbf{M} , I express the solution at time t as:

$$\begin{aligned}J(t) &= \frac{A(0)v_{(2)1} - J(0)v_{(2)2}}{v_{(2)1}v_{(1)2} - v_{(2)2}v_{(1)1}}v_{(1)1}e^{\lambda_1 t} + \frac{J(0)v_{(1)2} - A(0)v_{(1)1}}{v_{(2)1}v_{(1)2} - v_{(2)2}v_{(1)1}}v_{(2)1}e^{\lambda_2 t} \\ A(t) &= \frac{A(0)v_{(2)1} - J(0)v_{(2)2}}{v_{(2)1}v_{(1)2} - v_{(2)2}v_{(1)1}}v_{(1)2}e^{\lambda_1 t} + \frac{J(0)v_{(1)2} - A(0)v_{(1)1}}{v_{(2)1}v_{(1)2} - v_{(2)2}v_{(1)1}}v_{(2)2}e^{\lambda_2 t}\end{aligned}\tag{3}$$

where $v_{(i)j}$ is the j^{th} element of the i^{th} eigenvector corresponding to eigenvalue λ_i of \mathbf{M} . This solution describes simple structured population dynamics in an undisturbed environment, but by eigendecomposing the system I isolate the time parameter t which will eventually allow me to study demographic dynamics as a direct function of period length between disturbances. To make the solutions explicit with respect to disturbance cycle period T , I let $t = T$, and at time T multiply the structure by S_J and S_A to impose juvenile- and adult-specific mortality associated with disturbance. The combined system can be expressed as the matrix \mathbf{P} (Appendix I, Equation S10):

$$\mathbf{P} = \begin{bmatrix} S_J \frac{[(\mathbf{v}_{(1)2} e^{\lambda_2 T} \mathbf{v}_{(1)2} - \mathbf{v}_{(1)1} e^{\lambda_1 T} \mathbf{v}_{(2)2})]}{\mathbf{v}_{(2)1} \mathbf{v}_{(1)2} - \mathbf{v}_{(2)2} \mathbf{v}_{(1)1}} & S_J \frac{[(\mathbf{v}_{(1)1} e^{\lambda_1 T} \mathbf{v}_{(2)1} - \mathbf{v}_{(1)2} e^{\lambda_2 T} \mathbf{v}_{(1)1})]}{\mathbf{v}_{(2)1} \mathbf{v}_{(1)2} - \mathbf{v}_{(2)2} \mathbf{v}_{(1)1}} \\ S_A \frac{[(\mathbf{v}_{(2)2} e^{\lambda_2 T} \mathbf{v}_{(1)2} - \mathbf{v}_{(1)2} e^{\lambda_1 T} \mathbf{v}_{(2)2})]}{\mathbf{v}_{(2)1} \mathbf{v}_{(1)2} - \mathbf{v}_{(2)2} \mathbf{v}_{(1)1}} & S_A \frac{[(\mathbf{v}_{(1)2} e^{\lambda_1 T} \mathbf{v}_{(2)1} - \mathbf{v}_{(2)2} e^{\lambda_2 T} \mathbf{v}_{(1)1})]}{\mathbf{v}_{(2)1} \mathbf{v}_{(1)2} - \mathbf{v}_{(2)2} \mathbf{v}_{(1)1}} \end{bmatrix} \quad (4)$$

Matrix-multiplying initial abundances by \mathbf{P} would thus give stage structure after existing in a constant environment for time T and experiencing a disturbance event that incurs stage-specific mortalities. More interestingly, I use this framework to ask: what are the consequences of different combinations of life history traits on the fitness of a population given that it resides in disturbance regime T ?

2.3.2 Fitness

Given the general framework of cyclically perturbed stage-structured population dynamics, I ask how the predicted fitness of the population is influenced by the periodicity of environmental cycles. The dominant eigenvalue (λ) of a population transition matrix is a widely used measure of relative fitness because it represents how well the population will perform in the long run compared to other hypothetical populations with different life history strategies (Stearns 1992; Caswell 2001). This metric, equivalent to ‘ r ’ in demography and life history theory, does not capture consequences of short-term transient dynamics (Koons et al. 2005; Stott et al. 2011), but has been useful for drawing broad life history evolution predictions and conceptualizing relative fitness that match well with empirical observations (Charlesworth 1994; Caswell 2001; Stearns 1992). In stochastic environments fluctuations in instantaneous growth rates may lead λ to give inaccurate evolutionary predictions. In systems that can be modelled by periodic switching between environments, however, eigenvalues and eigenvectors of the matrix product of constituent matrices describing the different environmental states can be used for demographic and life history analyses

in exactly the same way as they are used in time-invariant theory (Skellam 1967; Caswell 2001). My matrix \mathbf{P} is equivalent to periodic models since the system switches between an undisturbed phase and disturbance, and the switching periodicity and population matrix elements do not fluctuate randomly (see Appendix I, Fig. SI-1.1 for simulation results). Thus, here I use the dominant eigenvalue of \mathbf{P} (hereafter referred to as λ_P) as the measure of relative fitness to compare the theoretical performance of life history strategies in a periodically time-variant framework, and characterize general selective pressures on life history strategies as a function of cycle periodicity.

2.3.3 Life history trade-offs

Life history evolution is a matter of optimization because limited resources must be allocated into various biological processes such as survival and reproduction involving trade-offs (Stearns 1989, 1992). The exact shapes of trade-off functions in organisms are famously difficult to measure, let alone justify in model assumptions (Pease and Bull 1988; Stearns 1989). Here I take a conservative approach and assume simple linear trade-offs to investigate general patterns in optimality as a function of the environment without making more complex physiological assumptions. To express a trade-off between any two traits in the construction of a fitness landscape, I computationally set the vector of the range of values of one trait in decreasing order as the other increases, imposing a negative slope between the two traits. When two traits do not trade off, one of the traits remains at the mean of its range as the other varies through its own range. I varied the combinatory inclusions of trade-offs among the four key parameters (μ , maturation rate; f , reproduction rate; d , background juvenile survival; and γ , background adult survival) to create model variants and investigate their relative fit to the data.

2.3.4 Fitness landscapes and optimal life history strategies

All realizations of \mathbf{P} —and thus the construction of fitness landscapes—must be constrained within the space of the interacting life history parameters, μ , d , f , and γ . In this presentation I constrained the space with known *T. californicus* life history ranges and trade-offs to demonstrate one example of the usage of this framework, but constraints can be set flexibly to represent any given species (see Appendix I, SI-1.2.5 for descriptions and citations for parameterization).

Using λ_P I construct fitness landscapes for μ and f simultaneously for each model. Here I focus on μ and f because they are life history traits for which I can collect large amounts of paired data in *T. californicus*, but it should be noted that fitness landscapes can be created for any life history trait in the original system of differential equations. For each landscape, I scan across the range of μ or f for a given value of T , while varying all other traits according to trade-off relationships included in the given model. Therefore I construct a vertical gradient of relative λ_P per T . To construct a landscape, I calculate gradients of relative λ_P across the horizontal axis of T . The optimal trait per T is the trait that maximizes λ_P per T . Finally, to get the curve of optimal trait values across the axis of T I track values associated with maximum λ_P across T .

2.3.5 Empirical investigation in *Tigriopus californicus*

Tigriopus californicus is a copepod found widely along the North American Pacific coast (see Appendix I, SI-1.2.1 for detailed description of natural history). Dense populations reside in rock pools above the intertidal zone at varying heights (Dethier 1980; Powlik 1998, 1999), which accordingly experience tide cycle disturbance at varying periodicities. When tide levels cyclically reach pool heights and waves wash through pools, *T. californicus* cling onto the rocky benthos in order to prevent being flushed down to open water or to the lower intertidal zone (Dethier 1980).

If they are washed down, predators that do not occur in *T. californicus* pools feed on them quickly, and re-colonization of *T. californicus* into the pools appear to be low (Dethier 1980; Dybdahl 1995). Despite clinging, tidal disturbance was shown to always decrease population size, and in particular, incur heightened juvenile mortality (Appendix I, Fig. SI-1.4).

I sampled 19 isolated populations across two sites in northern Washington, USA (Neah Bay, Friday Harbor) in order to capture a wide gradient of disturbance periodicities (see Appendix I, SI-1.2.2-1.2.4 for detailed description of data collection). I quantified the periodicity of tidal disturbance in each pool via timeseries analysis of pool temperature data over 4 months at 5-minute intervals, taking abnormal drops in temperature as signals of wave flush (Appendix I, SI-1.2.2). I siphoned entire isolated populations out of rock pools, and subsampled individuals after homogenizing them, to get representative population samples. I reared 30 mating pairs captured from each population in common garden settings. In these lines I measured rate of maturity (μ in the model) and rate of reproduction (f in the model) (see Appendix I, SI-1.2.4 for detailed description of trait measurements).

2.3.6 Likelihood and model fitting

I calculated the log-likelihoods of the optimality curves of the two focal life history traits μ and f produced by each model variant given the variance and covariance of the μ and f data. Each model is a different trade-off model (Appendix I, Fig. SI-1.2, Table SI-1.2). Every model has the same number of estimated parameters because they only differ in how the parameters trade off in the construction of the fitness landscapes, which is included computationally by aligning parameter range sequences in reverse order. Therefore model selection criteria that penalize number of parameters such as AIC were not used. Each model produces optimality curves (dominant

eigenvalue of matrix \mathbf{P} across gradient of disturbance period T) of μ and f given trade-off relationships. I searched for the maximum log-likelihood of each model given μ and f data simultaneously within the space of $S_A \geq S_J$ and compared maximum log-likelihoods of the 13 model variants.

2.4 RESULTS

2.4.1 Cycle periodicity alters optimal life history predictions

Classic life history theory balances costs and benefits of key biological investments such as development, reproduction, and survival to predict fitness profiles of life history traits (Stearns 1992; Charnov et al. 2001; Roff et al. 2006). Here I incorporated these classic balance considerations but imposed cyclical perturbations to population structure and asked if the fitness predictions change as a function of environmental cycle periodicity. Using this framework, I analyzed the role of cost (slope of trade-off, Fig. 2.1A) on the fitness profile of a life history trait (maturation rate) in two scenarios: one in which period length is long enough (e.g. to fit more than 10 generations in a period) that the effect of discrete cycles on the evolution of life history rates should be small (Fig. 2.1B), and another in which period length is at a similar timescale to generation time (Fig. 2.1C). The former approaches classic formulations of optimal life history predictions based on trade-offs alone (Roff et al. 2006). The latter shows that external periodic

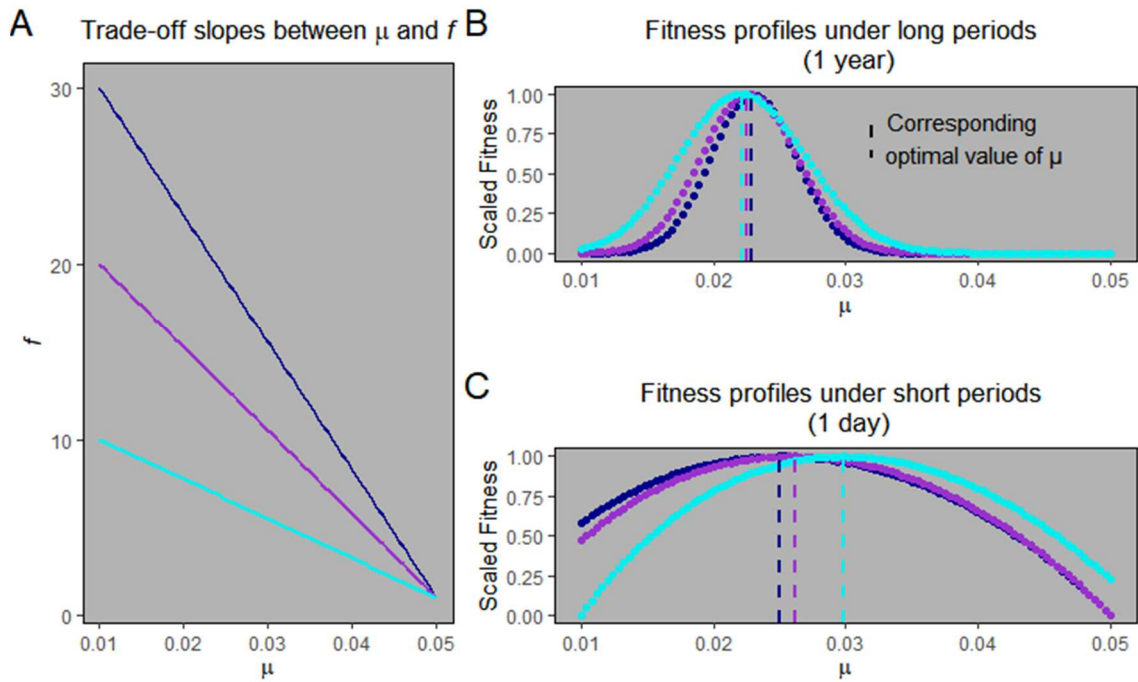


Figure 2.1 Three hypothetical cost functions between μ —rate at which juveniles mature into reproducing adults—and f —adult fecundity—are analyzed while setting linear trade-offs between μ and f , and between those two traits and their respective stage-specific background survival rates (d and γ). Stage-specific survival terms associated with cyclical disturbance are set at $S_A = 0.9$ & $S_J = 0.6$. Colors of cost functions in A correspond to colors of fitness profiles of μ in B and C. Dashed lines in B and C show peaks of fitness profiles which correspond to optimal values of μ . Periodicity of cyclical perturbation to population structure is set to be much greater than generation time in B ($T=365$), and at a relevant time scale ($<$ generation time) in C ($T=1$). Under short periods (C), all cost functions produce higher optimal μ values, wider fitness profiles, and an exactly reversed relationship between cost and optimality compared to long periods (B).

perturbations significantly change optimality predictions. In the latter scenario all trade-off cost assumptions predict higher optimal values of maturation rate compared to the former. The shape of fitness profiles is also flatter in the latter scenario, which may suggest weaker selection or that larger variance of maturation rate can be maintained within a population under shorter disturbance cycles. Lastly, the relationship between trade-off cost and optimality is reversed between the two scenarios: the lowest cost case produces the lowest optimal maturation rate under long periods but the highest optimum under short periods, and vice versa. These results show that the periodicity

with which harsh environmental conditions arrive and affect survival modifies the expected reproductive value of individuals, and significantly alters relative fitness of strategies with which individuals invest biological resources into life history traits.

2.4.2 Periodicity and trade-offs interact to produce diverse life histories

Optimal life history varies nonlinearly as a function of disturbance cycle period, even with assumptions of simple linear trade-offs between traits (Fig. 2.2). This nonlinearity implies that changes in the evolutionary optimum of a life history trait can be of very different magnitudes even with the same magnitude change in periodicity, depending on the initial period length.

Shapes of optimality curves (optimal traits vs. period) can vary dramatically depending on which life history trade-offs are included (Appendix I, Fig. SI-1.2). For example, when maturation trades off with background juvenile survival and fecundity (Fig. SI-1.2G), optimal maturation rate is expected to decrease and optimal fecundity is expected to increase as period length increases; on the other hand, if maturation trades off with background adult survival and fecundity instead (Fig. SI-1.2I), directions of expected trends in both optimal traits as period length changes are the opposite of the former case. Similarly, when maturation trades off with background adult survival, optimal maturation rate and fecundity are both expected to increase with period length (Fig. SI-1.2C), but both are expected to decline with period length if background juvenile survival trades off with background adult survival (Fig. SI-1.2E). Collectively, this broad range of cases examined demonstrates that the way in which external environmental cycles determine what combination of life history traits is evolutionarily optimal depends heavily on how traits trade off of one another internally. In the next section I show that the model that includes known trade-offs in *T. californicus* has the highest likelihood given *T. californicus*-specific life history data; but it is

important to note that no one model is necessarily better than another in a general sense because different species in nature will have different levels of complexity and rank order of trade-offs between life history traits (Roff et al. 2006; Stearns 1989; Schluter et al. 1991).

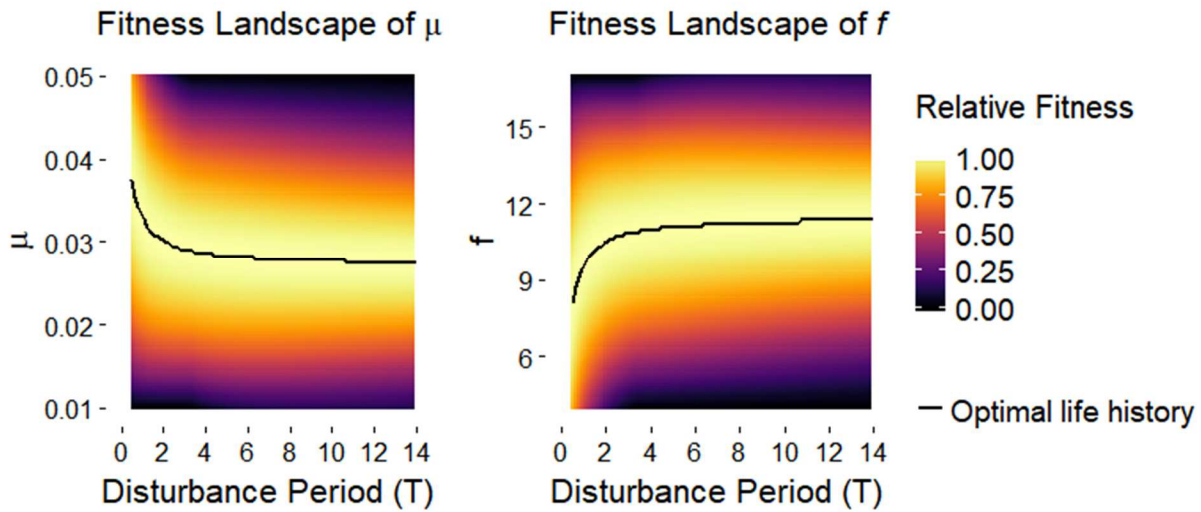


Figure 2.2 Example fitness landscapes of two focal life history traits, μ (rate of maturity) and f (reproductive rate) which assumes lower juvenile survival with each disturbance event ($S_A = 0.9$, $S_J = 0.6$), and trade-offs between μ and f , between μ and d , and between f and γ . Heat shows normalized fitness of a life history strategy compared to all other strategies in a disturbance regime (T). Curves track the optimal (maximum fitness) life history trait across T .

2.4.3 *Tigriopus* trade-offs predict life history variation across a periodicity gradient

Temperature time series analyses confirmed that there is a broad range of disturbance cycle periodicities across *T. californicus* pools across the two regions (Appendix I, SI-1.2.1; Fig. SI-1.4A, B; Table SI-1.1). These sampled pools provided a gradient of periodic regimes against which I tested optimal life history predictions. Daily temperature regimes, which may contribute to life history differences (Willett 2010; Kelly et al. 2013), were not significantly different among pools of varying periodicity regimes across the two regions (Fig. SI-1.5). Disturbance always caused

higher juvenile mortality than adult mortality in subsampled disturbance events, with mean juvenile mortality of 41% and mean adult mortality of 6% (Fig. SI-1.4C).

Life history traits shift as disturbance period changes across *T. californicus* populations (Fig. 2.3), mirroring the shape predicted by the model (Fig. 2.2). The best model (likelihood maximizing when μ and f are fit simultaneously, represented by Fig. 2.2) was the one that assumed trade-offs between maturation rate and fecundity, between maturation and juvenile survival, and between fecundity and adult survival, consistent with known trade-offs in *T. californicus* (Appendix I, SI-1.2.1). Raw data collected for μ and f per maternal line in my populations also support a general negative relationship between μ and f (electronic supplementary material, Fig. S6). Finally, model variants with double or tertiary trade-off assumptions generally fit better than ones with only single trade-offs (see Appendix I, Fig. SI-1.2 and Table SI-1.2 for the full list of models). These comparisons among model variants suggest that multidimensional trade-off relationships—which are typically avoided in empirical measurements or model assumptions of life history evolution (Pease and Bull 1988; Stearns 1989), but gaining some attention (Salguero-Gómez et al. 2016; Cohen et al. 2017)—may actually be important in predicting life history optimization in cyclical environments because trade-off consequences change as a function of cycle period.

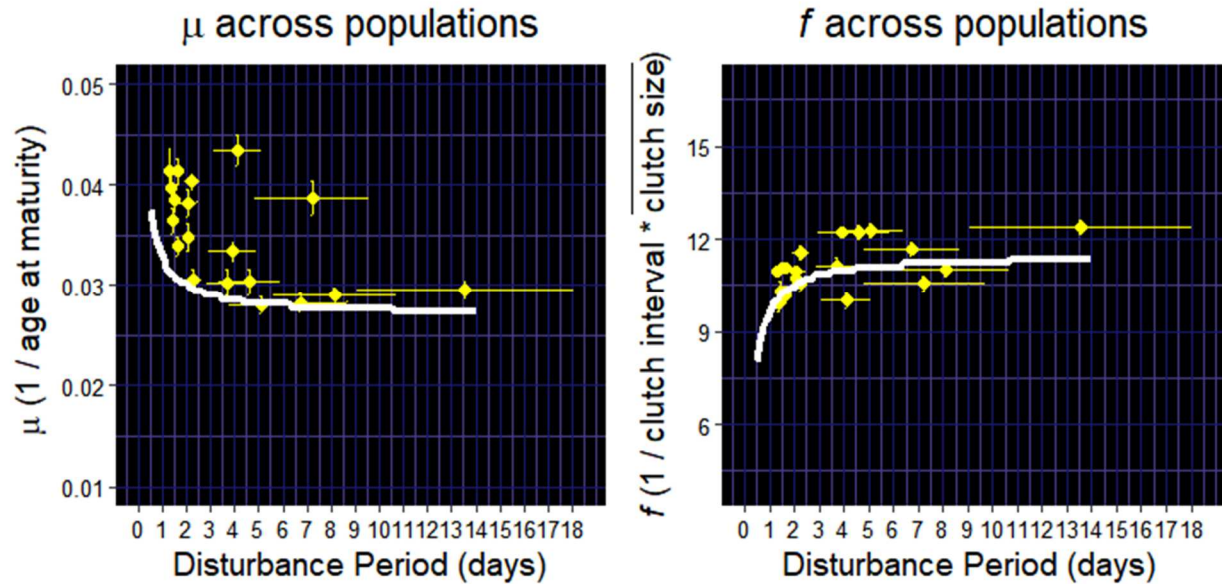


Figure 2.3 Mean (\pm se) values of the two focal life history traits μ and f across 19 *T. californicus* populations, against mean (\pm se) disturbance period determined by timeseries analysis of wave disturbance signals in each pool. Curves are optimal life history functions across periodicity (T) fit simultaneously to μ and f .

2.5 DISCUSSION

Ecologists have long assumed that environmental cycles are important for life cycle-related traits. But growing knowledge of phenological shifts has generated confusion regarding how environmental cycles shape life history strategies and thus transition rates of life cycle phases. A long-accepted tenet in life history evolution theory is that the mean and variance of population structure perturbations shape life history variation (Law 1979; Michod 1979; Charlesworth 1994; Reznick et al. 1996). Results here show that the temporal nature of such perturbations, such as the period length of environmental cycles, should interact strongly with general life history trade-off architectures in determining evolutionarily optimal traits. The interactive link between environmental cycles and life history optimality may be facilitated by the concept of reproductive value. Reproductive value is the expected contribution of an individual at a particular age or stage

to the population through current and future reproduction, determined by biological trade-offs and survival through time (Fisher 1930; Stearns 1992). Reproductive value is a central evaluation for fitness and evolution because it represents the aggregate consequence of trade-offs among many important life history traits (Goodman 1982). Naturally, the realization of current and future reproduction must depend on current and future environmental conditions for survival experienced by individuals. Thus it can be expected that, in predictably cyclical environments that periodically incur harsh conditions for survival, the period length of cycles will have a tractable influence on which life history strategy should perform best in the long term. A version of the model tuned with known *T. californicus* trade-offs successfully predicted the shape of life history variation across natural periodicity regimes, demonstrating the power of this interactive effect.

A fundamental question in ecology and evolution is why life histories are so diverse in nature. Divergent trends in phenological shifts among species in fact offer a current, global opportunity to study the production of life history diversity. Here I show that the interaction between environmental cycles and life history trade-offs is a simple mechanism that can account for large variations in life histories. First, due to the non-linear relationships between cycle period and optimal traits, the same magnitude of period change can induce different magnitudes of life history evolution between two populations of a species that are in different cyclical regimes (Fig. 2.2). Second, different trade-offs produce varying shapes of optimality curves (Appendix I, Fig. SI-1.2), and thus the same change in period can induce an increase, decrease, or no change in a life history trait for different species in the same system depending on what trade-offs are biologically important for those species. Environmental cycle periodicity is diverse across systems (such as growing season lengths across a latitudinal gradient), and trade-off architectures among populations and species vary widely due to physiological constraints, environmental conditions,

and reaction norms (Stearns 1989). Combined, cycles and trade-offs can produce a wide array of predicted life history strategies. Testing this mechanism in species that are controlled by different trade-offs, either across populations in different cyclical regimes or within a single population through time in a habitat undergoing a change in cycle periodicity—for instance due to climate change—will provide fruitful avenues for further exploring this perspective.

2.5.1 Stochasticity, ESS models, and gene flow

Cycles in nature, of course, are not perfectly periodic. The present study focuses on the consideration of period, or interval length between autocorrelated events. The mechanistic influence of fundamentally cyclical environments on life history evolution is noticeably understudied compared to probabilistic expectations in stochastic environments (Lande et al. 2017), even though regular cycles on various time scales are common in nature. Periodic models can be used to address a real aspect of nature that is difficult or impossible to address explicitly with stochastic models: cyclicity. Here, I take advantage of the fact that periodic models allow the use of matrix properties such as the dominant eigenvalue to infer relative fitness within a fluctuating system (Skellam 1967; Caswell 2001) and analyze conditions for optimization. By doing so I uncover a novel mechanistic relationship between cyclicity and life history evolution. However, cyclicity and stochasticity are both important aspects of nature. For instance, stochastic fluctuations in instantaneous population growth rate can significantly modify evolutionary trajectories predicted by time-invariant or periodic theoretical assumptions (Tuljapurkar 1982; Koons et al. 2005; Stott et al. 2011). Studying the relative influences of periodicity and stochasticity on optimal strategy, and on how quickly a population evolves to its predicted optimal strategy, are the obvious next steps that will add more richness to the perspective offered here.

Optimality curves in my model framework represent variations in evolutionary stable strategies (ESS) because I take the long-run growth rate of populations (dominant eigenvalue of \mathbf{P}) as the measure of fitness as is commonly done in demography and life history theory. ESS models are useful for the purpose of predicting general directions of selection over a long term. ESS models take a non-genetic perspective on broad selective forces, although a genetic justification for optimization of a quantitative trait is given by the fact that a mutation can invade the population if it confers a higher r on its carriers (Charlesworth 1994). Optimization models and quantitative genetics models are approximately equal for constrained multivariate systems (Charlesworth 1990). Nonetheless, results found here are inconclusive with respect to what a population's evolutionary trajectory from one optimum to another should look like in an environment undergoing change in cycle periodicity. Antagonistic selection on correlated traits imposed by different environmental variables associated with seasonal fluctuations, such as photoperiod and temperature, might cause deviations from ESS predictions. Evolutionary trajectories could be altered if bottlenecks are created by a sequence of disturbances and constrain the standing genetic variation subject to selection. In *T. californicus*, selection on optimal life histories may be obscured if high gene flow among nearby populations exists due to wave transport. However, colonization rates and genetic exchange have been repeatedly observed to be low in this system (Burton and Feldman 1981; Burton 1987, 1997), and demographic dynamics given high mortality rates caused by tidal disturbance likely overwhelm population genetic dynamics on the time scale of tide cycles. In this study I deliberately chose populations that were deemed to be well isolated given field observations. But the level of gene flow may vary depending on locality due to habitat characteristics, and may contribute to some of the variance within populations and deviations of population means from ESS predictions. Nonetheless, my model

fitting results suggest that ESS assumptions predict *T. californicus* life histories reasonably well given a population's periodic regime.

2.5.2 Trade-off functions

Trade-offs between traits can be nonlinear, and multidimensional architectures of trade-offs can be extremely difficult to measure (Stearns 1989; Schluter et al. 1991; Pease and Bull 1988). Here I have taken the conservative approach of assuming linear trade-offs among modeled life history variables, which biologically equate to strictly substitutable energetic currencies divided between different traits, to focus on the demonstration that consequent optimality curves across periodicity are nonlinear, and that a diverse set of optimality curves can be produced with different trade-offs. The simple linear assumption still performs well, at least with *T. californicus* life history data from my sample populations. However to test this framework further in different species, different functions can and should be used if the relationship between two traits is known to be nonlinear.

2.5.3 Links to evolution of seasonal phenologies

In seasonal environments cyclical arrival of harsh meteorological conditions (e.g. winter) can incur large demographic perturbations and thus strongly influence population dynamics (Rathcke and Lacey 1985; Remmel et al. 2009). Here I show that if periodic arrivals of disturbance incur significant demographic perturbations, individuals and their lineages that have life history strategies that are non-optimal in the context of their environment's cyclicity will have lower long-term fitness; thus, cyclical perturbations play an important role in driving the evolution of life history transition rates.

One unresolved paradox in phenology is that various species in the same community (e.g. those in different trophic levels) undergoing the same change in abiotic seasonal cycles often exhibit phenological shifts of vastly different magnitudes, or even in opposite directions. Here my results suggest that an interaction between environmental cycles and general biological trade-off relationships among fitness-related traits might contribute to life history and phenological divergence.

Period is not the only parameter of cycles, however. Particularly for seasons, cycle amplitude may also shape phenologies in important ways, and is shifting with climate change in many natural systems [e.g. seasonal CO₂ cycle amplitude (Keeling et al. 1996; Angert et al. 2005)]. Amplitude of seasonal cycles may play two roles for evolution. First, amplitude is associated with intensity of disturbance, which can be explored with survivorship functions in my theoretical framework. If the pattern of stage-specific mortality associated with cyclical disturbance is clear, such as in *T. californicus* and many seasonal species, then heightened intensity of cyclical disturbance will likely increase strength of selection. Second, amplitude reflects the rate of environmental change within cycle phases. Rate of change may be important for cue-detection and plastic responses. For example many plants in seasonal environments are well known for tracking growing degree-days as a way of taking cues on the passing of the seasons (Wolkovich et al. 2012). In my theoretical framework, cyclical disturbances arrive without warning and simply incur repeated penalties on individuals and cohorts that had non-optimal life history strategies for the given regime. In reality there may be a number of continuously changing environmental variables in *T. californicus* pools such as salinity, and I cannot exclude the possibility that, like plants, birds, or many aquatic invertebrates, *T. californicus* possess biological mechanisms to use cues from continuously changing parameters to plastically alter their phenotypes. Nonetheless, I was able to

predict variation in *T. californicus* life histories across a periodicity gradient in the environment without accounting for plasticity, suggesting that plastic responses might not have a strong effect on life history evolution in response to cyclicity. Future phenological work should directly compare the relative roles of demographic influences such as those discussed here and plastic response to cues that can be tracked along continuous cycles.

When considering phenological evolution in cyclical environments, the relative scaling of life cycles and environmental cycles becomes important. For instance, a perennial species must endure multiple seasonal cycle periods per generation. An annual species' generation on the other hand fits within a single cycle period. In both cases, consequences of fitness-related phenotypes in one generation carry over to subsequent generations via intergenerational trade-offs in life histories (Stearns 1992), but the trajectory of evolution may differ between the two because of the number of cycle periods a generation experiences. Further, the model framework presented here assumes overlapping generations but many annual organisms have non-overlapping generations and synchronous phenologies. The evolutionary consequences of non-overlapping generations and synchronization in a population in cyclical environments should be explored further.

Phenology is the study of how life cycle schedules are fit to environmental cycles. A phenological trait is a manifestation of the aggregate life history strategy of a species (Post et al. 2008), and expression timings of traits are ultimately controlled by transition rates between life history stages (Forrest and Miller-Rushing 2010). Phenological studies typically measure one representative phenotype such as flowering time in association with proximate drivers such as temperature or precipitation. But phenotypes covary and therefore one must consider trade-offs and competing selective forces with a whole-life perspective in order to understand the evolution of cyclical phenological traits. Here I placed such connections in the general context of

environmental cycles, of which the annual seasonal cycle is one example, and tested mechanistic predictions on the relatively short timescale of tide cycles which yielded large amounts of data across many cycle periods and generations quickly. This framework provides a basis for analyzing, comparing, and predicting adaptive phenological shifts in changing seasonal environments.

2.6 ACKNOWLEDGEMENTS

I thank G. Dwyer, M. Pascual, C.A. Pfister, T.D. Price, S.C. Stearns, J.T. Wootton, and two anonymous reviewers for helpful discussions and comments on earlier drafts. K. Miranda and T. Bowyer provided assistance in the field and with trait measurements. I am grateful to the Makah Tribe in Neah Bay, Friday Harbor Laboratories, and M. and D. Hurd for granting access to their lands for field data collection. This work was supported by University of Chicago Hinds Fund, DOE GAANN, and NSF LTREB grant (DEB-1556874).

3 Slower environmental cycles increase life history variation within populations

3.1 Abstract

Populations in nature are comprised of individual life histories, whose variation underpins ecological and evolutionary processes. Yet the forces of environmental selection that shape intrapopulation life history variation are still not well understood, and efforts have largely centered around random (stochastic) fluctuations of the environment. However, a ubiquitous mode of environmental fluctuation in nature is cyclical, whose periodicities can change independently of stochasticity. Here we test theoretically-based hypotheses for whether shortened ('Fast') or lengthened ('Slow') environmental cycles should generate higher intrapopulation variation of life-history phenotypes. We show, through a combination of agent-based modelling and a multi-generational laboratory selection experiment using the tidepool copepod *Tigriopus californicus*, that slower environmental cycles maintain higher levels of intrapopulation variation. Surprisingly, the effect of environmental periodicity on variation was much stronger than that of stochasticity. Thus, our results show that it is important to consider periodicity of fluctuating environments for studying life history variation.

3.2 INTRODUCTION

Individual variation in populations provides the raw material for natural selection, influences how demographic dynamics (e.g. population growth, extinction) unfold (Kendall and Fox 2002), how multiple species interact to shape community dynamics (Bolnick et al. 2011), and how species' responses to global change are mediated (Moran et al. 2016). Understanding the factors that generate and maintain trait variation within populations is thus a central goal of ecology and evolution. Contributions to the total phenotypic variance observed in a population are classically partitioned into genetic and environmental components, and their interactions (Bull 1987; Falconer 1996; Lynch and Walsh 1998). While the mapping of genotypic variance to phenotypic variance has been a main pillar of quantitative genetics and evolutionary studies for several decades, how environmental variance shapes phenotypic variance remains relatively less understood. Often, the environmental variance component is relegated to subsume any causally unexplained variations in the observed phenotypes, such as those that are assumed to arise from random environmental noise experienced during development and growth. For quantifying regimes of environmental variance, stochasticity (random fluctuation) is typically the tool that is used. Theoretical effort has been concentrated on exploring the different outcomes of stable versus stochastic environment assumptions for ecological and evolutionary dynamics (Metcalf and Koons 2007; Coulson and Tuljapurkar 2008; Vindenes et al. 2008; Tuljapurkar et al. 2009; Sæther and Engen 2015; Vindenes and Langangen 2015; Koons et al. 2016; Lande et al. 2017; Engen et al. 2020).

Though stochastic variables can closely approximate real temporal variability of environments and lend useful ecological and evolutionary insights, randomness overlooks a pervasive mode of environmental fluctuations in nature: periodic oscillations. Many environmental cycles in nature are periodically forced by a fundamental driver, such as the

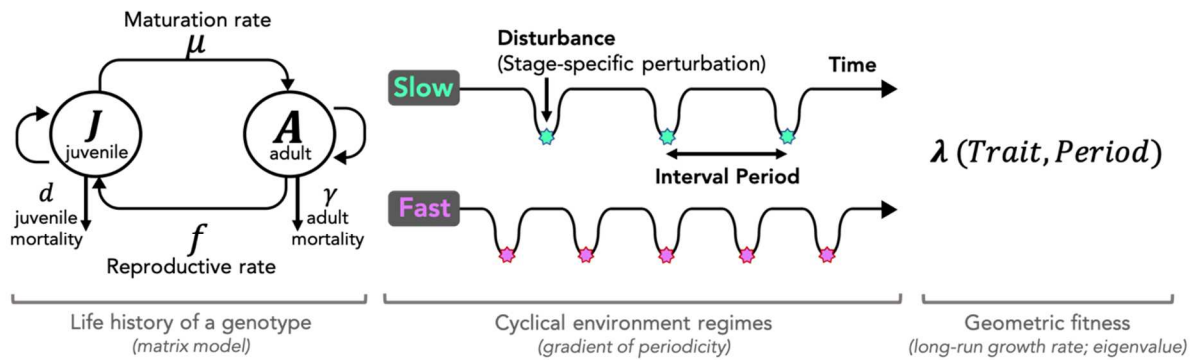
revolution of the Earth around the Sun that causes seasonality, or the lunar cycle that controls the tides. Stochastic models can indeed be used to characterize environments with frequency spectra that may be indistinguishable from fundamentally cyclical but noisy environments, for example by using a random variable for event timing drawn from a Gaussian distribution with a mean periodicity and a standard deviation that scales the amount of temporal stochasticity (Lytle 2001). Autocorrelative functions can be added to stochastic models (Vasseur and Yodzis 2004; Metcalf and Koons 2007; Wieczynski et al. 2018) to approximate noisy environments with some time-lagged memory. However, the distinct influences of periodicity and noise—two important axes of environmental fluctuations—on ecological and evolutionary processes remain an important target of study. One reason is that periodicity and noise can vary orthogonally. For example, the period length of warm (‘growing’) seasons optimal for biological activity varies clinally across latitudes (shorter towards higher latitudes) independently from change in stochasticity of seasonality driven by climate change (Easterling et al. 2000; Zhu et al. 2012; Xu et al. 2013). Even non-externally forced regimes that have emergent cyclical behavior due to internal system dynamics, such as fire, show orthogonal variations of average frequency and stochasticity (Westerling et al. 2006; Marlon et al. 2009; Moritz et al. 2012).

Models of periodic environments have shown that periodicity has significant impacts on population dynamics (Tuljapurkar 1985; Caswell and Trevisan 1994) and life-history evolution (Park 2019). Yet, these are concerned with population-level properties such as optimal or mean traits. For studying the environment’s role in shaping variability among individuals of a population, stochasticity remains the main conceptual framework (Bull 1987; Canino-Koning et al. 2019; van Daalen and Caswell 2020). Here we investigate how variance in life-history traits within populations is influenced by environment periodicity and stochasticity separately.

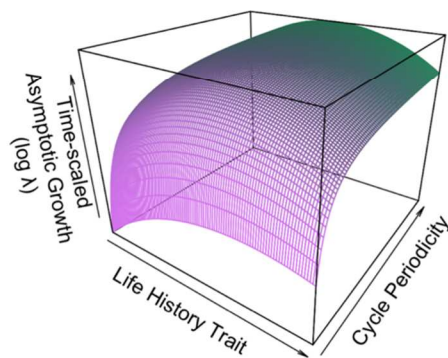
Specifically, we consider the case where environmental fluctuations are on similar timescales as generation time, population size is free to change, and generations overlap.

Two hypotheses for variance are given by a recent theoretical fitness landscape model of life histories in cyclically disturbed environments (Park 2019). In this simple deterministic framework (Fig. 3.1A), the asymptotic growth rate of a genotype is given as a function of its life-history traits, trade-offs among them, and the periodicity of the environment, calculated as the dominant eigenvalue (λ) of the underlying vital rates summarized in a matrix model. As the main output, a fitness landscape is given by scanning across possible life histories and environment periodicities (Fig. 3.1B). Here we ask how the topography of the landscape relates to the variance of traits as across environmental periodicity. We take two representatives from the periodicity spectrum, henceforth “Fast” (low period) and “Slow” (high period) environments. On one hand, relative $\log \lambda$ (scaled to $\max \log \lambda$ in each regime) shows a sharper profile in the Slow regime (Fig. 3.1C, left panel), which might indicate stronger stabilizing selection and thus lower variance than in the Fast regime. On the other hand, when seen in absolute terms (scaled by length of the projection interval), the entire profile in the Slow regime consists of higher magnitudes of asymptotic growth rate (Fig. 3.1C, right panel), which indicates high persistence of all genotypes. In other words, even suboptimal genotypes in Slow environments can proliferate and remain in the population in high numbers due to less frequent disturbances. Contrastingly, in Fast environments, all genotypes are much closer to $\log \lambda = 0$, which represents extinction. This discrepancy in the heights of profiles between Fast and Slow regimes presents an interplay between natural selection and drift: natural selection governs the relative probability of genotype survival, but drift, whose effect scales with population size, influences how many genotypes stochastically cross the line of extinction at the tails of the profiles and reduce variance in the population.

(A) Model framework



(B) Fitness landscape



(C) Contrasting hypotheses for variance

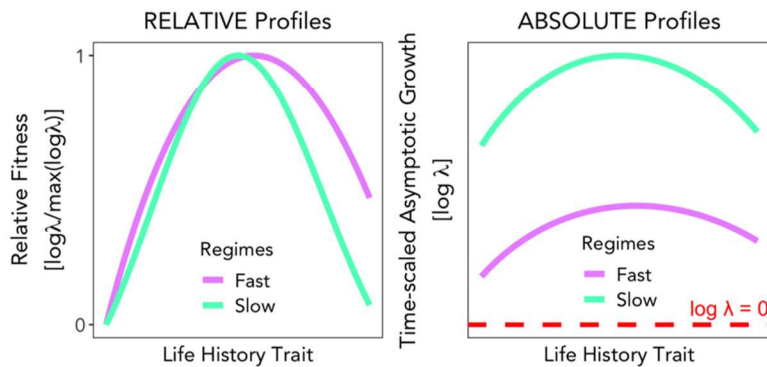


Figure 3.1 Optimality model of life histories in cyclical environments, and hypotheses for variance. (A) The deterministic theoretical model (Park 2019) takes the life-history strategy of a genotype—which consists of life-history traits and trade-offs among them—and calculates the asymptotic growth rate (dominant eigenvalue λ of the matrix model) as a continuous function of traits and environmental periodicity. (B) The resulting landscape gives optimal life histories (peaks on trait axis) across the axis of environmental cycle periodicity. Note that asymptotic growth on the z-axis is scaled by the matrix projection intervals which vary along the cycle periodicity axis. Here we take two near-extreme cases of periodicity, namely “Fast” (low period) and “Slow” (high period), and investigate trait distribution hypotheses. (C) Relative (to the optimal trait in each regime) vs. absolute asymptotic growth rate profiles across the trait axis give contrasting hypotheses for whether higher variance should be expected in Fast or Slow environments.

Here we test these two hypotheses—higher variance expected in Fast environments due to a weaker selection profile vs. higher variance in Slow environments due to broad proliferation of suboptimal genotypes—with an agent-based model of life-history evolution in cyclically and stochastically disturbed environments. We further corroborate our simulations with a life-history

selection experiment in the lab. We used the copepod *Tigriopus californicus* found in periodically disturbed tidepools of the Pacific Northwest, USA to parameterize our simulations and conduct the experiment. We explicitly differentiate environmental periodicity and stochasticity, and show that these two subcomponents of environmental fluctuations have distinct contributions to intraspecific life history variation, and that periodicity plays a surprisingly large role.

3.3 METHODS

*3.3.1 Demography and life history of *Tigriopus californicus**

T. californicus, a harpacticoid marine copepod, forms dense populations typically reaching thousands of individuals in <1L of water in small rock pools above the intertidal zone along the Pacific coastline of North America (Dethier 1980; Powlik 1999). Individuals develop through distinct stages from eggs to nauplii to copepodids to reproducing adults. After mating, females produce a series of clutches of eggs every few days until death; generation time ranges between 20~30 days (Burton et al. 1979). Pools containing populations experience wave disturbance from the tide cycle at measurably consistent periodicities depending on the height of the pool relative to the tide line; this periodicity across populations ranges from every 2-3 days to two weeks (Park 2019). Whenever populations are disturbed periodically by waves, *T. californicus* cling to the benthos of their shallow pools to avoid being washed out; yet many are dislodged to the lower intertidal zones where predators such as sculpin and anemones feed on them quickly (Dethier 1980; Dybdahl 1995). Predation of washed-out individuals and the difficulty of returning to home pools are hypothesized as mechanisms that restrict exchange between pools and intensify local adaptation even among neighboring pools (Burton and Feldman 1981). These wash-out disturbances decrease population size periodically, but more importantly they incur stage-specific

mortality by disproportionately killing more juveniles than adults (Park 2019). We used extreme representatives of disturbance cycle periods in nature to parameterize the Fast (period = 3 days) and Slow (Period = 14 days) cycle regimes of both the simulations and laboratory experiment here.

3.3.2 Agent-based model (ABM) of life-history evolution in fluctuating environments

We simulated selection dynamics in populations of genotypes with varying life-history traits. We subjected these *in silico* populations, parameterized for the *T. californicus* system, to deterministically cyclical, and stochastic fluctuation regimes and tracked *i*-state configurations (developmental states of individuals) through time. Then we analyzed the distributions of life-history traits of the surviving genotypes. See S1 for schematic of the ABM.

Birth, growth & death of individuals

We initiated each population with a set of n genotypes $i = \{1 \dots n\}$, each defined by two life-history phenotypes: maturation rate $\{\mu_1, \dots, \mu_n\}$ and fecundity $\{f_1, \dots, f_n\}$. Each individual progressively grows through states $s_i = [0, 3.0]$, transitioning through life-history stages where 0 = new-born, $[0, 1.0)$ = reproductively immature juvenile, $[1.0, 3.0)$ = reproductively mature adult, and 3.0 = end of life. At the beginning of each simulation, the population begins at $n = 5000$, and consists of a mix of *i*-states such that there is a 25:1 ratio of juveniles:adults, which was the approximate steady-state stage-structure from our exploratory simulations, but initial states within each stage (juvenile or adult) are randomly drawn from a uniform distribution. Then each individual i grows (state updated) at increments of μ_i per time-step. Therefore, genotypes reach reproductive maturity in different amounts of time, spend different amounts of time as reproductive adults, and have different lifespans. As soon as juveniles reach $s_i = 1.0$, they begin

reproducing continuously following a Poisson process with rate f_i . This continuous manner of reproduction is a good approximation of the reproductive pattern of *T. californicus*. Maturation rate μ_i and fecundity f_i are linearly negatively correlated, denoting a trade-off, following findings in other studies of *T. californicus* (Dybdahl 1995; Hong and Shurin 2015) and parameterized from (Park 2019) such that $f_i = 1 / (4 * \mu_i)$. The set of initial μ_i spanned [0.02,0.04] and f_i spanned [6.25,12.50], which represent the ranges of previously measured values of these traits (Park 2019). When a mature individual reproduces, it appends a number of offspring per time-step to the population vector, where number $\sim Pois(f_i)$. All offspring begin life at $s_i = 0$. Note that the adults modeled are more precisely female adults, as is the convention in stage-structured demographic models of two-sex populations (Caswell 2000) that are focused on the sex that limits reproductive and population growth processes. Nevertheless, males might introduce genetic variance via recombination. Further, other sources such as mutations and plasticity can cause imperfect inheritance of parental traits to offspring, so the μ_i and f_i of the newborn offspring are copies of those of their parent plus a small error drawn from a normal distribution with mean 0 and variance $0.01 * \bar{\mu}$ for maturation and $0.01 * \bar{f}$ for fecundity,, where $\bar{\mu}$ and \bar{f} are global means from the initial sets.

There are four ways in which mortality occurs. First, juvenile maturation rate μ_n and adult fecundity f_n trade off with juvenile and adult survival probabilities (i.e. positively covary with mortality), respectively. These trade-offs are not only known central pillars of life-history theory (Stearns 1989; Cohen et al. 2017), but have been previously measured in *T. californicus*. Mortality of juveniles ($s_i < 1.0$) is a Poisson process with rate $5 \times \mu_i$ (maturation rate), and mortality of adults ($s_i > 1.0$) is a Poisson process with rate $0.001 \times f_i$ (fecundity), parameterized following (Park 2019). Second, density-dependent mortality is applied to all individuals regardless of state.

Density-dependent mortality per time-step is a non-linear function of density N_t , where $N_t \times 0.001 \times \left(1 + \frac{N_t}{250000}\right)$ random individuals are excised from the population. Minimum background mortality rate of 0.001 in optimal conditions and scaling factor of 250,000 assuming a typical 10L *Tigriopus* pool were estimated from previously reported values (Dybdahl 1995; Powlik 1999; Hong and Shurin 2015). Third, when an individual reaches state $s_i = 3.0$, it reaches end of life and dies. Finally, environmental disturbance, either periodic or stochastic, removes a random 30% of juveniles ($s_i < 1.0$) from the population vector.

Environmental fluctuation regimes

We evolved these *in silico* populations under four different environmental fluctuation regimes: deterministic Fast cycles (periodicity = 3 time-steps), deterministic Slow cycles (periodicity = 14 time-steps), and stochastic analogs of each wherein disturbance timings were drawn randomly from a uniform distribution, $timing \sim U(0, T)$ where $T = length\ of\ simulations$, but such that the total number of disturbance events was equivalent to the deterministic analogs so that total mortality would be comparable. These periodicities were determined from the measured tidal disturbance periodicity spectrum across natural *T. californicus* pools (Park 2019), on the daily scale. Life-history traits μ and f , and the mortality rates were also scaled to the daily scale.

Phenotypic variance

We simulated 100 realizations of evolving populations within each of the four fluctuation regimes. For each of the realizations we tracked i -state configurations of individuals in the population, and the distributions of maturation rates $\{\mu_1, \dots, \mu_n\}$ and fecundities $\{f_1, \dots, f_n\}$ in the population. We

ran each simulation for 150 time-steps, which is equivalent to 150 days or 5~6 generations of *T. californicus*, equal to the length of the lab experiment.

3.3.3 Multi-generational life history selection experiment

Prior to the experiment, we initiated a laboratory stock population of *T. californicus* collected from pool populations in northwest Washington State, USA, maintained in a 4-liter tank under a 12-hour photoperiod cycle at 20°C in a Percival growth chamber for 4 months (3~4 generations). We used a medium of 35‰ artificial seawater solution (Instant Ocean) in DI water and 0.4g/L concentration of Spirulina powder for food. Food was added twice weekly ad libitum during the pre-experiment rearing. See S2 for a schematic for the experiment.

At the start of the experiment, we initiated replicate experimental populations with 100 mating pairs and 100 juveniles each, randomly selected from the stock population. We maintained each population in 500ml of 35‰ artificial seawater solution and 0.4g/L Spirulina. We assigned eight replicate populations randomly to each of three treatments: deterministic Fast, deterministic Slow, or stochastic Slow. Treatment assignment determined the frequency and distribution of disturbance over the 5-month span of the experiment. Fast treatment replicates were disturbed exactly every 3 days, Slow replicates every 14 days, and stochastic Slow replicates on random days dispersed by intervals drawn from a uniform distribution, but such that the total number of disturbance events during the span of the experiment was equal to that of the deterministic Slow treatment. Due to logistical constraints, we did not include a stochastic analog of the Fast treatment. We administered disturbance in the form of juvenile-specific mortality, emulating what occurs in natural *T. californicus* pools from periodic tide disturbance. To do so, we designed a two-layered cylindrical container with 200µm mesh at the bottom of the inner container, whose gaps would let

only juveniles to pass. Thus, on a replicate population's pre-designated disturbance day, we 1) extracted the meshed inner container, leaving only the juveniles in the medium inside the outer container, 2) thoroughly swirled and discarded 150mL of the well-mixed solution with juveniles to administer 30% juvenile mortality, 3) reinserted the meshed container thereby rejoining the juveniles and adults of the population, and finally 4) refilled the container to 500mL to replenish medium and food. An equivalent amount of food was added to the deterministic and stochastic Slow treatment replicates at the same 3-day interval to match the replenishment rate of Fast treatment replicates. All populations were kept in a growth chamber at 20°C and a 12-hour photoperiod cycle, and rotated randomly within the chamber every week.

Following five months of the disturbance treatments, we selected 30 random gravid females from each replicate population (3 treatments \times 8 replicate populations \times 30 individuals) by visually checking for adult females with red egg sacs. These gravid females were used to measure fecundity (f), and their offspring were used to measure maturation rate (μ). Each gravid female was kept in a separate 3.4mL well containing the same medium and 0.4g/L *Spirulina*, refreshed regularly with an eyedropper.

Fecundity (f) measurements

For each female the production of the first clutch of live juveniles, then the appearance of newly hatched clutches was monitored every 12 hours. Once a clutch production was observed, the whole clutch of juveniles was cleared from the well immediately using a pipette, leaving the female isolated in the well again with fresh medium and food. The time gaps between clutches were thus recorded in increments of 12 hours until each reproducing female had deposited up to 3 successive clutches. Then the mean 'clutch interval' per female was calculated. The size of each clutch was

not measured due to logistical constraints, but a global average of 47.32 was assumed for all females which was measured in a previous study using individuals from the same natural population sources used here (Park 2019). Fecundity was thus calculated as $\overline{clutch\ size} / \overline{clutch\ interval}$ per female.

Maturation rate (μ) measurements

We collected newborn nauplii from the second clutch of each female with a pipette immediately after hatching. From this clutch 20 nauplii were randomly selected and put into a single 6.9mL well containing the same medium and 0.4g/L *Spirulina*. Food was replenished regularly with an eyedropper and the siblings were allowed to mature and sib-mate. This ensured that all individuals in each mating group started life at the same time. We monitored mating groups from each female parent and recorded when the first egg sac appeared on a female as the earliest and surest sign of sexual maturity. Immediately after a gravid female appeared we removed her from the well to avoid counting subsequent clutches of the same female. Then we monitored each well in 12-hour increments until 2 gravid females appeared in total per well, and calculated the mean age at sexual maturity of the offspring produced per original parental female.

3.3.4 Statistical analyses

At the endpoints of the simulations, we analyzed if intrapopulation variances of phenotypes (σ^2_{μ} and σ^2_f within each realization) varied between environmental fluctuation regimes with a series of Welch's two-sample t-tests using log-transformed variances assuming unequal size and variance.

For the experiment, we similarly calculated phenotypic variance within each laboratory

population at the end of the selection period. To accommodate the non-normal distributions and unequal numbers of phenotype measurements in replicate populations, we conducted a Monte Carlo permutation test to analyze differences in intrapopulation variances between any pair of treatments A and B. First, we randomly sampled groups of 30 individual-level phenotypic measurements from the global dataset containing the measurements across all treatments and all replicates. We selected N such samples, where $N = a + b$, and a = number of replicates in treatment A, and b = number of replicates in treatment B. We calculated the variances of these N samples, which comprised the universal probability density function (PDF) central to such permutation tests. From the universal PDF we then randomly sampled, with replacement, the same number of variance estimates as there were replicates per treatment, and calculated $mean(b \text{ variance samples}) - mean(a \text{ variance samples})$. We permuted this calculation 50,000 times, which formed the null distribution of variance estimate differences between treatments. To test the hypothesis that the observed intrapopulation variances differed between any two experimental treatments, we computed the empirical *observed difference* = $mean(\text{variance measurements of replicates in Treatment B}) - mean(\text{variance measurements of replicates in Treatment A})$, and computed *p-value* = proportion of the permutation distribution \geq observed difference (S3). We conducted this permutation hypothesis test to compare Slow vs. Fast, and deterministic vs. stochastic Slow intrapopulation variance differences, for both μ and f .

3.4 RESULTS

3.4.1 Shifting distributions in simulated populations during transience

In all evolutionary simulation realizations, the within-population means of maturation rate (Fig. 3.2A&B) and fecundity (Fig. 3.2C&D) both showed concordant shifting patterns during the first

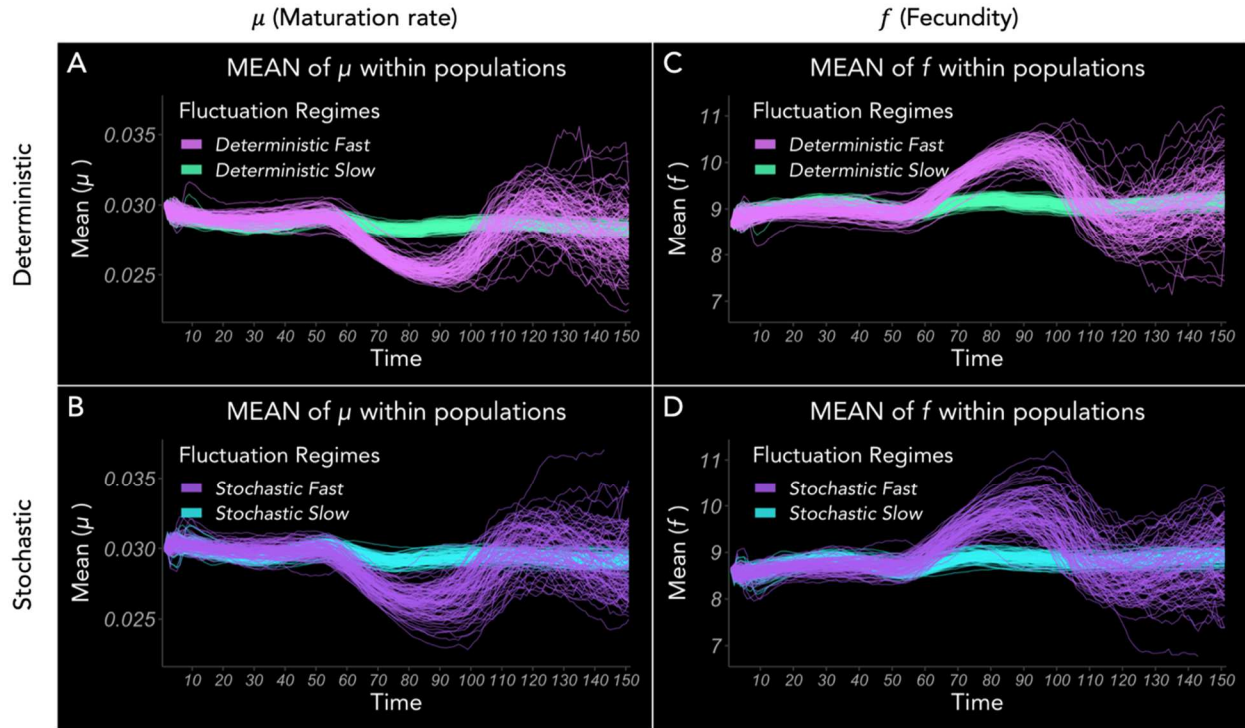


Figure 3.2 Means of life-history traits evolving in simulated populations. (A) and (B) show evolving mean of μ (maturation rate) in deterministic and stochastic regimes, respectively; (C) and (D) show evolving mean of f (fecundity) in deterministic and stochastic regimes, respectively. Each scenario is repeated for 100 realizations.

few generations. Particularly, under all environmental fluctuation regimes, there was an initial shift towards higher mean f due to an initial short-term proliferation of fast reproducers and, correspondingly, lower mean μ , reflecting the trade-off between the two (Fig. 3.3). That shift, which was more pronounced in Fast environments due to higher juvenile mortality from more frequent disturbances, was counteracted in 1~2 generations by costs associated with high reproduction, causing a resurgence in frequency of faster-maturing (higher μ) genotypes. This compensatory trend of means reflects an inter-generational consequence of a short-term benefit in life-history change. Then, approaching the end of the simulations, approximately after 5~6 generations, the distributions began to narrow (Fig. 3.3). Deterministically periodic regimes and their stochastic analogs (same number of disturbance events but randomly dispersed) produced

qualitatively very similar trends over time (Fig. 3.2A vs. B, and C vs. D), showing that mean periodicity had a stronger influence on life-history dynamics than temporal stochasticity of the environment (Fig. 3.2).

Purifying selection on μ through time under Fast Fluctuation

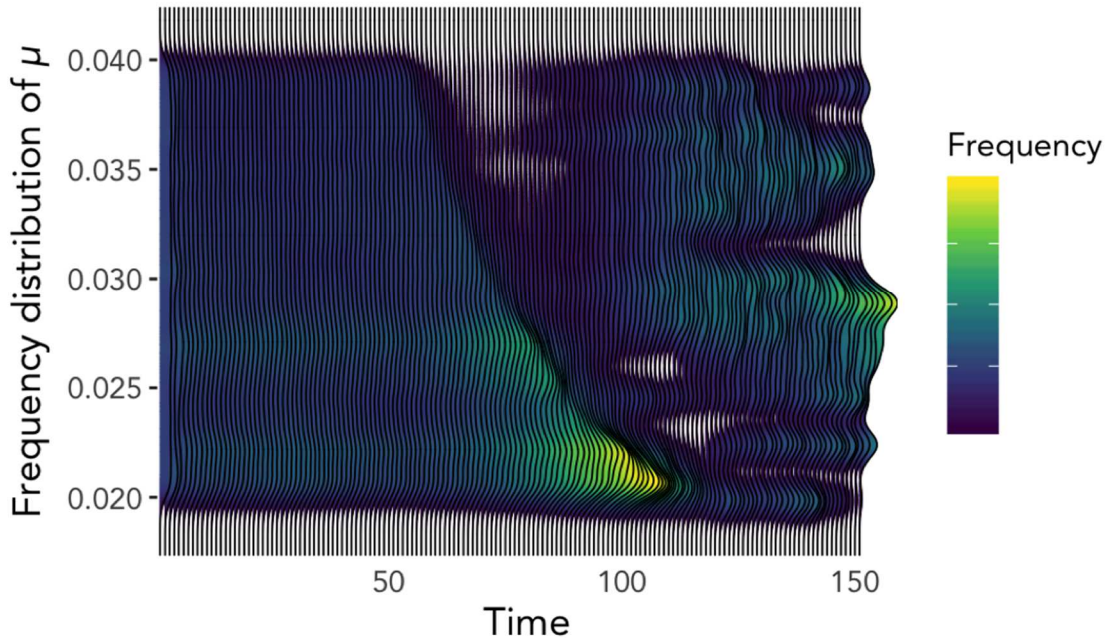


Figure 3.3 Purifying selection in action. Morphing distribution of μ (maturation rate) in one example realization of a population under Fast environmental fluctuation shows early selection towards lower μ ; this reflects short-term benefit for fast reproducers (high f) that are simply adding more offspring that resemble them quickly. Thereafter, costs associated with high reproduction allow alternate phenotypes to resurge in frequency ($\sim t=75$), which momentarily raises population mean as well as variance. Soon, the distribution narrows towards an optimum and variance declines (yellow peak at $t=150$).

3.4.2 Higher variance in Slow simulated environments

Life-history variances were distinctively higher in Slow compared to Fast regimes at the end of the simulation period, for both traits (Fig. 3.4; S5). Variance trajectories over the first few generations were driven by the same processes that drove concordant shifts in trait means, namely the early proliferation of high f & low μ phenotypes (producing the initial decrease in variance),

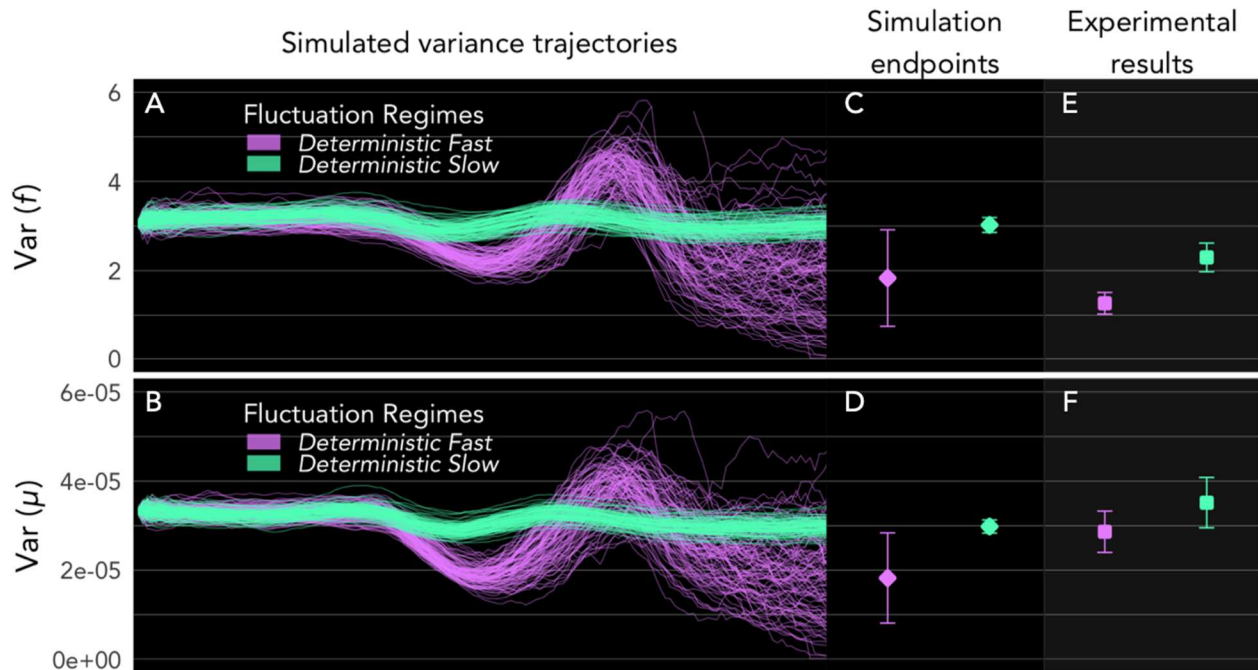


Figure 3.4 Higher phenotypic variance in Slow environments in simulation and in experiment. (A-B) Simulated trajectories of intrapopulation variance over 150 time-steps (5~6 generations) exhibit common qualitative patterns of 1) dropping early on because fast reproducers proliferate quickly (by definition) and distributions become concentrated at high f and low μ values; 2) briefly spiking as alternate phenotypes rise in frequency due to life-history costs associated with high f and low μ ; and 3) beginning to gradually decline. (C-D) Intrapopulation variances at simulation endpoints are higher in Slow environments than Fast for both traits. Diamond points show means of variances in realizations (i.e. means of intrapopulation variance), and error bars the standard deviation among the realization variances. (E-F) Measurements of intrapopulation phenotypic variances after the 150-day experiment (5~6 generations) also showed higher variance in Slow treatments for both traits. Square points show means of intrapopulation variances among replicate populations, and error bars the standard error of the variance measurements.

followed by compensatory resurgence of alternate phenotype frequencies due to costs on extreme phenotypes (producing the momentary spike in variance), before the gradual decline in variance tracking purifying selection (Fig. 3.3). This decline was much faster in realizations under Fast fluctuation regimes than in those under Slow regimes (Figs. 3.4A-B). Comparing the endpoints of simulations (Fig. 3.4C-D; Fig. S5.2, Table S5.1), intrapopulation variances of both traits were dramatically higher in Slow environments, for both deterministic and stochastic cases.

Contrastingly, variance differences between deterministic and stochastic cases for both Fast and Slow regimes were not as strong or consistent. Maturation rate showed statistically stronger signatures of variance difference in deterministic and stochastic cases than fecundity. Overall, the strongest and most consistent driver of intrapopulation trait variance was the Fast-Slow distinction of the environment.

Trait	Experimental treatment variance comparison	p-value
f (fecundity)	Deterministic Fast vs. Deterministic Slow	0.005
	Deterministic Slow vs. Stochastic Slow	0.244
μ (maturation rate)	Deterministic Fast vs. Deterministic Slow	0.012
	Deterministic Slow vs. Stochastic Slow	0.418

Table 3.1 Comparing intrapopulation phenotypic variances among experimental populations. Hypothesis testing with Monte Carlo permutation showed that intrapopulation variances of both traits were significantly different between Fast and Slow treatments across replicate populations (p-values under significance level $\alpha = 0.05$ in bold). However, variances under Slow and Stochastic Slow treatments were not significantly different.

3.4.3 Experimental corroboration of higher variance in Slow environments

At the end of the *T. californicus* selection experiment that lasted for an equal number of days as time-steps in the simulations (5~6 generations), intrapopulation means of maturation rate (μ) and fecundity (f) did not show consistent signatures of statistical differences (S4), similar to simulation results. Intrapopulation variances, however, as in the simulation, were distinctively higher in the Slow cycle treatments than in the Fast for both traits (Fig. 3.4 E-F & Table 3.1). Variances in the stochastic Slow treatments were not different from those in the deterministic Slow treatments, for

both traits. Thus, overall, there was strong evidence that periodicity drove differences in intrapopulation variance much more strongly than the deterministic-stochastic environment distinction for both traits.

3.4.4 Speed of purifying selection and sustained variance in simulations

We found that the decline in variance seen by the end of the simulation period (scaled to match the length of the lab experiment) continued when the simulation ran for a longer period of time (300 time-steps) (Fig. 3.5), showing the emergent purifying selection dynamic in the agent-based simulations. We found that the variance decline becomes much steadier after about 5~6 generations, as the short-term benefits of extreme phenotypes and their time-lagged costs eventually stabilize and the populations narrow towards optima. This decline in variance in Fast regimes was already faster in the short-term transient phase (Fig. 3.4), and it continued to drop more precipitously than in Slow environments in the longer simulation (Fig. 3.5). Phenotypic

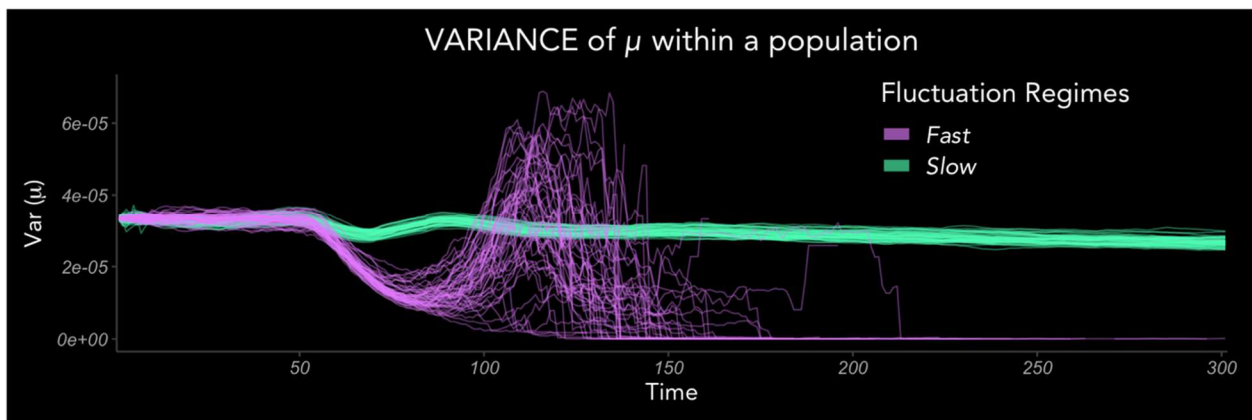


Figure 3.5 Sustained high variance in Slow environments. A longer simulation ($t=300$; 10~12 generations) of realizations for each regime, shows that phenotypic variances of populations in Slow environments steadily decrease as well, but much more gradually than those in Fast environments. Temporary spikes of variance in the Fast regime realizations are explained by compensatory resurgence of fast growers (high μ) after short-term dominance of fast reproducers. By $\sim t=150$, most simulated populations in the Fast regime have markedly low variance as a result of emergent purifying selection.

variance in Slow environments did decline very slowly because, despite the hypothesized stronger purifying selection (Fig. 3.1C), suboptimal phenotypes had higher λ than they would have in Fast environments and were thus sustained in the population.

3.5 DISCUSSION

Despite a growing scope for the *consequences* of individual phenotypic heterogeneity in ecology, there is still relatively little known about the environmental *causes* that shape heterogeneity in dynamic populations (Steiner et al. 2010; Moran et al. 2016; Hamel et al. 2018). Life-history fates are dependent on the very nature of the time sequence of the environment, strongly structured by the periodicity of cycles, beyond broad characterizations of temporal variance captured by environmental stochasticity. Thus, life history variations in cyclical environments, particularly in populations with overlapping generations where individuals born at different times experience very different time sequences of the environment through their lifetimes, present an interesting and broadly relevant puzzle (Tuljapurkar et al. 2020, 2021). Here we showed, through simulation and experiment grounded in evolutionary demographic fitness landscape predictions, that the periodicity of environmental fluctuations influences the level of life-history variance sustained within populations.

Oscillatory behavior of the environment, such as seasons or tides, is common in nature. We showed that the Fast-Slow axis of environmental oscillations created dramatic differences in the level of life history variance in populations. Phenotypic variance is a feature of transient phases of population dynamics, under the simple assumption that every population will converge to some theoretical optimum through perfect purifying selection in the limit. Equilibrium predictions may never be reached in real populations due to ever-present environmental and demographic

stochasticity in nature, and mutations; transient dynamics are thus important for understanding and predicting the trajectory of populations (Hastings 2004). We showed that the trajectory of phenotypic variance through transience differs radically depending on whether that population exists in a Fast (quick decline of variance) or Slow (gradual decline of variance) fluctuating environmental background.

The fitness profile of life-history traits across the spectrum of environmental periodicity varies in both sharpness (width) of relative fitness and overall magnitude (height) of absolute fitness (Fig. 3.1C). We asked whether phenotypic variance in transience would be more influenced by selection strength inferred from relative fitness, or magnitude of proliferation inferred from absolute fitness: weak selection might sustain variance, but all genotypes having high growth rates, despite stronger selection, reduces stochastic extinctions and could sustain variance as well. Within the parameter space of our investigations, the latter, conferred by longer periodicity of the environmental disturbance cycle, dramatically increased phenotypic variance despite density-dependent mortality. Importantly, higher population size did not strictly mean higher variance (Fig. 3.5; S6) because over a longer span of time, the optimal phenotypes eventually began to dominate via purifying selection and variance decreased despite growing population size. This suggests that the two drivers—selection strength and high overall growth rate—are indeed both at work, but the latter might be more influential for observed phenotypic variance than the former earlier on. Smaller population sizes increase the effect of drift, however, which can make long-term evolutionary outcomes more unpredictable. Indeed, we found that the spread of simulation realizations was much larger under Fast than Slow environments (Figs. 3.2 & 3.4). Future explorations of environmental fluctuation periodicity in the context of other study species could use our model framework to evaluate how the ratio between the environmental fluctuation period

and generation time of the species of interest (e.g. period \gg generation time, or vice versa) relates to the influence of periodicity in shaping phenotypic variance (Stearns 1976). Finally, our framework is well suited to explore the role of another important parameter of environmental fluctuations: amplitude. Amplitude can be approximated by the magnitude of mortality functions in our model to systematically analyze its effect on selection strength over time, and consequently the phenotypic variance in a population. Amplitude would be especially important in stochastic environments where extreme events significantly reduce genetic and phenotypic variation, and alter the course of subsequent evolutionary dynamics.

Beyond expanding theoretical understanding, climate change demonstrates a clear need to study the eco-evolutionary consequences of changing environmental cycles. While research has largely focused on the overall warming aspects of climate change, the length of the thermal growing season (the ‘climatic growing season’, e.g. the continuous frost-free period of the year) is consequently increasing in many ecosystems (Linderholm 2006; Parmesan 2006; Liu et al. 2018). Change in seasonality represents a change in annual intervals when most biological activity is optimal, or possible. Winters are conceptually analogous to periodic ‘disturbances’ and the length of intervening thermal growing seasons the ‘periodicity’ of that cycle. This perspective is particularly applicable to high latitude ecosystems. Conversely, longer summers represent a contraction of the biological window for winter-adapted species such as winter annual plants (Kimball et al. 2010). Thus, seasonal changes warp the temporal template upon which life histories unfold because life-histories are extremely time-dependent and balanced by trade-offs between current and future allocations crucial for fitness (e.g. timing of reproduction). Evolutionary consequences of seasonality expansions are not systematically understood: for example, phenologies of species (the timing of life-history events such as flowering) are shifting

incongruently and unpredictably in both direction (earlier or later) and magnitude (by how much). Dramatic shifts and variability of phenological responses within populations and between species documented worldwide suggest that the underlying cyclicality of the seasonal environment plays an important role in selectively shaping life-history trait distributions in ways that we do not understand well yet. Comparisons of species with different generation times, living in the same habitat undergoing the same directional change in seasonality, should be enlightening for understanding divergent responses in life history trait distributions as a function of the ratio between generation time and seasonality change.

Of crucial importance for understanding life-history evolution in cyclically disturbed environments, particularly in populations with overlapping generations, is that disturbance events are not necessarily ‘selection events’ in the traditional sense because demographic-specific mortality incurred by events are non-selective with respect to life-history strategy. For instance, juveniles of the same age or stage that are killed by disturbance may have taken very different amounts of time to mature to that point (via low vs. high μ). Selectively advantageous vital rates, instead, are determined by integrating the probabilistic costs, benefits, and reproductive consequences of individuals’ life-history decisions in the context of recent and forthcoming disturbances over entire lifetimes and over generations. If those disturbances or fluctuations are predictable, then over multiple generations the ultimate ‘winning’ strategy and distribution around it emerges. If environmental fluctuations are on much longer timescales than generations, then fluctuations are often conceived to impose ‘fluctuating selection’, where the population might adaptively track the environment over generations (Hairston et al. 2005; Bell 2010). In contrast, our investigations are in the realm in which generation time is roughly similar to environmental fluctuations. In circumstances where generation time is much longer than the periodicity of

environmental fluctuations, mechanisms other than life histories that mediate the effect of fluctuations on much shorter timescales, such as physiological or behavioral plasticity, may be targets of selection (Moran 1992; Gross et al. 2010; Lande 2014; Scheiner et al. 2020). However, relative time scale similarity of life history and environmental fluctuations is characteristic of many birds, insects, and annual plant systems. In such cases, we argue, the environmental fluctuation regimes—defined by parameters like periodicity—are agents of selection themselves that shape life history distributions in populations.

3.6 ACKNOWLEDGEMENTS

We thank the Makah Tribe of Washington State, USA for their partnership and support in our field collection work. We thank Greg Dwyer, David Iles, Mercedes Pascual, Cathy Pfister, Trevor Price, and Stephen Stearns for helpful discussions regarding literature review, study design, and analysis, and for comments that improved manuscript drafts. We thank Zoe Dellaert, Dalton Hammond, Khashiff Miranda, Nora Spadoni, and Mélusine Velde for their help with laboratory experiment work. Special thanks to Tim Morton for critical equipment and logistics assistance with laboratory work. JSP and JTW were supported by the National Science Foundation (OCE 1851489 & DEB 1556874).

4 Synthesis and Epilogue

Despite all the complex noise we often struggle to understand or capture, nature exhibits undeniable regularities in the way it fluctuates through time. Geophysical fixtures that exist outside the influence of ecological and evolutionary processes, that is to say planetary-scale dynamics like the regular revolution of the Earth and the lunar pull of the tides, apply a common force to all natural systems above which more idiosyncratic “noises” play out. It is useful to distinguish periodicity and stochasticity for two reasons, one philosophical and one practical. Philosophically, the underlying deterministic periodicities of the environment are a truly global theme—which is rare—and thus offer a deeply unifying and systematic perspective on all the wonderfully creative innovations organisms have evolved to make good use of time. I explored the idea of periodic environments as a unifying theme of biology in Chapter 1. Practically, periodicity and stochasticity can vary from space to space or change through time orthogonally. Orthogonal variations of periodicity and stochasticity, and their distinct effects on the ecology and evolution of dynamic populations, will be especially useful for studying the consequences of climate change. In Chapters 2 and 3, I quantitatively showed the powerful role of periodic fluctuations on life history evolution through a theoretical model, an examination of a natural system, a long-term laboratory experiment, and an agent-based simulation model.

It is useful to speculate why the disciplines of ecology and evolution have largely focused on stochastic characterizations of fluctuating environments, as a way to see that the focus was a result of human biases instead of an accurate reflection of the relative prevalence of stochastic noise over periodicity in nature. Quantifying periodicity and understanding its quantitative effects on ecology and evolution require immense data collection effort. To understand annual patterns,

for example, many years of continuous data collection might be required. The shorter the dataset, the more likely it is to appear stochastic despite an underlying periodic driver. Conversely, the longer the dataset, the more likely it might be to capture changes in periodicity due to factors like changing seasonality under climate change, thus complicating the analysis of the role of periodicity on biotic dynamics. It is easy to understand the desire to capture such complicated processes with powerfully simple probabilistic distributions developed in disciplines of statistics, mathematics, and physics in the face of such challenges and, often, given sparse ecological data.

Further motivating the overemphasis of randomness in nature, stochastically simulated environments can have long-term power spectra of the environment that can qualitatively look indistinguishable from environments that are periodically driven by an external force but have some noise on top of it. For studying general long-term dynamics of populations like population size, where populations are treated as collections of particles, simple stochastic characterizations of environmental fluctuations might indeed be sufficient. However, life histories are complex optimization properties that depend on the exact sequence of environments, as opposed to summary statistics of variability over some chunk of time. To illustrate this point, below I demonstrate a simple model. The punchline is that regularity with respect to an external clock, not just statistical predictability, matters for evolutionary fitness.

Consider four environmental scenarios defined by different underlying processes:

- (1) Random (stochastic) fluctuation;
- (2) “Noisy Cyclical” (deterministically cyclical fluctuation but with stochastic noise);
- (3) Negatively autocorrelated (‘self-correcting’) fluctuation; and
- (4) Positively autocorrelated (‘feedback loop’) fluctuation.

Each of the above scenarios models a sequence of event intervals. Events may be disturbances, or, in the context of seasonal systems, less favorable seasons (i.e. winter) expressed as discrete events. In tidal systems, like in *Tigriopus californicus*, events are high-tide wash-out events of pools. Much like in my dissertation work, consider that whenever events occur, a population experiences mortality as well as some structural perturbation (proportion of stages such as juveniles and adults). Within event intervals, populations continue their normal growth, determined by a simple model. Additionally, I let some continuous trait, in this case juvenile survival, to vary nonlinearly as a function of time since previous disturbance, around some mean interval (Fig 4.1).

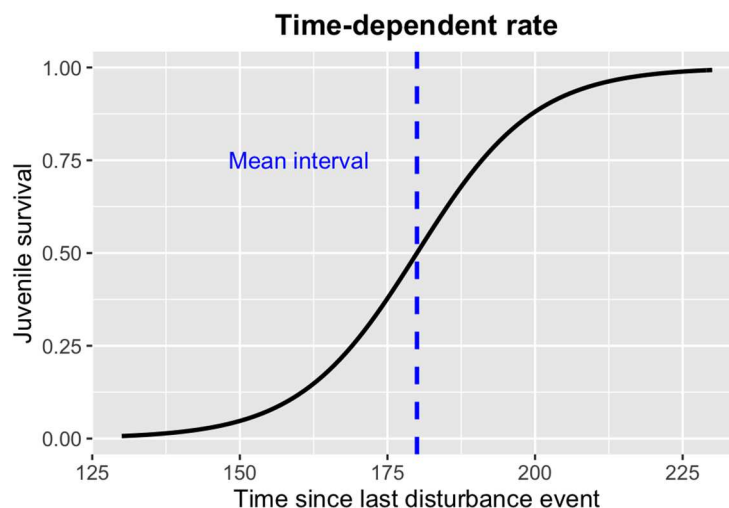


Figure 4.1 Nonlinear functional response of a life history trait (juvenile survival) as a function of time since last disturbance event.

More specifically, let each of the scenarios be modelled this way:

- (1) **Random fluctuation**: each subsequent interval is drawn from a normal distribution.
- (2) **Noisy Cyclical**: there are clocked 'due times' for events that are pre-determined (e.g. a calendar), and noise is added to each event as deviations from the clocked timing, drawn from a normal distribution. Then, event intervals are calculated as gaps between adjacent

realized events.

- (3) **Negatively autocorrelated fluctuation:** an AR(1) process with a negative autoregressive term (-0.7 in this arbitrary example), with error drawn from a normal distribution and added to the sequence of event intervals, such that

$$X_t = \overline{interval} - 0.7X_{t-1} + \varepsilon_t, \text{ where } \varepsilon_t \sim N(0, \sigma).$$

- (4) **Positively autocorrelated fluctuation:** an AR(1) process with a positive autoregressive term (+0.7 in this arbitrary example), with error drawn from a normal distribution and added to the sequence of event intervals, such that

$$X_t = \overline{interval} + 0.7X_{t-1} + \varepsilon_t, \text{ where } \varepsilon_t \sim N(0, \sigma).$$

Given the above processes, I simulate timeseries of event intervals for 500 time-steps to evaluate what they look like (Fig. 4.2). For subsequent analyses I dial up or down the strength of noise (σ) to see its effect on fitness. To illustrate the differences among the environment types, here I set the error rate at $\sigma = 0.1 * \overline{interval}$.

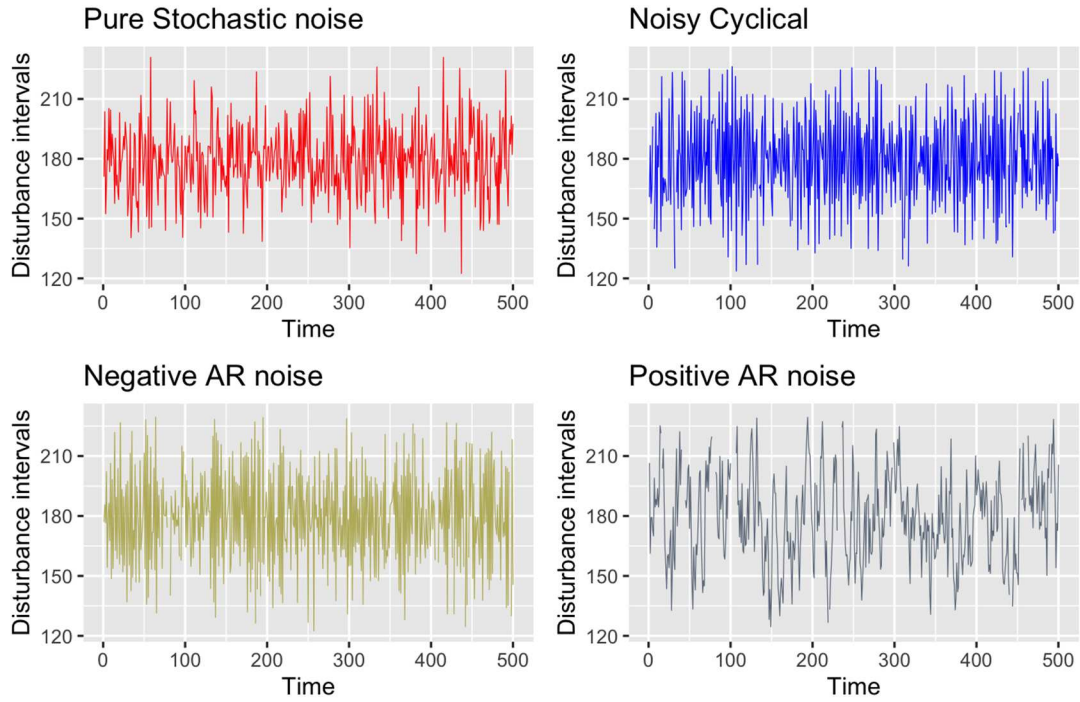


Figure 4.2 Timeseries of disturbance event intervals in the four environmental fluctuation scenarios considered.

I can also visualize the frequency distribution of event intervals under the four environment scenarios (Fig. 4.3); the point is that they are qualitatively nearly indistinguishable:

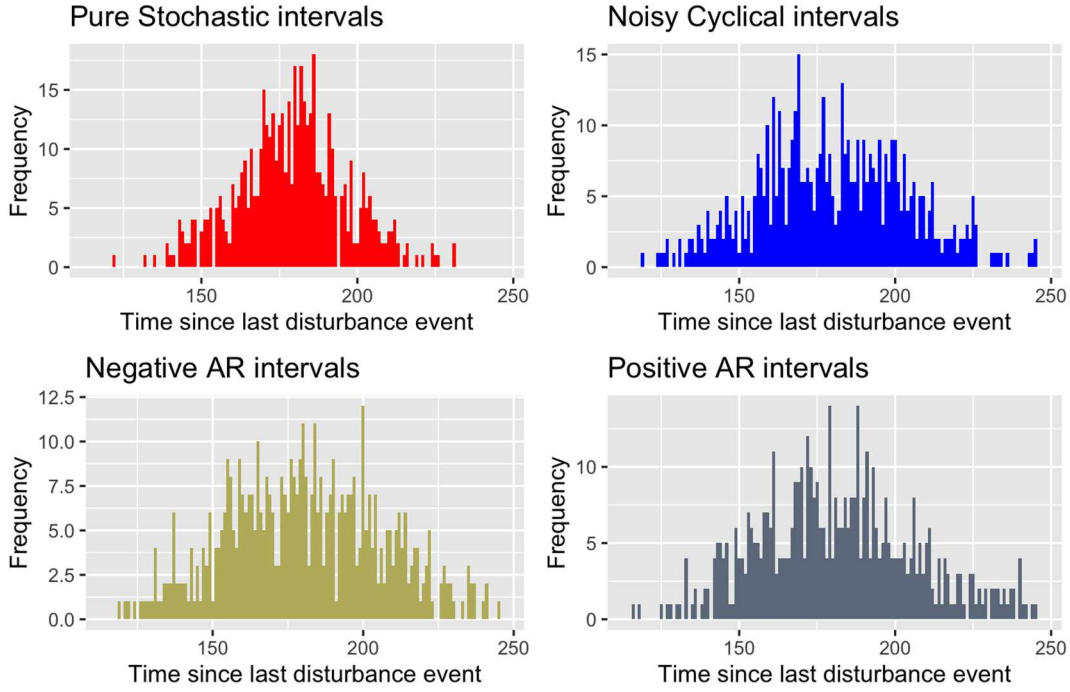


Figure 4.3 Frequency distributions of disturbance event intervals in the four environmental fluctuations scenarios considered.

Next, I ask how the fitness of a lineage that embodies a specific life history strategy is affected by the strength of environmental noise, across all four scenarios. Fitness here is defined as long-term stochastic growth rate of a population of a genotype defined by life history strategy. Life history strategy is the set of life history traits, defined in the discrete-time population model:

$$J_{t+1} = A_t f;$$

$$A_{t+1} = A_t S_A + J_t S_J,$$

where J = number of juveniles, A = number of adults, S_J and S_A are juvenile- and adult-specific survival rates, and f = fecundity. S_J here will vary logistically as a function of time since last event, and \bar{S}_J will set the shape of the logistic curve relative to $\overline{interval}$.

As an illustrative example, I set $S_A = 0.95$, $f = 0.2$, and $S_J = 0.5$. The following plot shows how the fitness of this particular set of traits (life history strategy) changes under the four environmental noise scenarios, as strength of the noise increases (Fig. 4.4). The stationary environment case (black line), of course, has no noise component and thus remains flat, but is shown for comparison.

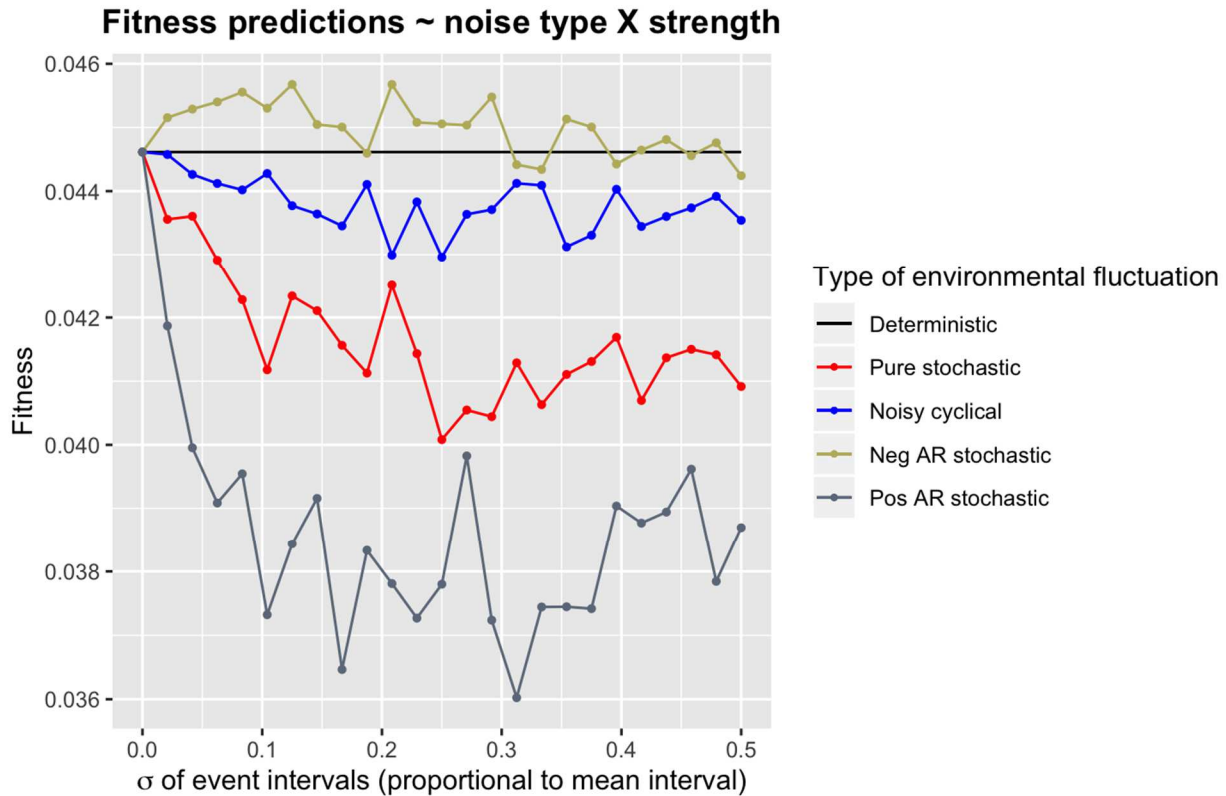


Figure 4.4 Response in fitness predictions as standard deviation (σ) of event intervals—i.e. amount of noise—increases, across the four environmental fluctuation scenarios considered.

It is clear that fitness is not only very different across environment scenarios but also changes with strength of noise very differently, despite the fact that frequency distributions of event intervals are qualitatively very similar. The main message is that environments that look similar, and indeed can be captured with the same mathematically convenient probabilistic distribution function (e.g. Gaussian noise), have different fitness consequences for the same life

history strategy depending on the generating process of the noise in the environment.

To investigate how exactly the generating process of environmental noise has rippling effects on fitness, I compute distributions of consecutive negative deviations from the mean interval—consecutive disturbance events that happen more quickly or ‘sooner’ than the expectation—to see if compounding deviations contribute to long-term fitness consequences (Fig. 4.5).

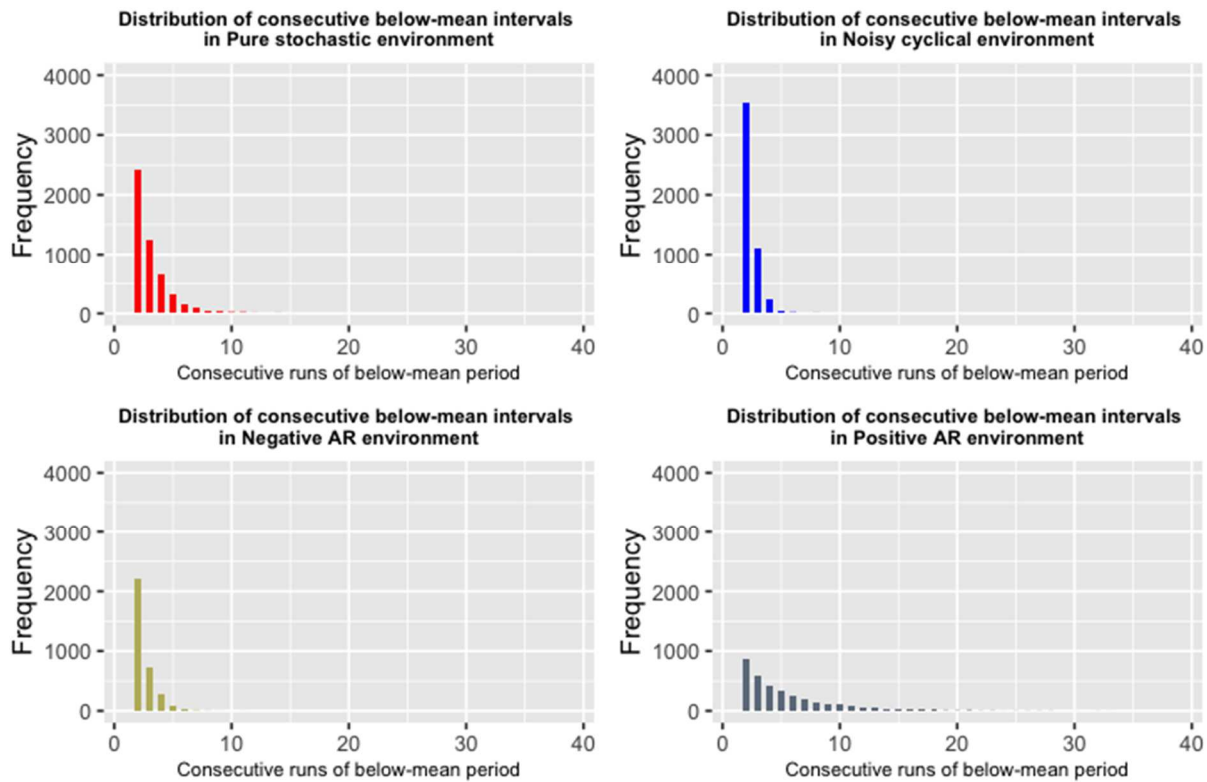


Figure 4.5 Frequency distributions of consecutive events with negative deviations from the mean interval, across the four environmental fluctuation scenarios considered.

These distributions of consecutive unfavorable (below-mean) deviations match with the height order among the fitness \sim stochasticity curves of the four environments. The Positive AR

stochastic scenario is the most right-skewed in the distribution of consecutive below-mean intervals, therefore long-term fitness is lowest due to the compounding of unfavorable intervals. This is a good simple check of the model in that I want positive autoregression to mean that a below-mean interval is likely to be followed by another below-mean interval. Pure stochastic is next in right-skewness, and its fitness ~ stochasticity curve is also the second lowest. Noisy cyclical and Negative AR stochastic are much less right-skewed, and their fitness ~ stochasticity curves are accordingly higher. The Negative AR stochastic scenario has much fewer consecutive below-mean intervals in total (shorter bars in the histogram), which also make sense by the way it was modelled (self-correcting), and its fitness ~ stochasticity curve is accordingly highest.

Due to Jensen's Inequality resulting from the nonlinear functional response of the focal trait with respect to time since last event, negative and positive deviations from mean interval have unequal effects on population processes. Therefore, the tracked consecutive deviations have compounding effects on fitness. Here the example focal trait was juvenile survival, but many other life history traits crucial for fitness such as reproductive output depend similarly on the recovery of the environment from recent perturbations.

This simple example illustrates the point that summary probabilistic representations of environment variability, often the default tool for modelling population dynamics and life history evolution, may be insufficient in teasing apart the generating processes of variability and their eco-evolutionary consequences. Nuanced but real differences in the geophysical forces that underlie environmental variability are crucial for life histories, whose evolution is an integration of the exact sequence of the environment through an organism's lifetime, and through the existence of the population. In my dissertation I have strived to elucidate the underappreciated role of cyclical environments on the evolution of life histories. In Chapter 1, I highlighted the pervasiveness of

cyclical environments, implications for phenology in an era of climate change, and basic ecological and evolutionary questions on which this perspective sheds light. In Chapter 2, I demonstrated the power of periodic oscillations in driving evolutionary divergence of life histories across many real, natural populations. In Chapter 3, I showed that periodicity interacts with natural selection to dictate levels of phenotypic variance maintained in populations.

Many insights that drove me forward in my PhD research were possible because of the synergistic combination of theory, fieldwork, and laboratory experimental work. Cross-pollination was both educational and constantly refreshing. But first and foremost, I believe that my true inspiration came from the quiet observations I made of the cyclical turnovers of flies and mosquitoes while spending undistracted summers in remote reaches of the Canadian tundra during my undergraduate years, yet unencumbered by the rigid conventions of disciplines. These observations, which I later realized are representative of many systems around the world – flowering plants, seasonal insects, migratory birds – continued to be a source of motivation during particularly foggy moments of the more mature theoretical ruminations of my PhD years. My personal experience of anchoring my focus in the simple, undeniable observations while enduring the confusion of research mirrors what I view as a good philosophy in the continued quest to understand the fundamental role of cyclicity of nature on complex biotic processes: that through the static, through all the noise, there is some governing force that is real, and thus worth studying.

Appendix I: Supporting Information for Chapter 2 (Cyclical environments drive variation in life history strategies: a general theory of cyclical phenology)

SI-1.1 MODEL DESCRIPTION

SI-1.1.1 Continuous stage-structured population dynamics

First I express the dynamics of Juveniles and Adults of a population in the *absence of disturbance* with a simple system of ordinary differential equations:

$$\begin{aligned}\frac{dJ}{dt} &= -(\mu + d)J + fA \\ \frac{dA}{dt} &= \mu J - \gamma A\end{aligned}\tag{S1}$$

where μ is the rate at which juveniles mature into reproducing adults, d is intrinsic juvenile mortality rate, f is reproductive rate of adults, and γ is intrinsic adult mortality rate. This system, in matrix form, can be expressed as:

$$\mathbf{M} = \begin{bmatrix} -(\mu + d) & f \\ \mu & -\gamma \end{bmatrix}\tag{S2}$$

The vector of solutions $\langle J(t), A(t) \rangle$ can be expressed as $C_1 v_{\lambda_1} e^{\lambda_1 t} + C_2 v_{\lambda_2} e^{\lambda_2 t}$, thus

$$\begin{aligned}J(t) &= C_1 v_{(1)1} e^{\lambda_1 t} + C_2 v_{(2)1} e^{\lambda_2 t} \\ A(t) &= C_1 v_{(1)2} e^{\lambda_1 t} + C_2 v_{(2)2} e^{\lambda_2 t}\end{aligned}\tag{S3}$$

where $v_{(i)j}$ is the j^{th} element of eigenvector i , associated with eigenvalue λ_i of \mathbf{M} .

To obtain the full solution I must solve for λ_1 , λ_2 and $v_{(i)j}$ of \mathbf{M} , as well as the constants C_1 and C_2 in terms of the eigenvalues and eigenvectors.

Let the abundance in each stage at $t = 0$ be:

$$\begin{aligned} J(0) &= C_1 v_{(1)1} + C_2 v_{(2)1} \\ A(0) &= C_1 v_{(1)2} + C_2 v_{(2)2} \end{aligned} \tag{S4}$$

Rearranging, I find:

$$\begin{aligned} C_1 &= \frac{A(0) - C_2 v_{(2)2}}{v_{(1)2}} \\ C_2 &= \frac{J(0) - C_1 v_{(1)1}}{v_{(2)1}} \end{aligned} \tag{S5}$$

and substituting C_2 into C_1 I find:

$$\begin{aligned} C_1 &= \frac{A(0) - \frac{J(0) - C_1 v_{(1)1}}{v_{(2)1}} v_{(2)2}}{v_{(1)2}} = \frac{A(0)}{v_{(1)2}} - \frac{(J(0) - C_1 v_{(1)1}) v_{(2)2}}{v_{(2)1} v_{(1)2}} \\ C_1 \left[1 - \frac{v_{(1)1} v_{(2)2}}{v_{(2)1} v_{(1)2}} \right] &= \frac{A(0)}{v_{(1)2}} - J(0) \frac{v_{(2)2}}{v_{(2)1} v_{(1)2}} \\ C_1 \left[\frac{v_{(2)1} v_{(1)2} - v_{(1)1} v_{(2)2}}{v_{(2)1} v_{(1)2}} \right] &= \frac{A(0)}{v_{(1)2}} - J(0) \frac{v_{(2)2}}{v_{(2)1} v_{(1)2}} \\ C_1 &= \frac{A(0) v_{(2)1} - J(0) v_{(2)2}}{v_{(2)1} v_{(1)2} - v_{(2)2} v_{(1)1}} \end{aligned} \tag{S6}$$

And similarly, I solve for C_2 :

$$C_2 = \frac{J(0)v_{(1)2} - A(0)v_{(1)1}}{v_{(2)1}v_{(1)2} - v_{(2)2}v_{(1)1}} \quad (S7)$$

Finally, substituting (S6) and (S7) into (S3), I find the solution for abundances of Juveniles and Adults at time t in the absence of disturbance:

$$\begin{aligned} J(t) &= \frac{A(0)v_{(2)1} - J(0)v_{(2)2}}{v_{(2)1}v_{(1)2} - v_{(2)2}v_{(1)1}} v_{(1)1} e^{\lambda_1 t} + \frac{J(0)v_{(1)2} - A(0)v_{(1)1}}{v_{(2)1}v_{(1)2} - v_{(2)2}v_{(1)1}} v_{(2)1} e^{\lambda_2 t} \\ A(t) &= \frac{A(0)v_{(2)1} - J(0)v_{(2)2}}{v_{(2)1}v_{(1)2} - v_{(2)2}v_{(1)1}} v_{(1)2} e^{\lambda_1 t} + \frac{J(0)v_{(1)2} - A(0)v_{(1)1}}{v_{(2)1}v_{(1)2} - v_{(2)2}v_{(1)1}} v_{(2)2} e^{\lambda_2 t} \end{aligned} \quad (S8)$$

This is the solution for demographic dynamics in the absence of disturbance, i.e. dynamics *between disturbance events*. Now I incorporate periodic disturbance and then lastly calculate population fitness as a result of periodicity of disturbance.

Note that the sole purpose of expanding the solution into the form (S8) is to isolate t , which will be used to incorporate periodic disturbance.

SI-1.1.2 Incorporating periodic disturbance

Let $J_w(t)$ and $A_w(t)$ describe the changes in the two stages through time before the first disturbance, and $J_{w+1}(t)$ and $A_{w+1}(t)$ before the second disturbance, and so on. Let T = length of each phase between disturbance events. Therefore, $J_w(T)$ and $A_w(T)$ are abundances immediately

before the first disturbance, and $J_{w+1}(0)$ and $A_{w+1}(0)$ immediately after the first disturbance, and so on. Let S_J and S_A describe *survival rates* of each stage when disturbance occurs, so that:

$$\begin{aligned} J_{w+1}(0) &= S_J J_w(T) \\ A_{w+1}(0) &= S_A A_w(T) \end{aligned} \quad (\text{S9})$$

Thus,

$$\begin{aligned} \vec{N}_{w+1} &= \begin{bmatrix} S_J J_w(T) \\ S_A A_w(T) \end{bmatrix} = \vec{N}_w \\ &= \begin{bmatrix} S_J \left[\frac{A_w(0)v_{(2)1} - J_w(0)v_{(2)2}}{v_{(2)1}v_{(1)2} - v_{(2)2}v_{(1)1}} v_{(1)1}e^{\lambda_1 T} + \frac{J_w(0)v_{(1)2} - A_w(0)v_{(1)1}}{v_{(2)1}v_{(1)2} - v_{(2)2}v_{(1)1}} v_{(1)2}e^{\lambda_2 T} \right] \\ S_A \left[\frac{A_w(0)v_{(2)1} - J_w(0)v_{(2)2}}{v_{(2)1}v_{(1)2} - v_{(2)2}v_{(1)1}} v_{(1)2}e^{\lambda_1 T} + \frac{J_w(0)v_{(1)2} - A_w(0)v_{(1)1}}{v_{(2)1}v_{(1)2} - v_{(2)2}v_{(1)1}} v_{(2)2}e^{\lambda_2 T} \right] \end{bmatrix} = \mathbf{P} \begin{bmatrix} J_w(0) \\ A_w(0) \end{bmatrix} \\ &= \begin{bmatrix} \frac{J_w(0)S_J[(v_{(1)2}e^{\lambda_2 T}v_{(1)2} - v_{(1)1}e^{\lambda_1 T}v_{(2)2})]}{v_{(2)1}v_{(1)2} - v_{(2)2}v_{(1)1}} + \frac{A_w(0)S_J[(v_{(1)1}e^{\lambda_1 T}v_{(2)1} - v_{(1)2}e^{\lambda_2 T}v_{(1)1})]}{v_{(2)1}v_{(1)2} - v_{(2)2}v_{(1)1}} \\ \frac{J_w(0)S_A[(v_{(2)2}e^{\lambda_2 T}v_{(1)2} - v_{(1)2}e^{\lambda_1 T}v_{(2)2})]}{v_{(2)1}v_{(1)2} - v_{(2)2}v_{(1)1}} + \frac{A_w(0)S_A[(v_{(1)2}e^{\lambda_1 T}v_{(2)1} - v_{(2)2}e^{\lambda_2 T}v_{(1)1})]}{v_{(2)1}v_{(1)2} - v_{(2)2}v_{(1)1}} \end{bmatrix} = \mathbf{P} \begin{bmatrix} J_w(0) \\ A_w(0) \end{bmatrix} \end{aligned}$$

$$\mathbf{P} = \begin{bmatrix} S_J \frac{[(v_{(1)2}e^{\lambda_2 T}v_{(1)2} - v_{(1)1}e^{\lambda_1 T}v_{(2)2})]}{v_{(2)1}v_{(1)2} - v_{(2)2}v_{(1)1}} & S_J \frac{[(v_{(1)1}e^{\lambda_1 T}v_{(2)1} - v_{(1)2}e^{\lambda_2 T}v_{(1)1})]}{v_{(2)1}v_{(1)2} - v_{(2)2}v_{(1)1}} \\ S_A \frac{[(v_{(2)2}e^{\lambda_2 T}v_{(1)2} - v_{(1)2}e^{\lambda_1 T}v_{(2)2})]}{v_{(2)1}v_{(1)2} - v_{(2)2}v_{(1)1}} & S_A \frac{[(v_{(1)2}e^{\lambda_1 T}v_{(2)1} - v_{(2)2}e^{\lambda_2 T}v_{(1)1})]}{v_{(2)1}v_{(1)2} - v_{(2)2}v_{(1)1}} \end{bmatrix} \quad (\text{S10})$$

where \mathbf{P} is the matrix that relates the initial abundances of the two stages (\vec{N}_w) to those after disturbance (\vec{N}_{w+1}), via the length of the undisturbed phase, i.e. periodicity of disturbance (T), and the survival rate of each stage when disturbance occurs (S_J and S_A).

SI-1.1.3 Fitness of a periodically disturbed population

Iterative multiplications of \mathbf{P} to the initial population structure will simulate dynamics of the structure over many periodic disturbance cycles. Since periodicity in this model is not stochastic, \mathbf{P} is equivalent to periodic matrix product models (Skellam 1967; Caswell 2001) whose dominant eigenvalue gives the long-run growth rate of the population. And by extension the dominant eigenvalue of \mathbf{P} is an appropriate measure of the population's fitness in a given regime T . In order to construct the fitness landscape across values of a life history trait across periodicity (T) regimes, I pass a value of a life history trait through \mathbf{M} , allowing other life history traits to vary according to trade-off assumptions among traits, and calculate the dominant eigenvalue of the final matrix \mathbf{P} . Eigenvalues of \mathbf{P} are scaled against the highest eigenvalue per T in order to create a gradient per T . The life history trait per T that confers the highest fitness value is the optimal life history trait.

SI-1.2 DATA COLLECTION & ANALYSIS

SI-1.2.1 Tigriopus californicus

T. californicus has been a model species for marine phylogeography and population genetics research particularly due to its extensive latitudinal range and surprisingly strong local adaptation patterns (Burton & Feldman 1981; Burton *et al.* 1979; Edmands 2001; Edmands & Harrison 2003). Dense populations of *T. californicus* form in small pools, typically reaching tens of thousands of individuals in less than 10L of water (Dethier 1980; Powlik 1998, 1999). High tide levels periodically reach heights at which *T. californicus* pools occur and deliver wave disturbance. When waves flush through pools, normally free-swimming *T. californicus* dive and cling to the rock to avoid being washed out (Dethier 1980). Yet many are dislodged down to the mid and lower intertidal zones where predators such as sculpin and anemones feed on them quickly (Dethier 1980). Barriers of predation between pools are hypothesized as a mechanism that restricts

exchange between populations and enhances local patterns of genetic structure even among nearby pools (Dethier 1980; Dybdahl 1995). The egg-to-egg generation time of *T. californicus* is about three weeks (Burton *et al.* 1979), and high tide disturbance periodicity is on the order of days to weeks. Thus disturbance period is on a comparable time scale to generation time. The exact disturbance period for a given pool varies due to local tide patterns and height of pool on the rocky shore. Once juveniles mature into reproductive maturity, males and females form mating pairs, and each female is fertilized only once in her life and continuously produces successive clutches of juveniles until she dies (Burton 1985).

I sampled 19 populations for local disturbance regime and life history traits. Sample populations span two regions of the Strait of Juan de Fuca in northern Washington that experience very different high tide patterns, one near the mouth ('Neah Bay'), and one further inside the Strait ('Friday Harbor'). I chose the two regions based on the hypothesis that Neah Bay is subject to clearer differences in spring and neap tides, creating longer periods between tidal disturbances in general but also a broader spectrum of periods among pools depending on pool height on the shores, and that Friday Harbor experiences much more consistent and higher high tides, subjecting populations there to shorter disturbance period regimes in general. I specifically quantified local disturbance period for each population using high-resolution temperature time series data to verify this regional hypothesis.

In *T. californicus*, rate of maturation (inverse of age at maturity) and fecundity are known to trade off strongly (Dybdahl 1995; Edmands & Harrison 2003; Willett 2010; Hong & Shurin 2015). This trade-off is in fact widespread and known to covary and evolve rapidly in conjunction with one another in many plants and animals (Stearns & Koella 1986; Stearns 1989). I also found a strong negative correlation between the two traits across my 19 populations (Fig. 2). Intrinsic

survival rate of juveniles and adults are also known to trade off with maturation rate and adult fecundity, respectively, in *T. californicus* because energetically expensive osmoregulation and intracellular concentration of amino acids required in the harsh environment of rocky shores divert resources from reproduction and somatic growth (Goolish & Burton 1989; Dybdahl 1995).

SI-1.2.2 Local disturbance periods

Regional historical tide data were collected from National Oceanic and Atmospheric Administration's National Data Buoy Center. I adhered HOBO (Onset Co.) temperature loggers at the bottom of each pool that recorded temperature data at 5-minute intervals for up to 4 months. Oceanic water temperatures are typically significantly lower than rocky shore pool temperatures, so sudden drops in temperature were taken as signals of tidal wave disturbance. When high tide rises enough to reach a given pool, multiple waves create clusters of signals. Therefore I used a sliding window and identified negative derivatives in the timeseries that were below a significance threshold compared to their neighbors (7 standard deviations below mean of all derivatives within that day). This method deals well with stochasticity within days, as well as day-to-day variations caused by weather effects, and was ground-truthed by occasional visual checks of tidal disturbance. I then calculated mean period between days that contain signals of wave disturbance per pool.

SI-1.2.3 Disturbed demographic dynamics

In order to quantify the general impact that high tide wave disturbance has on *T. californicus* populations, I chose a subset of five of the sample pools that had not experienced tidal disturbance for at least 3 days, and measured population structures 5 hours before an impending high tide

disturbance and 5 hours after. To obtain comprehensive measurements of population structure and size at a given time point, I siphoned out entire volumes of water from pools using incrementally small plastic pipettes while squirting out small crevices and sucking out *T. californicus* individuals. I then vigorously swirled whole volumes in a uniform container (5-gallon bucket), took 50mL subsamples, and counted number of individuals in juvenile (nauplii and copepodites) and adult (both sexes) stages immediately under a scope. This method proved to yield consistent measurements of population structure, and provides a rare opportunity for sampling uniformly from known whole populations, quickly and easily. After the pre-disturbance structure measurements, I immediately returned all individuals to their pools to reinstate the populations. I chose nearby pools to determine whether pools exhibit high exchange of individuals when disturbance occurs, or if they exhibit a consistent pattern of structural change even if nearby, in line with previous studies that showed that mortality by predation in lower intertidal zones limit exchanges between pools.

SI-1.2.4 Life history measurements

I collected a random subsample of 30 mating adult pairs from each of the 19 populations after siphoning out the entire population. I kept each pair in an individual 6.9ml well filled with filtered local seawater (50 μ m) and 0.2g/l *Spirulina* powder in a common temperature environment. Once the pair copulated and separated, I extracted the male leaving only the female. In order to reduce potential lingering effects of variability in environmental conditions among home source pools, I let all fertilized females produce one clutch of eggs in the common garden setting before starting to measure fecundity. At 12 hour increments I checked for the production of a clutch of juveniles for every mother, transferred the mother to a fresh well if she had produced a clutch, recorded

interval between clutches, and repeated until up to 8 clutches were produced per female or she died. I then calculated mean clutch interval per female for each population. Clutch size is known to be highly variable among *T. californicus* individuals, as well as among clutches per individual (Kelly *et al.* 2013), and clutch interval may be a better indicator of rate of reproduction that respond to selection experiments. I measured clutch size of the second clutch for a subset of mothers across populations. Rate of reproduction (f in the model) of each mother is inverse of mean clutch interval * mean clutch size. To measure age at maturity, I isolated 20 juveniles from the second clutch produced from each mother and reared them in a 6.9mL well with the same conditions as above (Kelly *et al.* 2013). At 12 hour increments I checked for visible egg sacs in females in each cluster. Every time a gravid female appeared I extracted her from the well so that she would not be counted twice. I recorded time to maturity for 5 females in a clutch from one mother. Rate of maturation (μ in the model) is the inverse of mean age at maturity.

SI-1.2.5 Parameterization for model analysis

Using my own life history data and data from various other studies that reported *T. californicus* life history traits, I set broad constraints on parameters through which I explored model behavior. Literature sources include studies in nature across the geographical range of *T. californicus*, or experimental studies that measured life history traits in control treatments as basis for measuring effects of factors such as UV or pollutants (Burton *et al.* 1979; Dethier 1980; Willett 2010; Barnett & Kontogiannis 1975; Scott 1995). These constraints are: μ =[0.01,0.05], d =[0.01,0.4], f =[4,17], and γ =[0.01,0.2]. Rates are daily rates.

SI-1.3 SUPPLEMENTARY FIGURES

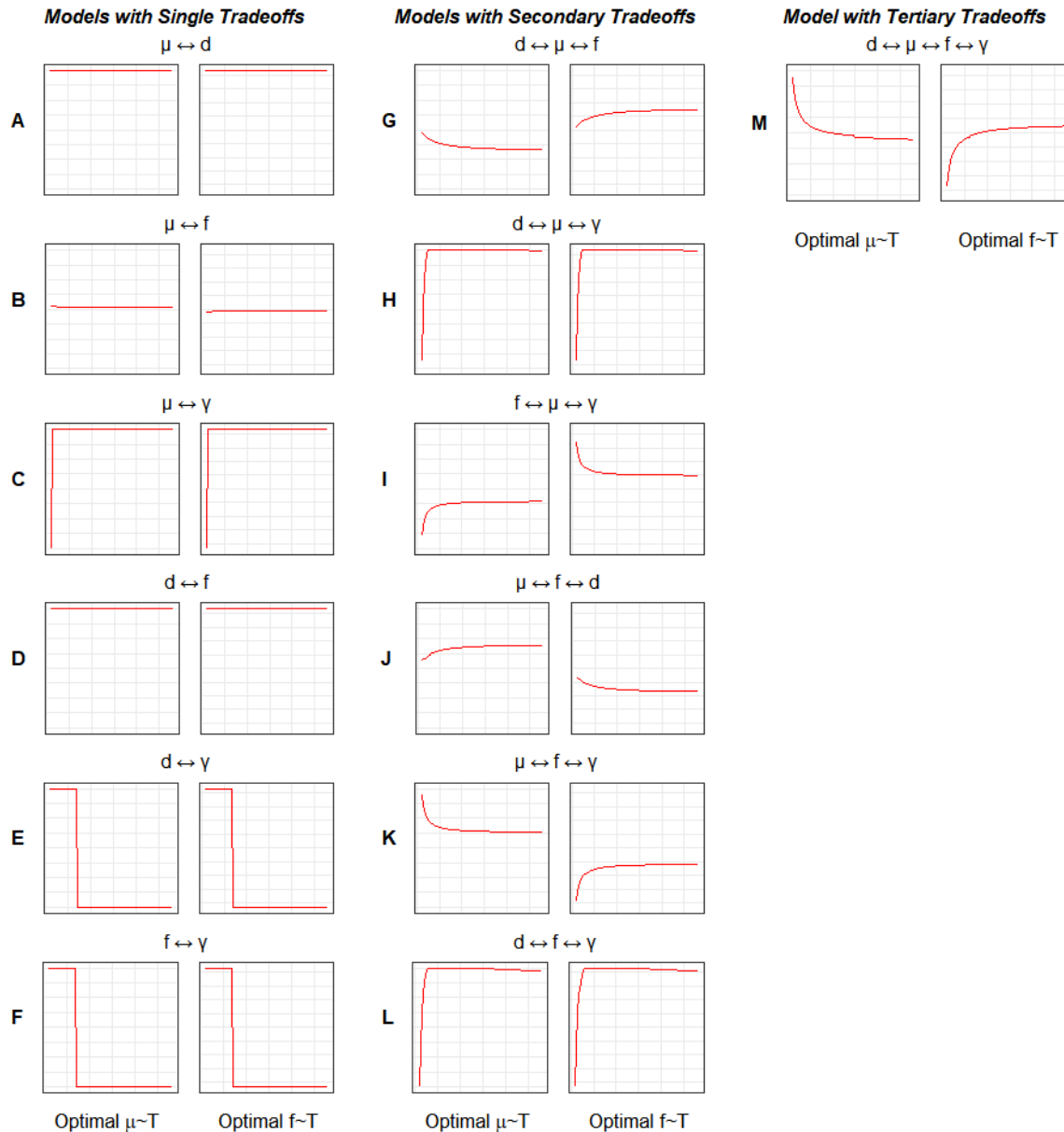


Figure SI-1.1 Optimality curves of all model variants which include varying life history trade-off assumptions. Each model's trade-off inclusion is denoted above the pair of plots by the double-sided arrow between traits. In each pair of plots the left panel is the curve representing optimal μ (fitness maximizing) across cycle period T , and right is optimal f across T . First column of paired plots contains models with single trade-offs, second column models with secondary trade-offs (but only ones that include μ or f out of all possible combinations among the four traits) and the last column the one model with tertiary trade-offs in which μ and f trade off with each other and with their respective stage mortalities d and γ . All realizations in this figure were run with $S_A > S_J$ (0.9, 0.6), which represent stage-specific (Adults vs. Juveniles) mortalities associated with cyclical disturbance. Magnitude of $S_A > S_J$ does not qualitatively change shapes of optimality curves.

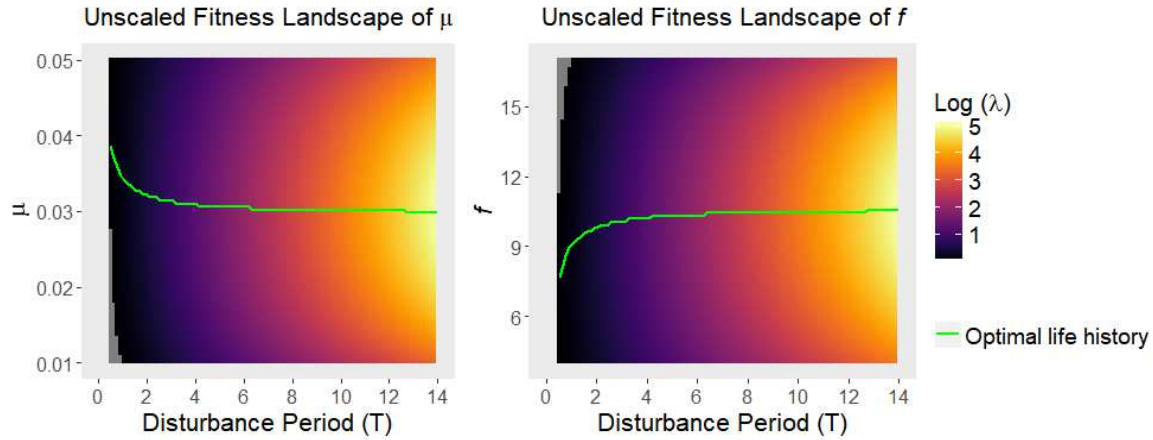


Figure SI-1.2 Landscapes of log-transformed absolute fitness (eigenvalue of P) as opposed to relative fitness (normalized per T , as in Figure 2 in main text). Areas of $\text{log}(\lambda) < 0$ would represent negative long-term population growth, therefore potential troughs in evolutionary trajectories. These areas are shown in gray, appearing in the bottom-left corner of the μ landscape and top-left corner of the f landscape. Curves of optimal life history across T are identical to those in relative fitness landscapes, and do not cross areas of $\text{log}(\lambda) < 0$. The general incline in $\text{log}(\lambda)$ as T increases is a result of higher long-term population growth due to less frequent disturbances.

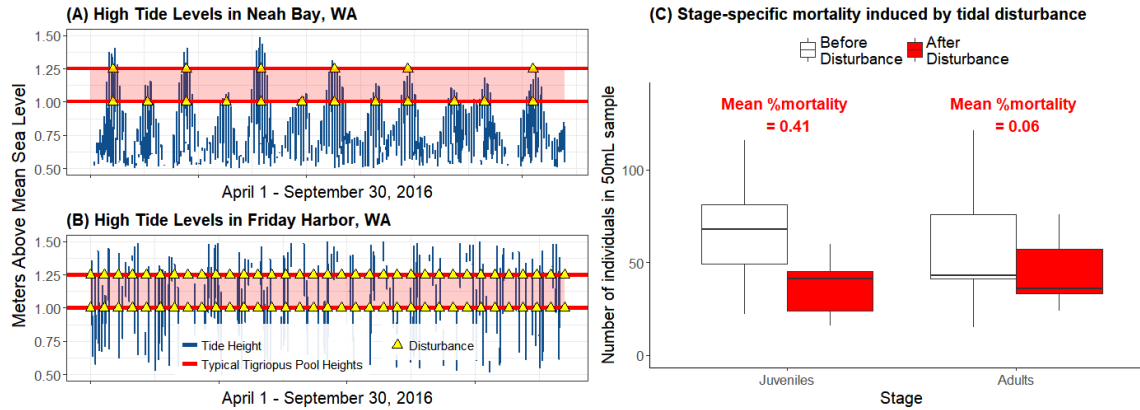


Figure SI-1.3 High tide periodicity regimes in Neah Bay (A) and Friday Harbor (B) in northern Washington, which are near the mouth of and further inside the Strait of Juan de Fuca respectively. Data are hourly tide heights from NOAA’s National Data Buoy Center (Stations # 9449880 and # 9443090 respectively). Red lines that bound red shaded areas show typical range of heights where *T. californicus* populations are found on rocky shores. Yellow triangles show hypothetical disturbance events when high tide reaches height of a *T. californicus* pool, to illustrate that pools in Neah Bay are generally subject to longer periods and a wider spectrum of periods, and pools in Friday Harbor are generally subject to shorter periods. Disturbance events generally induce higher mortality in juveniles than adults (C), incurring not only population decline but also structural perturbation.

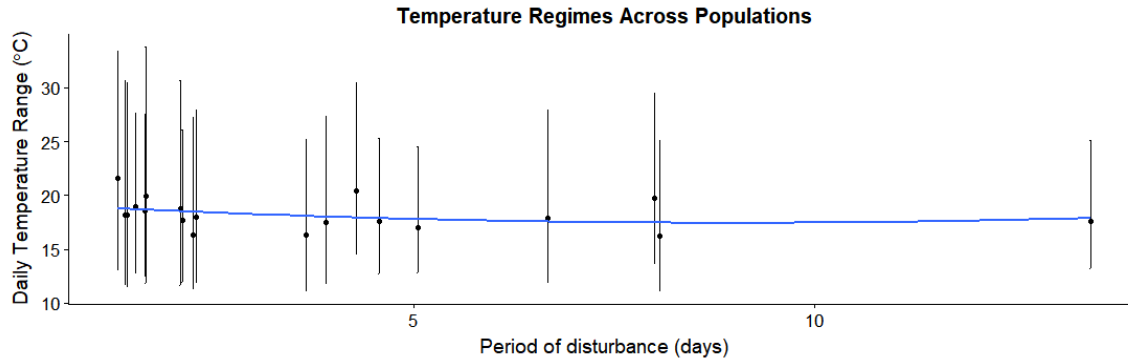


Figure SI-1.4 Temperature regimes of sample populations plotted against pools' tidal disturbance periods (data in Table S1), between June – September 2017. Point is mean daily mean temperature, and line spans mean daily minimum and mean daily maximum temperature per pool. Blue curve is second order polynomial fit on mean daily means. Generalized linear model (Mean daily mean \sim Period) showed non-significant difference across pools ($p = 0.28$).

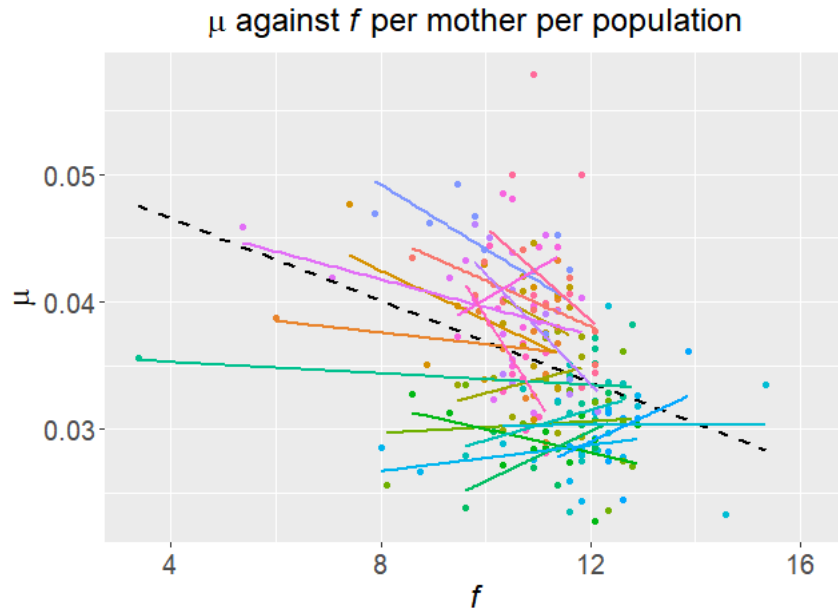


Figure SI-1.5 Observed trade-offs between μ and f per mother in each population. Each point is a pair of a mother (used for f measurement) and her clutch (used for μ measurement), and 19 independent populations are represented by different colors. Dashed black line is the regression of μ against f across all populations.

SI-1.4 SUPPLEMENTARY TABLES

Population #	Region	Period	Daily Min °C	Daily Mean °C	Daily Max °C
1181396	FH	8	13.556	19.693	29.477
20148877	FH	1.646	11.875	19.961	33.808
20148879	FH	1.3	13.052	21.56	33.413
2276020	FH	1.64	12.38	18.575	27.585
2278765	NB	8.067	11.067	16.209	25.123
2292396	NB	3.903	11.88	17.513	27.349
2401944	NB	4.56	12.755	17.618	25.273
906044	FH	1.414	11.501	18.179	30.421
9742335	NB	13.444	13.238	17.588	25.143
20148874	FH	2.079	11.656	18.757	30.623
20148876	FH	1.39	11.642	18.201	30.701
20148878	FH	2.103	11.958	17.677	26.048
2276018	FH	1.519	12.706	18.947	27.657
2276206	NB	2.236	11.233	16.361	27.273
2278766	NB	6.667	11.838	17.898	27.939
2382989	NB	3.655	11.154	16.303	25.168
906035	FH	2.278	11.842	17.997	27.966
9742332	NB	5.043	12.827	16.996	24.568
9742339	FH	4.278	14.493	20.424	30.471

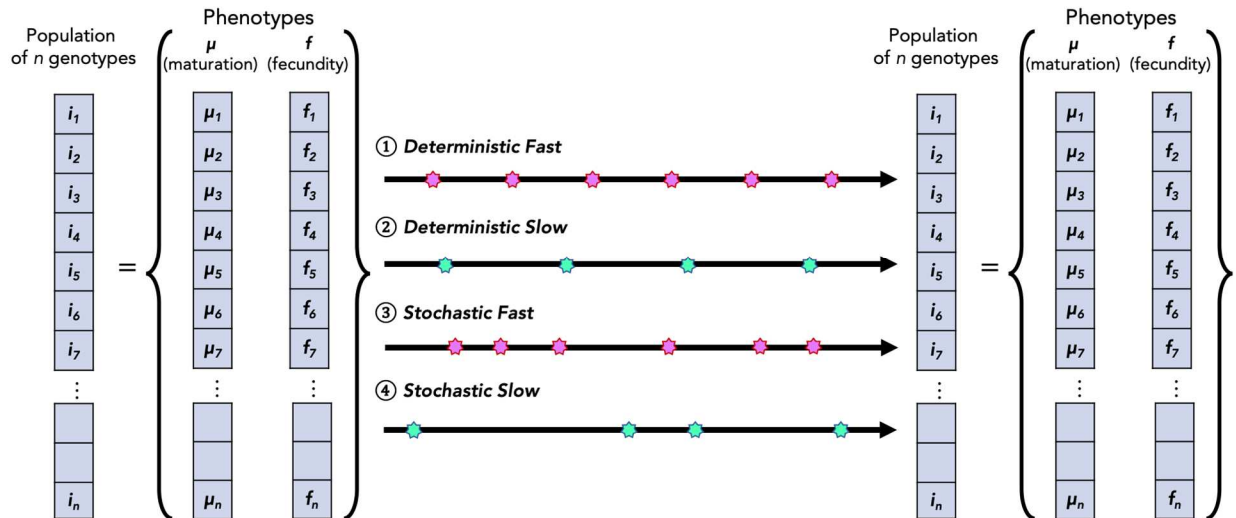
Table SI-1.1 Temperature regimes of all 19 sample pools decomposed into mean daily min, mean daily mean, and mean daily max (plotted in Fig. S1). Population # is arbitrary codes of HOBO temperature loggers that were used to obscure association of each pool with its region or disturbance regime while conducting analyses. “FH” is Friday Harbor and “NB” is Neah Bay. Period is result of time series analysis for each pool’s 5-minute interval temperature data over the summer of 2017 that detected signals of wave disturbance and their intervals.

Model (Trade-off)	Log-likelihood	Panel in Figure S2
$\mu \leftrightarrow d$	429.228	<i>A</i>
$\mu \leftrightarrow f$	431.774	<i>B</i>
$\mu \leftrightarrow \gamma$	429.228	<i>C</i>
$d \leftrightarrow f$	429.228	<i>D</i>
$d \leftrightarrow \gamma$	429.228	<i>E</i>
$f \leftrightarrow \gamma$	429.228	<i>F</i>
$d \leftrightarrow \mu \leftrightarrow f$	441.527	<i>G</i>
$d \leftrightarrow \mu \leftrightarrow \gamma$	431.431	<i>H</i>
$f \leftrightarrow \mu \leftrightarrow \gamma$	429.228	<i>I</i>
$\mu \leftrightarrow f \leftrightarrow d$	429.228	<i>J</i>
$\mu \leftrightarrow f \leftrightarrow \gamma$	441.709	<i>K</i>
$d \leftrightarrow f \leftrightarrow \gamma$	441.120	<i>L</i>
$\mathbf{d} \leftrightarrow \boldsymbol{\mu} \leftrightarrow \mathbf{f} \leftrightarrow \boldsymbol{\gamma}$	441.771	<i>M</i>

Table SI-1.2 Log-likelihoods of all models, obtained by maximum likelihood search through the space of $S_A \geq S_J$ (stage-specific mortalities associated with cyclical disturbance), while simultaneously fitting μ and f . Arrows denote trade-offs between life history traits. Model variants have different trade-off inclusions, but have the same number of estimated parameters because linear trade-offs were included computationally by setting parameter ranges of those traits in opposing (increasing vs. decreasing) order. Therefore model comparison criteria that penalize number of parameters were not needed. Highlighted (last model) is the best (likelihood-maximizing) model, which is reproduced as Figure 2 in the main text.

Appendix II: Supporting Information for Chapter 3 (Slower environmental cycles increase life-history variation within populations)

SI-2.1 Simulation schematic



Simulated populations are vectors of individuals, whose identities are defined by a pair of phenotypes μ (maturation rate) and f (fecundity). Each individual's continuous state $[0,3.0]$ is tracked throughout the simulation. Individuals grow, reproduce, and die following the below rules, and the population vector grows and shrinks through time accordingly.

Demographic dynamics

1. Individuals grow at their innate maturation rates (μ).
2. Individuals become mature at a certain point (state = 1.0), and start reproducing (adding new individuals to the population vector).
3. Offspring phenotypes are copies of the parent's (more specifically, their mother's, since mating is not modelled) with some error (e.g. recombination, mutation).

4. Juvenile maturation rate (μ) has a linear trade-off with juvenile intrinsic survival per time step (i.e. higher μ = higher mortality probability), and adult fecundity (f) has a linear trade-off with adult intrinsic survival (i.e. higher f = higher mortality probability).
5. Nonlinear density-dependent mortality applies equally across all individuals of all states.
6. Individuals senesce and die (excised from population vector) when they reach state = 3.0.

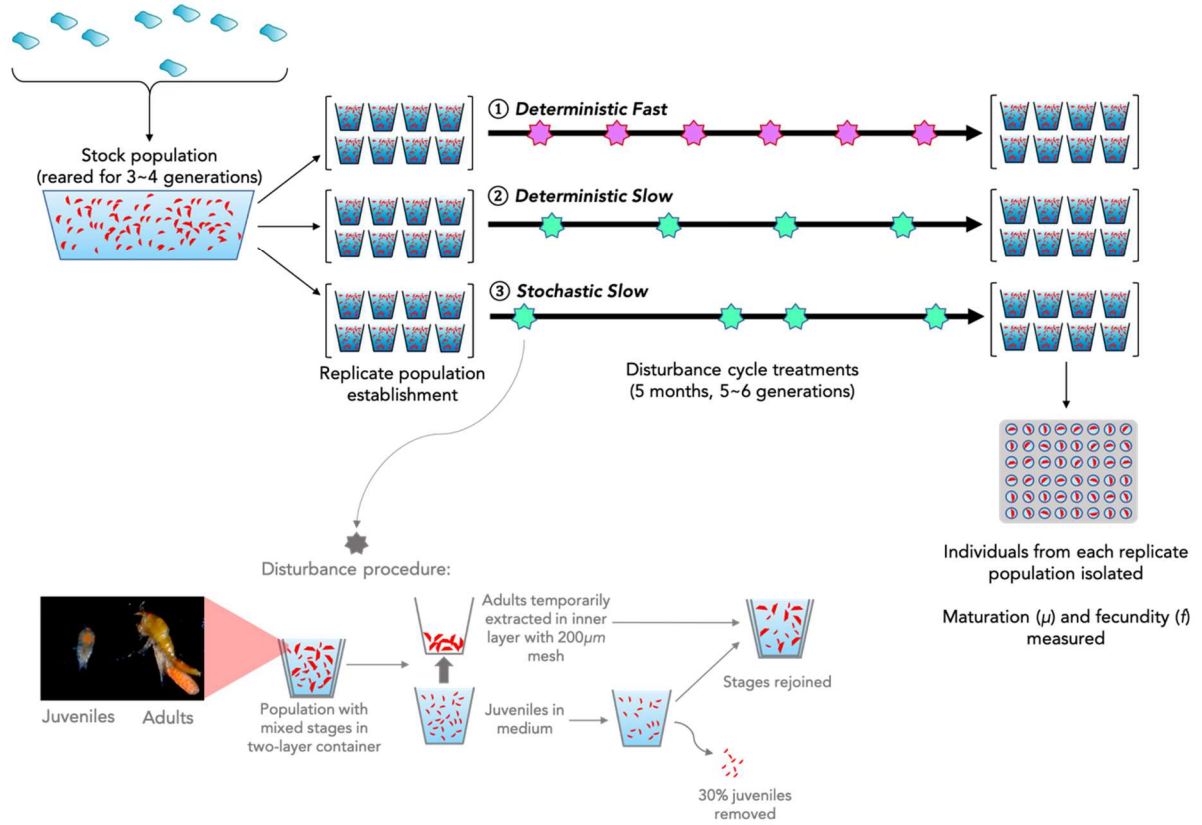
Periodic disturbance-induced death

1. The external environment disturbs the population, introducing stage-structure perturbation (i.e. heightened juvenile mortality) mirroring what happens in nature as well as what was administered in the lab experiment.
2. Four regimes were investigated as shown above – deterministic Fast, deterministic Slow, and stochastic analogs of each wherein the number of disturbances within the duration of the simulation was equal to their counterparts but intervals were random.

To study the dynamics of means and variances of phenotypes within simulated populations, we tracked the distributions of phenotypes represented by individuals of all states through time.

SI-2.2 Experimental schematic

Tidepool collection of *Tigriopus californicus*



SI-2.3 Permutation distributions of experimental population variances

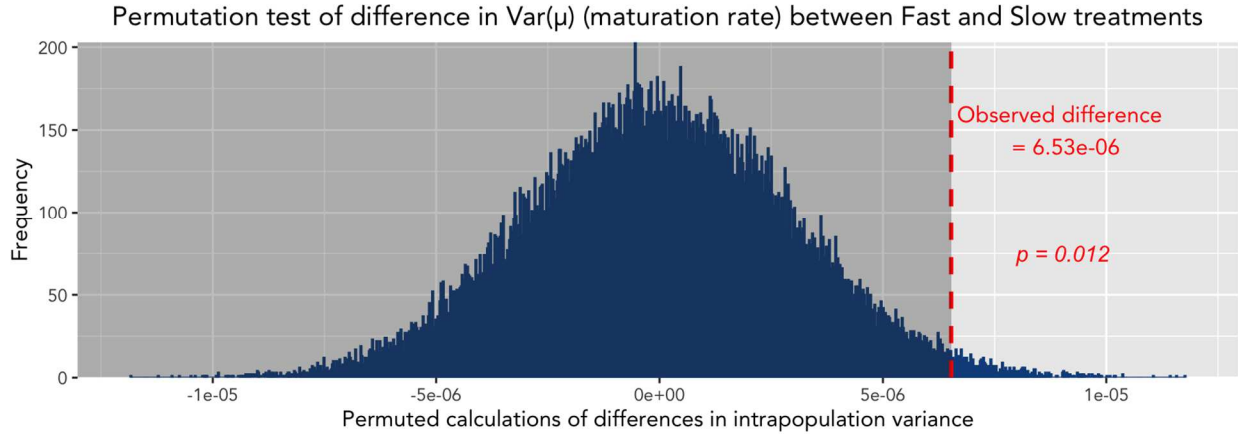


Figure SI-2.1 Permutation distribution used to calculate the p-value of the disparity between intrapopulation maturation rate variances of deterministic Fast and Slow treatment populations.

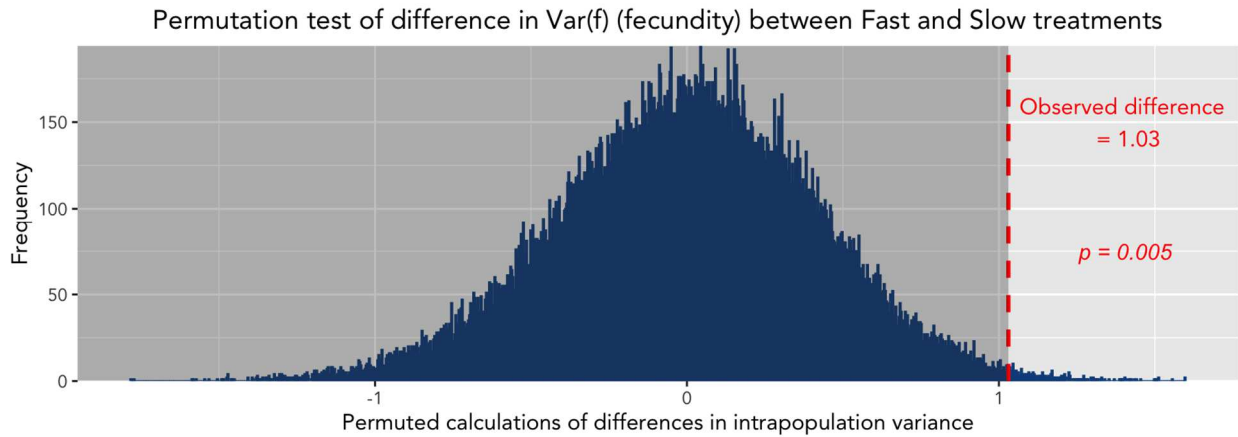


Figure SI-2.2 Permutation distribution used to calculate the p-value of the disparity between intrapopulation fecundity variances of deterministic Fast and Slow treatment populations.

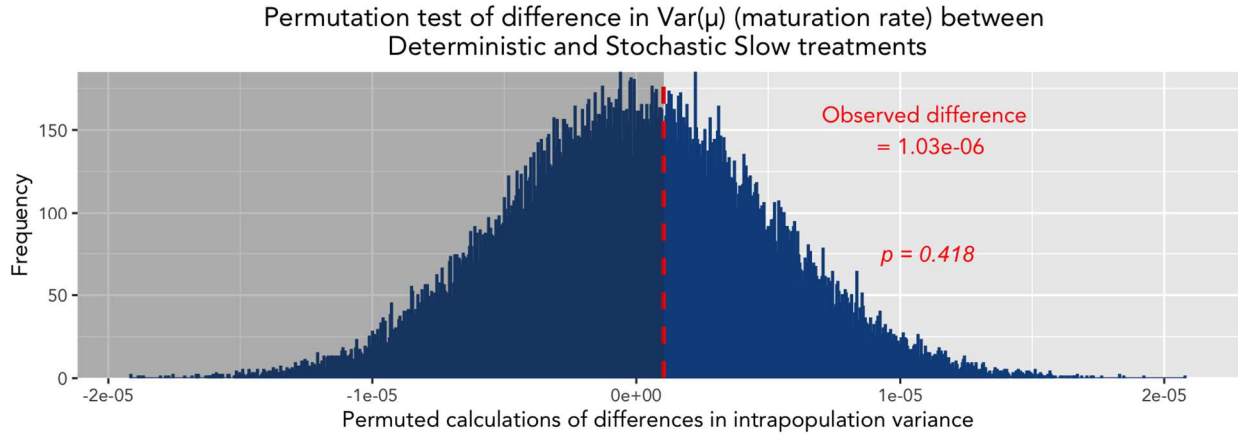


Figure SI-2.3 Permutation distribution used to calculate the p-value of the disparity between intrapopulation maturation rate variances of deterministic and stochastic Slow treatment populations.

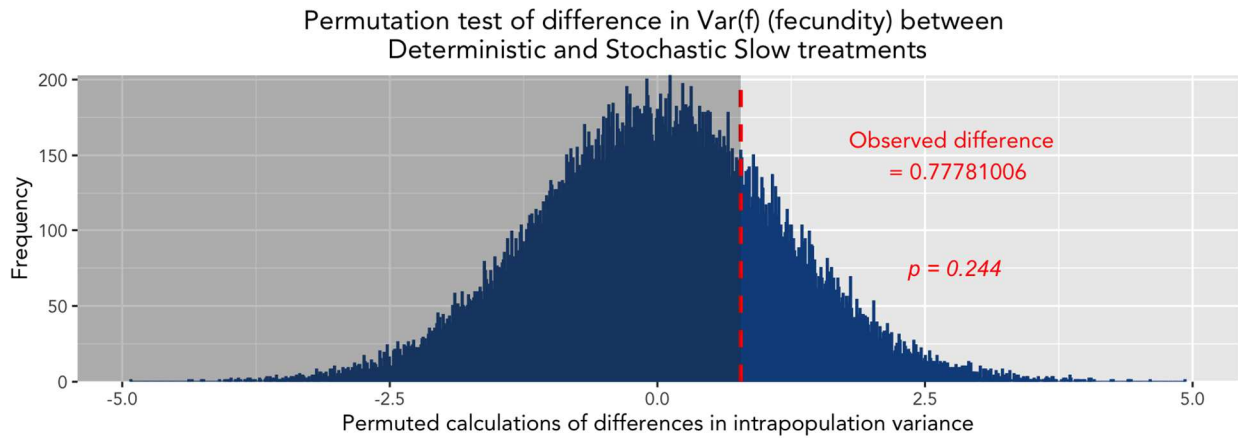


Figure SI-2.4 Permutation distribution used to calculate the p-value of the disparity between intrapopulation fecundity variances of deterministic and stochastic Slow treatment populations.

SI-2.4 Phenotypic means in experimental populations

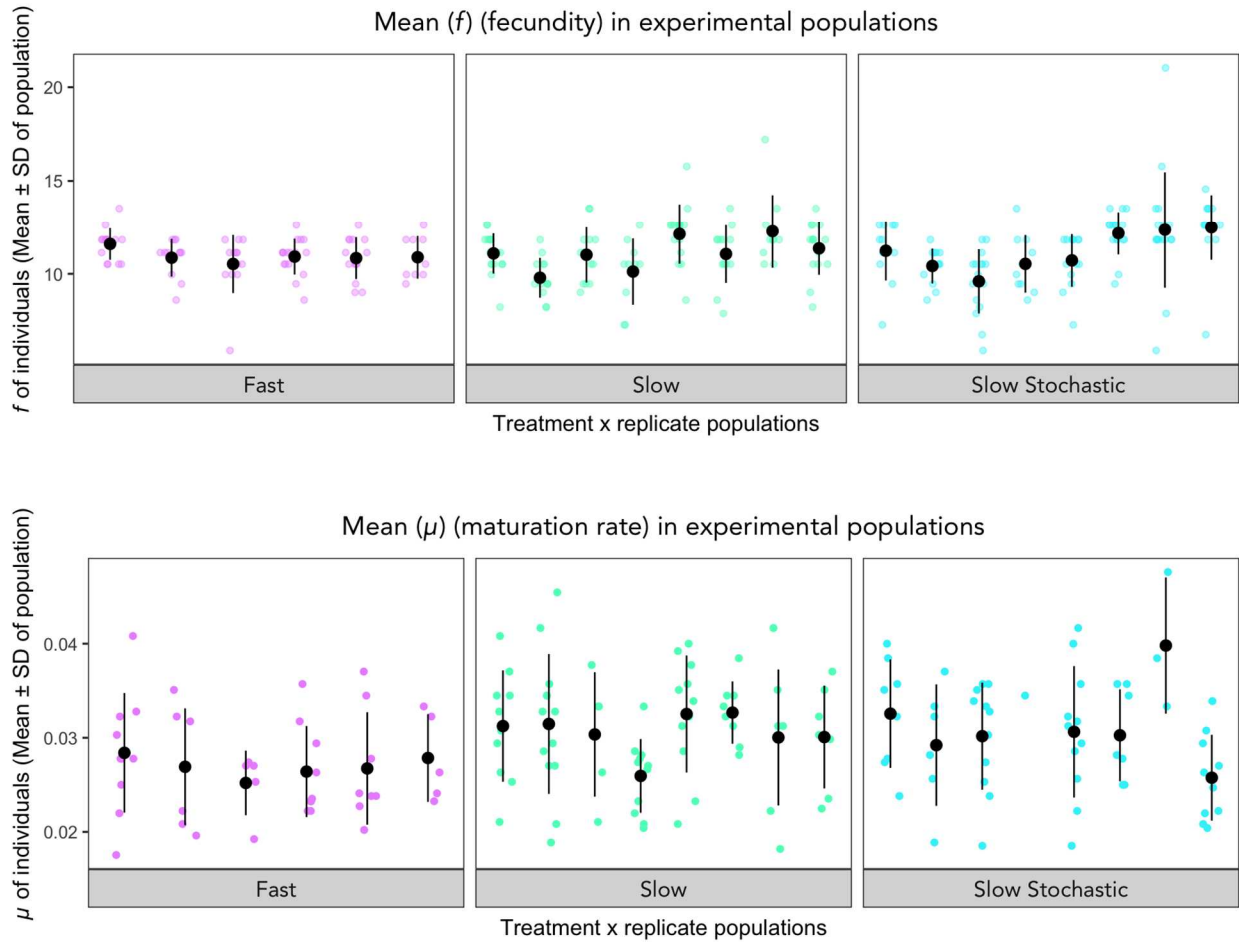


Figure SI-2.5 Phenotypic measurements from selection experiment. Colored scatter points show individual measurements, and black dots with bars show mean \pm sd of each replicate population. Panels show replicate populations of each treatment.

Trait	Treatment comparison	p-value
f	Fast vs. Slow	0.345
(reproductive rate)	Deterministic Slow vs. Stochastic Slow	0.879
μ	Fast vs. Slow	0.013
(maturation rate)	Deterministic Slow vs. Stochastic Slow	0.879

Table SI-2.1 Tests of differences in phenotypic means at the replicate population level. P-values are from two-tailed nonparametric Mann-Whitney tests using population means (black dots in Fig. SI-2.5).

SI-2.5 Deterministic vs. stochastic variance trajectories and endpoints

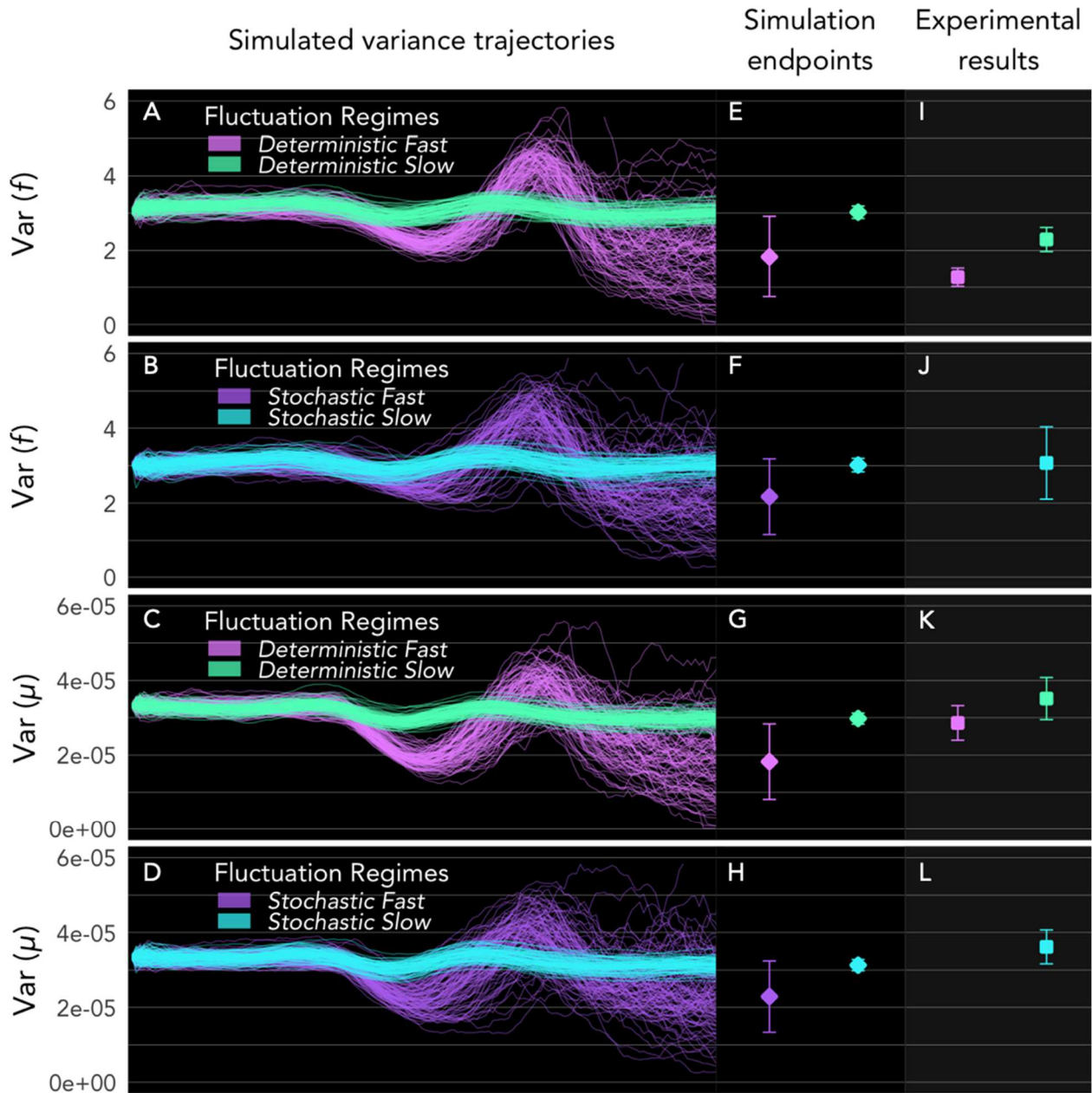


Figure SI-2.6 Intrapopulation variance trajectories of fecundity (f) and maturation rate (μ) in deterministic and stochastic simulation iterations. The deterministic panels (first and third rows; panels A, E & I, and C, G & K) are identical to Fig. 4 of main text. The second and fourth rows (panels B, F & J, and D, H & L) are the stochastic analogs. Note that in panels J and L, there is only one treatment, Stochastic Slow.

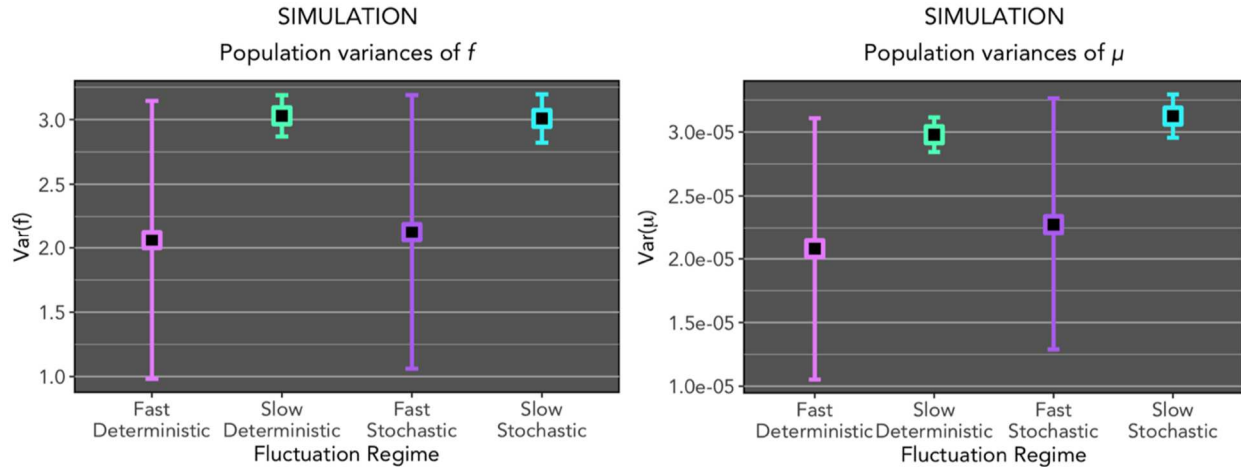


Figure SI-2.7 Simulation endpoint variances (identical data as second column of Fig. SI-2.6, presented for easier visual comparisons across treatments).

Trait	Simulation regime variance comparison	T-statistic	p-value
f (fecundity)	Deterministic Fast vs. Deterministic Slow	6.307	<0.001
	Stochastic Slow vs. Stochastic Fast	8.397	<0.001
	Deterministic Slow vs. Stochastic Slow	0.904	0.368
	Deterministic Fast vs. Stochastic Fast	-1.209	0.229
μ (maturation rate)	Deterministic Fast vs. Deterministic Slow	6.289	<0.001
	Stochastic Slow vs. Stochastic Fast	8.549	<0.001
	Deterministic Slow vs. Stochastic Slow	-6.72	<0.001
	Deterministic Fast vs. Stochastic Fast	-2.071	0.04

Table SI-2.2 Comparisons of intrapopulation phenotypic variances between simulation realizations. Welch’s two-sample t-tests with log-transformed measures of variance showed strong differences between Fast and Slow regimes for both traits, both in statistical significance and magnitude. Deterministic and stochastic analogs produced smaller, and less significant differences in intrapopulation variance overall (though more significant for μ than f).

SI-2.6 Population structure and size dynamics in simulations

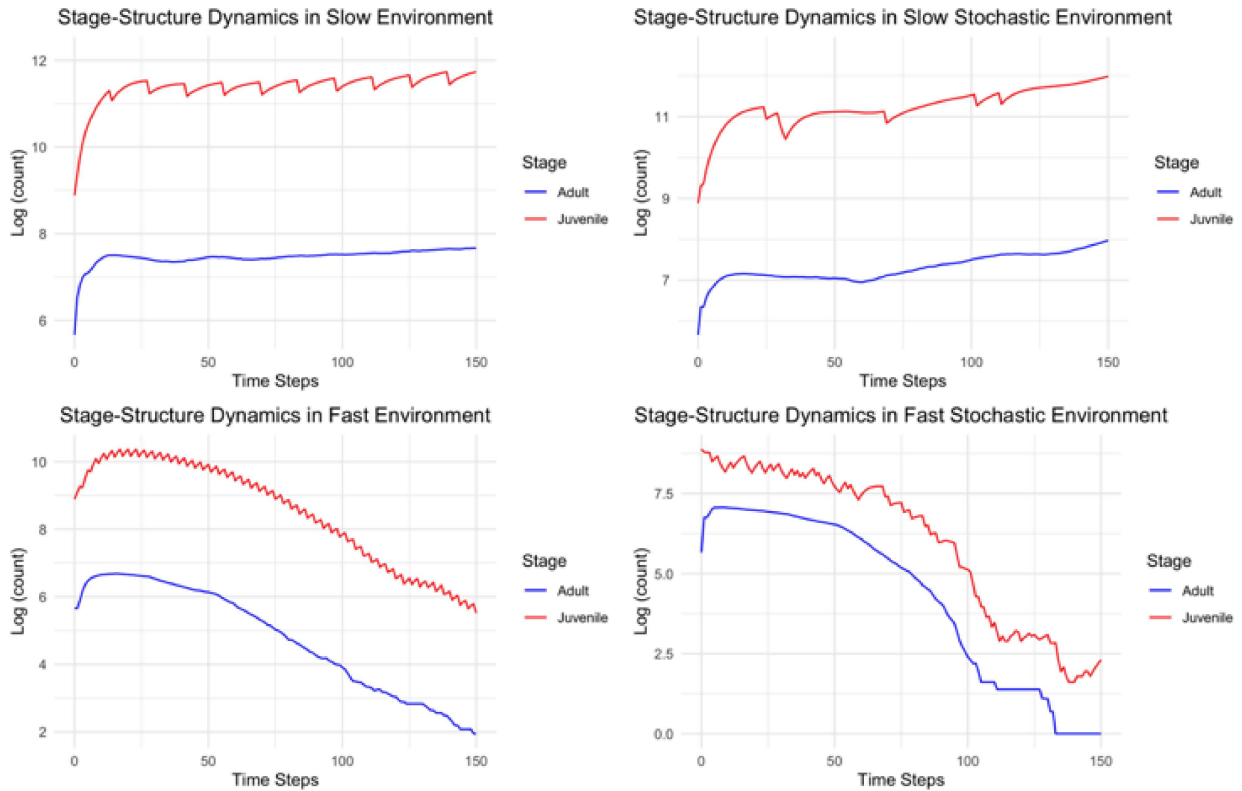


Figure SI-2.8 Stage-structure dynamics in deterministically and stochastically slow and fast regimes in one representative realization of the simulation.

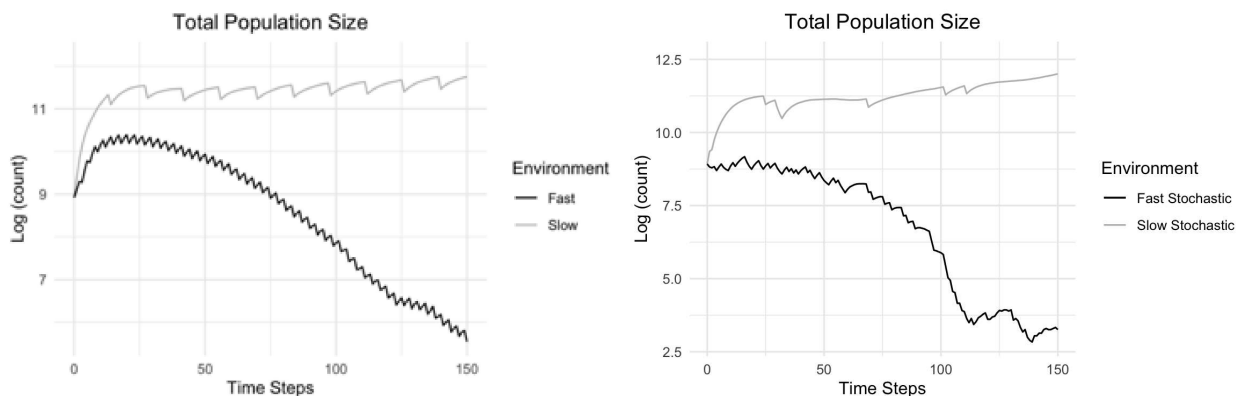


Figure SI-2.9 Population size dynamics in deterministically and stochastically slow and fast regimes in one representative realization of the simulation.

References

- Angert, A., S. Biraud, C. Bonfils, C. C. Henning, W. Buermann, J. Pinzon, C. J. Tucker, et al. 2005. Drier summers cancel out the CO₂ uptake enhancement induced by warmer springs. *Proceedings of the National Academy of Sciences* 102:10823–10827.
- Barnett, C. J., and J. E. Kontogiannis. 1975. The effect of crude oil fractions on the survival of a tidepool copepod, *Tigriopus californicus*. *Environmental Pollution* (1970) 8:45–54.
- Bartomeus, I., J. S. Ascher, D. Wagner, B. N. Danforth, S. Colla, S. Kornbluth, and R. Winfree. 2011. Climate-associated phenological advances in bee pollinators and bee-pollinated plants. *Proceedings of the National Academy of Sciences* 201115559.
- Bell, G. 2010. Fluctuating selection: the perpetual renewal of adaptation in variable environments. *Philosophical Transactions of the Royal Society B: Biological Sciences* 365:87–97.
- Bolnick, D. I., P. Amarasekare, M. S. Araújo, R. Bürger, J. M. Levine, M. Novak, V. H. W. Rudolf, et al. 2011. Why intraspecific trait variation matters in community ecology. *Trends in Ecology & Evolution* 26:183–192.
- Both, C., M. Van Asch, R. G. Bijlsma, A. B. Van Den Burg, and M. E. Visser. 2009. Climate change and unequal phenological changes across four trophic levels: constraints or adaptations? *Journal of Animal Ecology* 78:73–83.
- Bradshaw, W. E., and C. M. Holzapfel. 2008. Genetic response to rapid climate change: it's seasonal timing that matters. *Molecular ecology* 17:157–166.
- Bull, J. J. 1987. Evolution of Phenotypic Variance. *Evolution* 41:303–315.
- Burghardt, L. T., C. J. E. Metcalf, A. M. Wilczek, J. Schmitt, and K. Donohue. 2015. Modeling the Influence of Genetic and Environmental Variation on the Expression of Plant Life Cycles across Landscapes. *The American Naturalist* 185:212–227.
- Burton, R. S. 1985. Mating system of the intertidal copepod *Tigriopus californicus*. *Marine Biology* 86:247–252.
- Burton, R. S. 1987. Differentiation and integration of the genome in populations of the marine copepod *Tigriopus californicus*. *Evolution* 41:504–513.
- Burton, R. S. 1997. Genetic evidence for long term persistence of marine invertebrate populations in an ephemeral environment. *Evolution* 51:993–998.
- Burton, R., M. Feldman, and J. Curtsinger. 1979. Population Genetics of *Tigriopus californicus* (Copepoda: Harpacticoida): I. Population Structure Along the Central California Coast. *Marine Ecology Progress Series* 1:29–39.

- Burton, R. S., and M. W. Feldman. 1981. Population Genetics of *Tigriopus Californicus*. II. Differentiation Among Neighboring Populations. *Evolution* 35:1192–1205.
- Canino-Koning, R., M. J. Wiser, and C. Ofria. 2019. Fluctuating environments select for short-term phenotypic variation leading to long-term exploration. *PLOS Computational Biology* 15:e1006445.
- CaraDonna, P. J., A. M. Iler, and D. W. Inouye. 2014. Shifts in flowering phenology reshape a subalpine plant community. *Proceedings of the National Academy of Sciences* 111:4916–4921.
- Caswell, H. 2001. *Matrix population models: construction, analysis, and interpretation*. Sinauer Associates, Sunderland, Mass.
- Caswell, H., and M. C. Trevisan. 1994. Sensitivity Analysis of Periodic Matrix Models. *Ecology* 75:1299–1303.
- Charlesworth, B. 1990. Optimization models, quantitative genetics, and mutation. *Evolution* 44:520–538.
- Charlesworth, B. 1994. *Evolution in age-structured populations (Vol. 2)*. Cambridge University Press Cambridge.
- Charnov, E. L., and W. M. Schaffer. 1973. Life-history consequences of natural selection: Cole's result revisited. *The American Naturalist* 107:791–793.
- Charnov, E. L., T. F. Turner, and K. O. Winemiller. 2001. Reproductive constraints and the evolution of life histories with indeterminate growth. *Proceedings of the National Academy of Sciences* 98:9460–9464.
- Childs, D. Z., C. J. E. Metcalf, and M. Rees. 2010. Evolutionary bet-hedging in the real world: empirical evidence and challenges revealed by plants. *Proceedings of the Royal Society of London B: Biological Sciences* 277:3055–3064.
- Chuine, I. 2010. Why does phenology drive species distribution? *Philosophical Transactions of the Royal Society of London B: Biological Sciences* 365:3149–3160.
- Chmura, H. E., H. M. Kharouba, J. Ashander, S. M. Ehlman, E. B. Rivest, and L. H. Yang. 2019. The mechanisms of phenology: the patterns and processes of phenological shifts. *Ecological Monographs* 89:e01337.
- Cleland, E. E., I. Chuine, A. Menzel, H. A. Mooney, and M. D. Schwartz. 2007. Shifting plant phenology in response to global change. *Trends in Ecology & Evolution* 22:357–365.
- Cohen, A. A., C. Isaksson, and R. Salguero-Gómez. 2017. Co-existence of multiple trade-off currencies shapes evolutionary outcomes. *PLOS ONE* 12:e0189124.

- Cohen, J. M., M. J. Lajeunesse, and J. R. Rohr. 2018. A global synthesis of animal phenological responses to climate change. *Nature Climate Change* 8:224–228.
- Cole, L. C. 1954. The population consequences of life history phenomena. *The Quarterly Review of Biology* 29:103–137.
- Cook, R. E. 1979. Patterns of Juvenile Mortality and Recruitment in Plants. Pages 207–231 *in* *Topics in Plant Population Biology*. Palgrave, London.
- Coulson, T., and S. Tuljapurkar. 2008. The Dynamics of a Quantitative Trait in an Age-Structured Population Living in a Variable Environment. *The American Naturalist* 172:599–612.
- Dethier, M. N. 1980. Tidepools as refuges: Predation and the limits of the harpacticoid copepod *Tigriopus californicus* (Baker). *Journal of Experimental Marine Biology and Ecology* 42:99–111.
- Dybdahl, M. F. 1995. Selection on life-history traits across a wave exposure gradient in the tidepool copepod *Tigriopus californicus* (Baker). *Journal of Experimental Marine Biology and Ecology* 192:195–210.
- Easterling, D. R., G. A. Meehl, C. Parmesan, S. A. Changnon, T. R. Karl, and L. O. Mearns. 2000. Climate Extremes: Observations, Modeling, and Impacts. *Science* 289:2068–2074.
- Edmands, S. 2001. Phylogeography of the intertidal copepod *Tigriopus californicus* reveals substantially reduced population differentiation at northern latitudes. *Molecular Ecology* 10:1743–1750.
- Edmands, S., and J. S. Harrison. 2003. Molecular and quantitative trait variation within and among populations of the intertidal copepod *tigriopus californicus*. *Evolution* 57:2277–2285.
- Edwards, M., and A. J. Richardson. 2004. Impact of climate change on marine pelagic phenology and trophic mismatch. *Nature* 430:881–884.
- Ehrlén, J. 2015. Selection on flowering time in a life-cycle context. *Oikos* 124:92–101.
- Encinas-Viso, F., T. A. Revilla, and R. S. Etienne. 2012. Phenology drives mutualistic network structure and diversity. *Ecology Letters* 15:198–208.
- Engen, S., J. Wright, Y. G. Araya-Ajoy, and B.-E. Sæther. 2020. Phenotypic evolution in stochastic environments: The contribution of frequency- and density-dependent selection. *Evolution* 74:1923–1941.
- Ernande, B., U. Dieckmann, and M. Heino. 2004. Adaptive changes in harvested populations: plasticity and evolution of age and size at maturation. *Proceedings of the Royal Society of London B: Biological Sciences* 271:415–423.
- Falconer, D. S. 1996. *Introduction to quantitative genetics*. Pearson Education India.

- Fisher, R. A. 1930. The genetical theory of natural selection. The genetical theory of natural selection. Clarendon Press, Oxford, England.
- Forrest, J., and A. J. Miller-Rushing. 2010. Toward a synthetic understanding of the role of phenology in ecology and evolution. *Philosophical Transactions of the Royal Society of London B: Biological Sciences* 365:3101–3112.
- Gadgil, M., and W. H. Bossert. 1970. Life historical consequences of natural selection. *The American Naturalist* 104:1–24.
- Gezon, Z. J., R. J. Lindborg, A. Savage, and J. C. Daniels. 2018. Drifting Phenologies Cause Reduced Seasonality of Butterflies in Response to Increasing Temperatures. *Insects* 9:174.
- Goodman, D. 1982. Optimal Life Histories, Optimal Notation, and the Value of Reproductive Value. *The American Naturalist* 119:803–823.
- Goolish, E. M., and R. S. Burton. 1989. Energetics of Osmoregulation in an Intertidal Copepod: Effects of Anoxia and lipid Reserves on the Pattern of Free Amino Accumulation. *Functional Ecology* 3:81–89.
- Gremer, J. R., and D. L. Venable. 2014. Bet hedging in desert winter annual plants: optimal germination strategies in a variable environment. *Ecology Letters* 17:380–387.
- Gross, K., G. Pasinelli, and H. P. Kunc. 2010. Behavioral Plasticity Allows Short-Term Adjustment to a Novel Environment. *The American Naturalist* 176:456–464.
- Guisan, A., and N. E. Zimmermann. 2000. Predictive habitat distribution models in ecology. *Ecological Modelling* 135:147–186.
- Hairston, N. G., S. P. Ellner, M. A. Geber, T. Yoshida, and J. A. Fox. 2005. Rapid evolution and the convergence of ecological and evolutionary time. *Ecology Letters* 8:1114–1127.
- Hairston, N. G., and W. E. Walton. 1986. Rapid evolution of a life history trait. *Proceedings of the National Academy of Sciences* 83:4831–4833.
- Hamel, S., J.-M. Gaillard, and N. Yoccoz. 2018. Introduction to: Individual heterogeneity – the causes and consequences of a fundamental biological process. *Oikos* 127:643–647.
- Hart, R., and J. Salick. 2018. Vulnerability of phenological progressions over season and elevation to climate change: Rhododendrons of Mt. Yulong. *Perspectives in Plant Ecology, Evolution and Systematics* 34:129–139.
- Hastings, A. 2004. Transients: the key to long-term ecological understanding? *Trends in Ecology & Evolution* 19:39–45.
- Hastings, A., K. C. Abbott, K. Cuddington, T. Francis, G. Gellner, Y.-C. Lai, A. Morozov, et al. 2018. Transient phenomena in ecology. *Science* 361:990+.

- Helm, B., R. Ben-Shlomo, M. J. Sheriff, R. A. Hut, R. Foster, B. M. Barnes, and D. Dominoni. 2013. Annual rhythms that underlie phenology: biological time-keeping meets environmental change. *Proceedings of the Royal Society B: Biological Sciences* 280:20130016.
- Hong, B. C., and J. B. Shurin. 2015. Latitudinal variation in the response of tidepool copepods to mean and daily range in temperature. *Ecology* 96:2348–2359.
- Ims, R. A. 1990. On the Adaptive Value of Reproductive Synchrony as a Predator-Swamping Strategy. *The American Naturalist* 136:485–498.
- Inouye, D. W. 2008. Effects of Climate Change on Phenology, Frost Damage, and Floral Abundance of Montane Wildflowers. *Ecology* 89:353–362.
- Jenouvrier, S., and M. E. Visser. 2011. Climate change, phenological shifts, eco-evolutionary responses and population viability: toward a unifying predictive approach. *International Journal of Biometeorology* 55:905–919.
- Kaiser, T. S., B. Poehn, D. Szkiba, M. Preussner, F. J. Sedlazeck, A. Zrim, T. Neumann, et al. 2016. The genomic basis of circadian and circalunar timing adaptations in a midge. *Nature* 540:69–73.
- Katz, R. W., and B. G. Brown. 1992. Extreme events in a changing climate: Variability is more important than averages. *Climatic Change* 21:289–302.
- Keeley, J. E., and W. J. Bond. 1999. Mast Flowering and Semelparity in Bamboos: The Bamboo Fire Cycle Hypothesis. *The American Naturalist* 154:383–391.
- Keeling, C. D., J. F. S. Chin, and T. P. Whorf. 1996. Increased activity of northern vegetation inferred from atmospheric CO₂ measurements. *Nature* 382:146–149.
- Kelly, M. W., R. K. Grosberg, and E. Sanford. 2013. Trade-Offs, Geography, and Limits to Thermal Adaptation in a Tide Pool Copepod. *The American Naturalist* 181:846–854.
- Kendall, B. E., and G. A. Fox. 2002. Variation among Individuals and Reduced Demographic Stochasticity. *Conservation Biology* 16:109–116.
- Kerr, N. Z., T. Wepprich, F. S. Grevstad, E. B. Dopman, F. S. Chew, and E. E. Crone. 2020. Developmental trap or demographic bonanza? Opposing consequences of earlier phenology in a changing climate for a multivoltine butterfly. *Global Change Biology* 26:2014–2027.
- Kharouba, H. M., and E. M. Wolkovich. 2020. Disconnects between ecological theory and data in phenological mismatch research. *Nature Climate Change* 1–10.
- Kimball, S., A. L. Angert, T. E. Huxman, and D. L. Venable. 2010. Contemporary climate change in the Sonoran Desert favors cold-adapted species. *Global Change Biology* 16:1555–1565.

- Koons, D. N., J. B. Grand, B. Zinner, and R. F. Rockwell. 2005. Transient population dynamics: relations to life history and initial population state. *Ecological modelling* 185:283–297.
- Koons, D. N., D. T. Iles, M. Schaub, and H. Caswell. 2016. A life-history perspective on the demographic drivers of structured population dynamics in changing environments. *Ecology Letters* 19:1023–1031.
- Koons, D. N., C. J. E. Metcalf, and S. Tuljapurkar. 2008. Evolution of Delayed Reproduction in Uncertain Environments: A Life-History Perspective. *The American Naturalist* 172:797–805.
- Koons, D. N., S. Pavard, A. Baudisch, and J. E. Metcalf. 2009. Is life-history buffering or lability adaptive in stochastic environments? *Oikos* 118:972–980.
- Kukul, M. S., and S. Irmak. 2018. U.S. Agro-Climate in 20 th Century: Growing Degree Days, First and Last Frost, Growing Season Length, and Impacts on Crop Yields. *Scientific Reports* 8:6977.
- Lampert, W. 1989. The Adaptive Significance of Diel Vertical Migration of Zooplankton. *Functional Ecology* 3:21–27.
- Lande, R. 2014. Evolution of phenotypic plasticity and environmental tolerance of a labile quantitative character in a fluctuating environment. *Journal of Evolutionary Biology* 27:866–875.
- Lande, R., S. Engen, and B.-E. Sæther. 2017. Evolution of stochastic demography with life history tradeoffs in density-dependent age-structured populations. *Proceedings of the National Academy of Sciences* 114:11582–11590.
- Law, R. 1979. Optimal life histories under age-specific predation. *The American Naturalist* 114:399–417.
- Levin, S. A. 1992. The Problem of Pattern and Scale in Ecology: The Robert H. MacArthur Award Lecture. *Ecology* 73:1943–1967.
- Linderholm, H. W. 2006. Growing season changes in the last century. *Agricultural and Forest Meteorology* 137:1–14.
- Liu, Q., S. Piao, I. A. Janssens, Y. Fu, S. Peng, X. Lian, P. Ciais, et al. 2018. Extension of the growing season increases vegetation exposure to frost. *Nature Communications* 9:426.
- Lynch, M., and B. Walsh. 1998. *Genetics and analysis of quantitative traits* (Vol. 1). Sinauer Sunderland, MA.
- Lytle, D. A. 2001. Disturbance Regimes and Life-History Evolution. *The American Naturalist* 157:525–536.
- Lytle, D. A., and N. L. Poff. 2004. Adaptation to natural flow regimes. *Trends in Ecology & Evolution* 19:94–100.

- MacArthur, R. H., and E. O. Wilson. 1967. *The theory of island biogeography*. Princeton University Press.
- Marlon, J. R., P. J. Bartlein, M. K. Walsh, S. P. Harrison, K. J. Brown, M. E. Edwards, P. E. Higuera, et al. 2009. Wildfire responses to abrupt climate change in North America. *Proceedings of the National Academy of Sciences* 106:2519–2524.
- Menzel, A., T. H. Sparks, N. Estrella, E. Koch, A. Aasa, R. Ahas, K. Alm-Kübler, et al. 2006. European phenological response to climate change matches the warming pattern. *Global Change Biology* 12:1969–1976.
- Metcalf, C. J. E., and D. N. Koons. 2007. Environmental uncertainty, autocorrelation and the evolution of survival. *Proceedings of the Royal Society of London B: Biological Sciences* 274:2153–2160.
- Michod, R. E. 1979. Evolution of life histories in response to age-specific mortality factors. *The American Naturalist* 113:531–550.
- Miller-Rushing, A. J., T. T. Høye, D. W. Inouye, and E. Post. 2010. The effects of phenological mismatches on demography. *Philosophical Transactions of the Royal Society B: Biological Sciences* 365:3177–3186.
- Moran, E. V., F. Hartig, and D. M. Bell. 2016. Intraspecific trait variation across scales: implications for understanding global change responses. *Global Change Biology* 22:137–150.
- Moran, N. A. 1992. The Evolutionary Maintenance of Alternative Phenotypes. *The American Naturalist* 139:971–989.
- Moritz, M. A., M.-A. Parisien, E. Batllori, M. A. Krawchuk, J. V. Dorn, D. J. Ganz, and K. Hayhoe. 2012. Climate change and disruptions to global fire activity. *Ecosphere* 3:art49.
- Moyes, K., D. H. Nussey, M. N. Clements, F. E. Guinness, A. Morris, S. Morris, J. M. Pemberton, et al. 2011. Advancing breeding phenology in response to environmental change in a wild red deer population. *Global Change Biology* 17:2455–2469.
- Olsen, E. M., M. Heino, G. R. Lilly, M. J. Morgan, J. Brattey, B. Ernande, and U. Dieckmann. 2004. Maturation trends indicative of rapid evolution preceded the collapse of northern cod. *Nature* 428:932–935.
- Orzack, S. H. 1993. Life History Evolution and Population Dynamics in Variable Environments: Some Insights from Stochastic Demography. Pages 63–104 *in* *Adaptation in Stochastic Environments*, Lecture Notes in Biomathematics. Springer, Berlin, Heidelberg.
- Orzack, S. H., and S. Tuljapurkar. 2001. Reproductive Effort in Variable Environments, or Environmental Variation Is for the Birds. *Ecology* 82:2659–2665.

- Ozgul, A., D. Z. Childs, M. K. Oli, K. B. Armitage, D. T. Blumstein, L. E. Olson, S. Tuljapurkar, et al. 2010. Coupled dynamics of body mass and population growth in response to environmental change. *Nature* 466:482–485.
- Paniw, M., A. Ozgul, and R. Salguero-Gómez. 2018. Interactive life-history traits predict sensitivity of plants and animals to temporal autocorrelation. *Ecology Letters* 21:275–286.
- Park, J. S. 2019. Cyclical environments drive variation in life-history strategies: a general theory of cyclical phenology. *Proceedings of the Royal Society B: Biological Sciences* 286:20190214.
- Parmesan, C. 2006. Ecological and Evolutionary Responses to Recent Climate Change. *Annual Review of Ecology, Evolution, and Systematics* 37:637–669.
- Parmesan, C., and G. Yohe. 2003. A globally coherent fingerprint of climate change impacts across natural systems. *Nature* 421:37–42.
- Pau, S., E. M. Wolkovich, B. I. Cook, T. J. Davies, N. J. Kraft, K. Bolmgren, J. L. Betancourt, et al. 2011. Predicting phenology by integrating ecology, evolution and climate science. *Global Change Biology* 17:3633–3643.
- Pease, C. M., and J. J. Bull. 1988. A critique of methods for measuring life history trade-offs. *Journal of Evolutionary Biology* 1:293–303.
- Piao, S., Q. Liu, A. Chen, I. A. Janssens, Y. Fu, J. Dai, L. Liu, et al. 2019. Plant phenology and global climate change: Current progresses and challenges. *Global Change Biology* 25:1922–1940.
- Piao, S., X. Wang, T. Park, C. Chen, X. Lian, Y. He, J. W. Bjerke, et al. 2020. Characteristics, drivers and feedbacks of global greening. *Nature Reviews Earth & Environment* 1:14–27.
- Post, E. 2019. *Time in ecology: a theoretical framework [MPB 61] (Vol. 61)*. Princeton University Press.
- Post, E., and M. Avery. 2019. Phenological dynamics in pollinator-plant associations related to climate change. Pages 42–54 *in* T. E. Lovejoy and E. O. Wilson, eds. *Biodiversity and Climate Change*. Yale University Press.
- Post, E., M. C. Forchhammer, N. C. Stenseth, and T. V. Callaghan. 2001. The timing of life-history events in a changing climate. *Proceedings of the Royal Society of London B: Biological Sciences* 268:15–23.
- Post, E., J. Kerby, C. Pedersen, and H. Steltzer. 2016. Highly individualistic rates of plant phenological advance associated with arctic sea ice dynamics. *Biology letters* 12:20160332.
- Post, E. S., C. Pedersen, C. C. Wilmers, and M. C. Forchhammer. 2008. Phenological sequences reveal aggregate life history response to climatic warming. *Ecology* 89:363–370.

- Post, E., B. A. Steinman, and M. E. Mann. 2018. Acceleration of phenological advance and warming with latitude over the past century. *Scientific reports* 8:1–8.
- Post, E., and N. C. Stenseth. 1999. Climatic variability, plant phenology, and northern ungulates. *Ecology* 80:1322–1339.
- Powlik, J. J. 1998. Seasonal abundance and population flux of *Tigriopus californicus* (Copepoda: Harpacticoida) in Barkley sound, British Columbia. *Journal of the Marine Biological Association of the United Kingdom* 78:467–481.
- Powlik, J. J. 1999. Habitat characters of *Tigriopus californicus* (Copepoda: Harpacticoida), with notes on the dispersal of supralittoral fauna. *Journal of the Marine Biological Association of the United Kingdom* 79:85–92.
- Prevéy, J. S., C. Rixen, N. Rüger, T. T. Høye, A. D. Bjorkman, I. H. Myers-Smith, S. C. Elmendorf, et al. 2019. Warming shortens flowering seasons of tundra plant communities. *Nature Ecology & Evolution* 3:45.
- Primack, R. B., I. Ibáñez, H. Higuchi, S. D. Lee, A. J. Miller-Rushing, A. M. Wilson, and J. A. Silander. 2009. Spatial and interspecific variability in phenological responses to warming temperatures. *Biological Conservation* 142:2569–2577.
- Rathcke, B., and E. P. Lacey. 1985. Phenological Patterns of Terrestrial Plants. *Annual Review of Ecology and Systematics* 16:179–214.
- Reed, T. E., P. Gienapp, and M. E. Visser. 2015. Density dependence and microevolution interactively determine effects of phenology mismatch on population dynamics. *Oikos* 124:81–91.
- Rommel, T., T. Tammaru, and M. Maegi. 2009. Seasonal mortality trends in tree-feeding insects: a field experiment. *Ecological Entomology* 34:98–106.
- Reznick, D. 1982. The impact of predation on life history evolution in Trinidadian guppies: genetic basis of observed life history patterns. *Evolution* 36:1236–1250.
- Reznick, D. N., M. J. Butler, F. H. Rodd, and P. Ross. 1996. Life-history evolution in guppies (*Poecilia reticulata*) 6. Differential mortality as a mechanism for natural selection. *Evolution* 50:1651–1660.
- Richardson, A. D., T. A. Black, P. Ciais, N. Delbart, M. A. Friedl, N. Gobron, D. Y. Hollinger, et al. 2010. Influence of spring and autumn phenological transitions on forest ecosystem productivity. *Philosophical Transactions of the Royal Society of London B: Biological Sciences* 365:3227–3246.
- Richardson, A. D., K. Hufkens, T. Milliman, D. M. Aubrecht, M. E. Furze, B. Seyednasrollah, M. B. Krassovski, et al. 2018. Ecosystem warming extends vegetation activity but heightens vulnerability to cold temperatures. *Nature* 560:368–371.

- Ricklefs, R. E. 1987. Community Diversity: Relative Roles of Local and Regional Processes. *Science* 235:167–171.
- Roff, D. A. 1984. The Evolution of Life History Parameters in Teleosts. *Canadian Journal of Fisheries and Aquatic Sciences* 41:989–1000.
- Roff, D. A., E. Heibo, and L. A. Vøllestad. 2006. The importance of growth and mortality costs in the evolution of the optimal life history. *Journal of evolutionary biology* 19:1920–1930.
- Rudolf, V. H. W., and S. McCrory. 2018. Resource limitation alters effects of phenological shifts on inter-specific competition. *Oecologia* 188:515–523.
- Salguero-Gómez, R., O. R. Jones, E. Jongejans, S. P. Blomberg, D. J. Hodgson, C. Mbeau-Ache, P. A. Zuidema, et al. 2016. Fast–slow continuum and reproductive strategies structure plant life-history variation worldwide. *Proceedings of the National Academy of Sciences* 113:230–235.
- Sæther, B.-E., and S. Engen. 2015. The concept of fitness in fluctuating environments. *Trends in Ecology & Evolution* 30:273–281.
- Schär, C., P. L. Vidale, D. Lüthi, C. Frei, C. Häberli, M. A. Liniger, and C. Appenzeller. 2004. The role of increasing temperature variability in European summer heatwaves. *Nature* 427:332–336.
- Schauber, E. M., D. Kelly, P. Turchin, C. Simon, W. G. Lee, R. B. Allen, I. J. Payton, et al. 2002. Masting by eighteen New Zealand plant species: the role of temperature as a synchronizing cue. *Ecology* 83:1214–1225.
- Scheiner, S. M., M. Barfield, and R. D. Holt. 2020. The genetics of phenotypic plasticity. XVII. Response to climate change. *Evolutionary Applications* 13:388–399.
- Schluter, D., T. D. Price, and L. Rowe. 1991. Conflicting selection pressures and life history trade-offs. *Proc. R. Soc. Lond. B* 246:11–17.
- Schwartz, M. D. 2003. *Phenology: an integrative environmental science*. Springer.
- Schwartz, M. D., R. Ahas, and A. Aasa. 2006. Onset of spring starting earlier across the Northern Hemisphere. *Global Change Biology* 12:343–351.
- Scott, L. C. 1995. Survival and sex ratios of the intertidal copepod, *Tigriopus californicus*, following ultraviolet-B (290–320 nm) radiation exposure. *Marine Biology* 123:799–804.
- Sheriff, M. J., G. J. Kenagy, M. Richter, T. Lee, Ø. Tøien, F. Kohl, C. L. Buck, et al. 2011. Phenological variation in annual timing of hibernation and breeding in nearby populations of Arctic ground squirrels. *Proceedings of the Royal Society of London B: Biological Sciences* 278:2369–2375.

- Simmonds, E. G., E. F. Cole, B. C. Sheldon, and T. Coulson. 2020. Phenological asynchrony: a ticking time-bomb for seemingly stable populations? *Ecology Letters* 23:1766–1775.
- Simons, A. M., and M. O. Johnston. 2006. Environmental and Genetic Sources of Diversification in the Timing of Seed Germination: Implications for the Evolution of Bet Hedging. *Evolution* 60:2280–2292.
- Skellam, J. G. 1967. Seasonal periodicity in theoretical population ecology. Pages 179–205 *in* Proceedings of the 5th Berkeley symposium in mathematical statistics and probability (Vol. 4).
- Sletvold, N., and J. Ågren. 2015. Climate-dependent costs of reproduction: Survival and fecundity costs decline with length of the growing season and summer temperature. *Ecology Letters* 18:357–364.
- Smith, D. S., M. K. Lau, R. Jacobs, J. A. Monroy, S. M. Shuster, and T. G. Whitham. 2015. Rapid plant evolution in the presence of an introduced species alters community composition. *Oecologia* 179:563–572.
- Sponaugle, S., and R. K. Cowen. 1994. Larval durations and recruitment patterns of two Caribbean gobies (Gobiidae): contrasting early life histories in demersal spawners. *Marine Biology* 120:133–143.
- Stearns, S. C. 1976. Life-history tactics: a review of the ideas. *The Quarterly review of biology* 51:3–47.
- Stearns, S. C. 1989. Trade-Offs in Life-History Evolution. *Functional Ecology* 3:259–268.
- Stearns, S. C. 1992. *The Evolution of Life Histories*. Oxford University Press, Oxford.
- Stearns, S. C., M. Ackermann, M. Doebeli, and M. Kaiser. 2000. Experimental evolution of aging, growth, and reproduction in fruitflies. *Proceedings of the National Academy of Sciences* 97:3309–3313.
- Stearns, S. C., and J. C. Koella. 1986. The evolution of phenotypic plasticity in life-history traits: predictions of reaction norms for age and size at maturity. *Evolution* 40:893–913.
- Steiner, U. K., S. Tuljapurkar, and S. H. Orzack. 2010. Dynamic heterogeneity and life history variability in the kittiwake. *Journal of Animal Ecology* 79:436–444.
- Stott, I., S. Townley, and D. J. Hodgson. 2011. A framework for studying transient dynamics of population projection matrix models. *Ecology Letters* 14:959–970.
- Sugihara, G., and R. M. May. 1990. Nonlinear forecasting as a way of distinguishing chaos from measurement error in time series. *Nature* 344:734–741.

- Thackeray, S. J., P. A. Henrys, D. Hemming, J. R. Bell, M. S. Botham, S. Burthe, P. Helaouet, et al. 2016. Phenological sensitivity to climate across taxa and trophic levels. *Nature* 535:241–245.
- Thackeray, S. J., T. H. Sparks, M. Frederiksen, S. Burthe, P. J. Bacon, J. R. Bell, M. S. Botham, et al. 2010. Trophic level asynchrony in rates of phenological change for marine, freshwater and terrestrial environments. *Global Change Biology* 16:3304–3313.
- Todd, B. D., D. E. Scott, J. H. Pechmann, and J. W. Gibbons. 2010. Climate change correlates with rapid delays and advancements in reproductive timing in an amphibian community. *Proceedings of the Royal Society B: Biological Sciences* 278:2191–2197.
- Tuljapurkar, S. 1985. Population dynamics in variable environments. VI. Cyclical environments. *Theoretical Population Biology* 28:1–17.
- Tuljapurkar, S. D. 1982. Population dynamics in variable environments. III. Evolutionary dynamics of r-selection. *Theoretical Population Biology* 21:141–165.
- Tuljapurkar, S. 2013. *Population Dynamics in Variable Environments*. Springer Science & Business Media.
- Tuljapurkar, S., J.-M. Gaillard, and T. Coulson. 2009. From stochastic environments to life histories and back. *Philosophical Transactions of the Royal Society B: Biological Sciences* 364:1499–1509.
- Tuljapurkar, S., W. Zuo, T. Coulson, C. Horvitz, and J.-M. Gaillard. 2020. Skewed distributions of lifetime reproductive success: beyond mean and variance. *Ecology Letters* 23:748–756.
- Tuljapurkar, S., W. Zuo, T. Coulson, C. Horvitz, and J.-M. Gaillard. 2021. Distributions of LRS in varying environments. *Ecology Letters*.
- van Daalen, S., and H. Caswell. 2020. Variance as a life history outcome: Sensitivity analysis of the contributions of stochasticity and heterogeneity. *Ecological Modelling* 417:108856.
- van Schaik, C. P., J. W. Terborgh, and S. J. Wright. 1993. The Phenology of Tropical Forests: Adaptive Significance and Consequences for Primary Consumers. *Annual Review of Ecology and Systematics* 24:353–377.
- Varpe, Ø. 2017. Life History Adaptations to Seasonality. *Integrative and Comparative Biology* 57:943–960.
- Vasseur, D. A., and P. Yodzis. 2004. The color of environmental noise. *Ecology* 85:1146–1152.
- Vindenes, Y., S. Engen, and B. Sæther. 2008. Individual Heterogeneity in Vital Parameters and Demographic Stochasticity. *The American Naturalist* 171:455–467.
- Vindenes, Y., and Ø. Langangen. 2015. Individual heterogeneity in life histories and eco-evolutionary dynamics. *Ecology Letters* 18:417–432.

- Visser, M. E., S. P. Caro, K. van Oers, S. V. Schaper, and B. Helm. 2010. Phenology, seasonal timing and circannual rhythms: towards a unified framework. *Philosophical Transactions of the Royal Society of London B: Biological Sciences* 365:3113–3127.
- Walsh, M. R., and D. M. Post. 2011. Interpopulation variation in a fish predator drives evolutionary divergence in prey in lakes. *Proceedings of the Royal Society of London B: Biological Sciences* 278:2628–2637.
- Walther, G.-R., E. Post, P. Convey, A. Menzel, C. Parmesan, T. J. C. Beebee, J.-M. Fromentin, et al. 2002. Ecological responses to recent climate change. *Nature* 416:389–395.
- Waterton, J., and E. E. Cleland. 2016. Trade-off between early emergence and herbivore susceptibility mediates exotic success in an experimental California plant community. *Ecology and Evolution* 6:8942–8953.
- Westerling, A. L., H. G. Hidalgo, D. R. Cayan, and T. W. Swetnam. 2006. Warming and Earlier Spring Increase Western U.S. Forest Wildfire Activity. *Science* 313:940–943.
- Wieczynski, D. J., P. E. Turner, and D. A. Vasseur. 2018. Temporally Autocorrelated Environmental Fluctuations Inhibit the Evolution of Stress Tolerance. *The American Naturalist* 191:E195–E207.
- Wilczek, A. M., L. T. Burghardt, A. R. Cobb, M. D. Cooper, S. M. Welch, and J. Schmitt. 2010. Genetic and physiological bases for phenological responses to current and predicted climates. *Philosophical Transactions of the Royal Society B: Biological Sciences* 365:3129–3147.
- Willett, C. S. 2010. Potential fitness trade-offs for thermal tolerance in the intertidal copepod *Tigriopus californicus*. *Evolution* 64:2521–2534.
- Williams, C. M., G. J. Ragland, G. Betini, L. B. Buckley, Z. A. Cheviron, K. Donohue, J. Hereford, et al. 2017. Understanding Evolutionary Impacts of Seasonality: An Introduction to the Symposium. *Integrative and Comparative Biology* 57:921–933.
- Williams, J. W., and S. T. Jackson. 2007. Novel climates, no-analog communities, and ecological surprises. *Frontiers in Ecology and the Environment* 5:475–482.
- Winder, M., and D. E. Schindler. 2004. Climate Change Uncouples Trophic Interactions in an Aquatic Ecosystem. *Ecology* 85:2100–2106.
- Wolf, A. A., E. S. Zavaleta, and P. C. Selmants. 2017. Flowering phenology shifts in response to biodiversity loss. *Proceedings of the National Academy of Sciences* 201608357.
- Wolkovich, E. M., B. I. Cook, J. M. Allen, T. M. Crimmins, J. L. Betancourt, S. E. Travers, S. Pau, et al. 2012. Warming experiments underpredict plant phenological responses to climate change. *Nature* 485:494–497.

- Xu, L., R. B. Myneni, F. S. Chapin Iii, T. V. Callaghan, J. E. Pinzon, C. J. Tucker, Z. Zhu, et al. 2013. Temperature and vegetation seasonality diminishment over northern lands. *Nature Climate Change* 3:581–586.
- Zhu, W., H. Tian, X. Xu, Y. Pan, G. Chen, and W. Lin. 2012. Extension of the growing season due to delayed autumn over mid and high latitudes in North America during 1982–2006. *Global Ecology and Biogeography* 21:260–271.